

The Origin of Aromaticity: Aromatic Compounds as Intrinsic Topological Superconductors with Majorana Fermion

Kyoung Hwan Choi¹, and Dong Hack Suh^{1†}

*1 Advanced Materials & Chemical Engineering Building 311, 222 Wangsimni-ro, Seongdong-Gu,
Seoul, Korea, E-mail: dhsuh@hanyang.ac.kr*

Abstract

Topological superconductors have been discovered with recent advances in understanding the topological properties of condensed matters. These states have a full pairing gap in the bulk and gapless counter-propagating Majorana states at the boundary. A pair of Majorana zero modes is associated with each vortex. This understanding had a great influence on the theory of superconductivity and their following experiments, but its relevance to organic compounds was not closely observed. Here, we analyze the topological states of various polycyclic aromatic hydrocarbons (PAHs), including benzene, and reveal that they are topological superconductors. We have analyzed the momentum vectors of benzene and other PAHs through a semi-classical approach to confirm their non-trivial state. Their unique properties might be originated from the odd number of Kramers doublets in PAHs. The Hückel rule describing aromaticity can be reinterpreted with a topological viewpoint. It suggests that the $(4n+2)$ rule can be split into two pairs of $(2n+1)$ electrons each, namely, electrons and holes with spin up and down. Therefore, it always forms an odd number of Kramers' doublet. Moreover, n in the Hückel rule can be interpreted as the winding number in global next-nearest-neighbor (NNN) hopping. This work will re-establish the definition of aromaticity that has been known so far and extend the use of aromatic compounds as topological superconductors to quantum computers.

Introduction

The quantum state of matter is characterized not only by the structure of the energy spectrum but also by the nature of wave functions.¹ Of particular importance are topological properties of wave functions, i.e., properties that are invariant under small adiabatic deformation of the Hamiltonian. These properties can be specified by some topological invariant.

The quantum Hall (QH) effect² provides the first example of a non-trivial state of matter, where the quantized Hall conductance is a topological invariant and characterized by Chern number³. The quantum spin Hall (QSH) state has been theoretically predicted and experimentally observed in HgTe quantum wells.⁴⁻⁷ The QSH state is characterized by a Z_2 topological number⁸, gapless helical edge states^{9,10}, and winding number¹¹. Through these perceptions, the $^3\text{He-B}$ and the planar phase of the triplet superfluid superconductor belong to the time-reversal invariant (TRI) topological state of matter.^{12,13}

Following the generalization of the QSH state, the generalization of the TRI topological superconducting state can be obtained in a straightforward manner, and has gapless Majorana surface states protected by TR symmetry.¹⁴⁻¹⁶ The TRI superconductor can be classified by a Z_2 topological number in 2D. Furthermore, a TRI topological defect of a Z_2 non-trivial superconductor is accompanied by a Kramers' pair of Majorana fermions, an emergent quasi-particle with zero energy state.^{17,18} Because fundamental aspects of Majoranas and their non-Abelian braiding properties^{19,20} offer possible application in quantum computation^{21,22}, many examples of leading candidates to find Majoranas in superconductors are: the Moore-Read-type state in the fractional quantum Hall effect²³; vortices in two-dimensional (2D) p+ip spinless superconductors²⁴; and domain walls in 1D p-wave superconductors²⁵.

On the other hands, aromaticity is considered as one of the most important concepts in modern organic chemistry.²⁶ The term aromaticity/aromatic has a long history dating back to its first use in a chemical sense by Kekulé²⁷ and Erlenmeyer²⁸ in the 1860s. Similarly, as in

those days, in a modern sense the term is related either to some typical properties or to a specific structure.²⁹ In the last few decades it has been almost generally accepted that both terms, aromaticity and aromatic character, are associated with the ground-state properties of cyclic π -electron compounds which (i) are more stable than their chain analogues, (ii) have bond lengths between those typical of the single and double ones, and (iii) have a π -electron ring current that is induced when the system is exposed to external magnetic fields.

The recent study of topological aspects of PAHs has provided a more profound understanding of a non-trivial phase of PAHs. Organic crystal with pyrene derivatives shows topological photonics through Pancharatnam-Berry and wave retardation phase merging, wavefront shaping and waveguide on edges.³⁰ Magnetic properties and results of transport spectroscopy of pelletized organic crystal also demonstrate the intrinsic quantized spin waves on the pyrene derivative, coherent quantum phase slip (CQPS), and Majorana hinge and corner modes which are signatures of topological superconductors.³¹ However, the its origin remains unclear. Despite the the widespread use of “aromatic” and “aromaticity” in the current scientific literature, it has been defined on the empirical basis of experimental observables and quantities obtained from theoretical computations.³² Aromatic hydrocarbons generally refer to molecules that have $(4n+2)$ π electrons and follow the Hückel’s rule, which is composed of a benzenoid ring.

Here, we propose to investigate the momentum space of aromaticity by using a semi-classical approach. The momentum vectors of up- and down-spin of electrons and holes in various aromatic hydrocarbons are analyzed by the recent theoretical suggestion about time-reversal-invariant topological superconductors.¹⁷ In momentum space, it has been known that one pair of particles and the other pair of antiparticles must exist in zero energy state, and that all aromatic compounds have winding numbers, a topological invariant.³³ Given that, the physical meaning of the Hückel $(4n+2)$ rule should be reinterpreted as the odd number of

Kramers doublet for $(2n+1)$ up-spin and $(2n+1)$ down-spin particles and antiparticles, respectively and its n as closely to do with the winding number.

Results and discussion

Benzene as an exception compound to Peierls distortion

The geometry and energy of 1,3,5-cyclohexatriene has been suggested as a reference molecule for evaluating the extra stabilization energy of benzene.³⁴ Among various differences between two molecules, their bond length and binding energy seem to be the key factors. 1,3,5-cyclohexatriene has three alternating sequences of double and single bonds (A-B type), while benzene has six uniform bonds (A type). Benzene could be obtained without the existence of 1,3,5-cyclohexatriene. It is very contradictory because evenly spaced chains of interacting atoms with each one contributing an electron are more unstable than those with an alternating spaced chain, as in polyacetylene.^{35,36} It indicates that benzene is considered robust against Peierls distortion while 1,3,5-cyclohexatriene is not. (Fig. 1a) Although the Peierls distortion was perceived as a natural direction of stabilizing materials, the odd number of Kramers doublets resulting can make a system robust against it.^{10,37}

Momentum space and winding number of benzene

Almost no research has been done experimentally on the superconductivity of aromatic hydrocarbons (PAHs), but some theoretical research has been done.³⁸⁻⁴¹ Recently, their various topological properties, such as Pancharatnam-Berry and wave retardation phase merging, coherent quantum phase slip, and Majorana hinge and edge modes have been reported through experimental observations.^{30,31} These results allow PAHs including benzene to be considered as topological superconductors. Thus, the TRI topological superconductor model can be used for various PAHs. The BdG Hamiltonian is a block diagonal with only equal spin pairing and spin-up and -down electrons that form Cooper pairs with momentum pairing of $p_x + ip_y$ and p_x

- ip_y , respectively.¹⁷ In this situation, the quasiparticle operators ψ_\uparrow and ψ_\downarrow can be expressed in terms of the eigenstates of the BdG Hamiltonian as; $\psi_\uparrow(n) = [u(n)c_\uparrow(n) + v(n)c_\uparrow^\dagger(n)]$, $\psi_\downarrow(m) = [u^*(m)c_\downarrow(m) + v^*(m)c_\downarrow^\dagger(m)]$ where n and m are odd and even carbon numbers of PAHs, respectively, u and v and u^* and v^* are momentum vectors of electrons and holes, respectively. Additionally, $[\psi_\uparrow(n), \psi_\downarrow(m)]$ transforms as a Kramers' doublet which forbids a gap in the edge state spectrum once TRS is preserved by preventing the mixing of the spin-up and spin-down modes.

To explain benzene with the above situation, the odd-numbered carbons have the up-spin fermions and the even-number carbons have the down-spin fermions. (Fig. 2a) The u_k and v_k of benzene can be calculated from the position vectors of each of the electrons. (See Supplementary information). For instance, the up-spin electron and hole initially positioned at C1 moves to C3 for the electron and C5 for the hole by the quasiparticle operator $[\psi_\uparrow(1)]$. Therefore, $\vec{u}(1)$ and $\vec{v}(1)$ is positioned at (-0.313, -2.315) and (-2.310, -0.896), respectively. Contrary to this, the down-spin electron paired with the up-spin electron should have the opposite sign of the y axis momentum.¹⁷ To satisfy this, u_\downarrow^* and v_\downarrow^* must be matched with (-0.313, 2.315) and (-2.231, 0.896). This momentum is displayed when the electron and the hole positioned at C4 move to C2 for the electron $[\vec{u}^*(4)]$ and C6 for the hole $[\vec{v}^*(4)]$. Therefore, $[\psi_\uparrow(1), \psi_\downarrow(4)]$ can be interpreted as a Kramers doublet. In the same way, two different quasiparticle operators make Kramers doublets: one operator pairs which move up- and down-spin electrons from C3 to C5 (C2 to C6) is $[\psi_\uparrow(3), \psi_\downarrow(2)]$ and the other which moves up- and down-spin electrons from C5 to C1 (C6 to C4) is $[\psi_\uparrow(5), \psi_\downarrow(6)]$. Therefore, benzene can have three different Kramers doublets. It is the reason why benzene can be robust against Peierls distortion.

The relationship between these momentum vectors in the momentum space allows intuitive

perception of the non-trivial state of benzene through the winding number. The connections among $\vec{u}(1)$, $\vec{u}(3)$ and $\vec{u}(5)$ momentum vectors can create a single closed loop containing the position (0,0). (Fig. 2b) Therefore, the spin electrons rotating clockwise have the winding number as 1. The those among $\vec{u}^*(2)$, $\vec{u}^*(4)$ and $\vec{u}^*(6)$ can so make a single closed loop containing the (0,0) position counter-clockwise (Fig. 2b). As a result, down-spin electrons has the winding number as -1. Similarly, the winding numbers up- and down-spin holes are -1 and 1, respectively. (Fig. 2c) It is equivalent to helical superconductors predicted theoretically^{14,42} and its state is called “helical Majorana liquid”. It reflects the topological properties of PAHs well. It comes from the boundary of Z_2 topological superconductors and the mass term for the edge states is forbidden by TR symmetry. Up to this point, benzene has inherently a non-trivial state, and three pairs of quasiparticle operators create an odd number of Kramers doublets, causing chiral superconducting states with the chiral Majorana edge state.

The new interpretation of benzene could be extended to the entire PAHs governed by Hückel (4n+2) rule, a symbol of aromaticity. Two concepts are used to interpret benzene as a non-trivial state: One is the up-and down-spin electrons separated by odd- and even-number carbons, respectively. The other is odd numbers of Kramer doublets that enable their NNN hopping. Therefore, the Hückel (4n+2) rule can be split into two (2n+1) electrons for up-spin and down-spin, respectively. In this case, the up- and down-spin electrons are separated and the paired quasiparticle operators have odd numbers of Kramers doublets.

Momentum space and winding number of anthracene

Applying the new suggestion and extending it to PAHs with linear, bent and circular types the momentum vectors and calculated in naphthalene, anthracene, pyrene, phenanthrene, chrysene, and coronene. (Tables. S2-S16) During this process, two differences can be found compared to benzene. First, all momentum vectors that appear similarly located in momentum space have slightly different values. This trend was also observed in anthracene [$\vec{u}(1)$, $\vec{u}(3)$ and $\vec{u}(5)$]

and pyrene [$\vec{u}(1)$, $\vec{u}(3^b)$, $\vec{u}(13^b)$ and $\vec{u}(16^b)$], respectively. (Table. S5 and S7) It is very different from the momentum vectors in the crystals where two or three bases describe the whole system. Second, the Kramers doublet is not paired with in the same benzenoid ring. In anthracene, $\vec{u}(1)$ is paired with $\vec{u}^*(8)$, and $\vec{u}^*(3^a)$ is entangled with $\vec{u}^*(6^b)$ in pyrene. (Fig. 3a and b) It can be formed in the geometric relationship of point symmetry. Although the values of all up-and down-spin momentum vectors are slightly different, there are always momentum vectors that forms a pair of Kramers doublet in their molecules.

Global NNN hopping for exception molecules to the Hückel rule

PAH's topological interpretation also offers a new direction for the elusive parts of the Hückel rule. For example, pyrene is difficult to describe with the Hückel rule. Since pyrene is made up of 16 carbons, pyrene has n as 3.5. To explain this, several qualitative models (e.g., Platt's ring perimeter model⁴³, Clar's model⁴⁴ and Randić's conjugated circuits model⁴⁵) have been suggested to explain the aforementioned. The exception can be clear up by the extension of n based on the winding number of pyrene through global NNN hopping. Here, all fermions with identical spins return to their original position by hopping via the locations.

Anthracene's global NNN hopping involves seven up-spin and down-spin electrons. Therefore, the odd number of Kramers doublets was always guaranteed. On the other hand, anthracene's fermions create an Eulerian circuit because all anthracene vertices have an even degree. (Fig. 4a and b) Although momentum vectors in it are slightly different, the non-trivial state is guaranteed when fermions hop and eventually return to their initial position. Up-spin electrons rotate counter-clockwise by the same path in momentum space. Hence, the winding number is -1, while that of down-spin electrons is 1. (Fig. 4c and d)

However, for pyrene, there are eight up-and down-spin electrons. So, it can lead to Kramers doublets that is not robust to Peierls distortion. Two electrons should be excluded for robustness.

(Supplementary Fig. 53) Various methods are proposed to remove the electrons of each up-and down-spin fermion, but only in certain case, global NNN hopping can be preserved. Two odd vertices need to be an Eulerian trail and satisfy global NNN hopping. Thus, the starting momentum vector of global NNN hopping, $\vec{v}(13^a)$, is surely determined. It has a momentum vector of hole. Interestingly, it is excluded from the second run. (Fig. 5a) Although connections of momentum vectors of anthracene in momentum space make a closed-loop including the (0,0) position, a momentum vector of pyrene, $\vec{v}(13^a)$, is outside the closed loop of pyrene. It forms a half-integer winding number.⁴⁶

In other words, the number n in the Hückel rule represents the winding number formed in the process of global NNN hopping of the electronic state. Therefore, the topological interpretation of the Hückel rule helps to understand electronic states that are completely different from the previous ones of aromaticity. In aromatic molecules, electrons exist in a static state for Hückel rule, and the electrons are persistent circulating in a dynamic state.

To probe the reinterpretation of the Hückel rule, coronene, with the half integer n , with another exception of the Hückel rule, is investigated. It has 12 up- and down-spin electrons. For global NNN hopping, one up-spin electron and one down-spin electron should be excluded to obtain the odd number of Kramers doublet. In addition, the Eulerian trail is built to connect 11 up-spin electrons and one momentum vector. It is isolated in the second rotation of global NNN hopping of up-spin electrons having the momentum vector of down-spin. (Fig. 5c) Like pyrene, the unique momentum vector forms an exotic Kramer doublet between the up-spins, giving it a half-integer winding number. (Fig. 5d) However, the most significant difference between pyrene and coronene is that the winding number is 0.5 for pyrene in the global NNN hopping excluding this momentum vector, that is 1.5 for coronene. It was confirmed that the half-integer winding number in the Hückel rule could occur for forming an Euler trail during the global NNN hopping.

Conclusion

In conclusion, the electronic states of aromaticity, one of the most famous concepts in chemistry, has been empirically determined by many properties without the definition. Topological phenomena of PAHs led to reinterpret the aromaticity and the Hückel rule. We further tune the concepts of TRI topological superconductors to aromatic compounds. As a result, the new suggestion for aromatics implied that the up-and down-spins must form the odd number of Kramers doublets, and the number n represents the winding numbers during the global NNN hopping of all PAHs. It is not only means that the n value expands to a half integer, but also indicates that it is a topological invariant that represents a non-trivial state. In conclusion, all aromatic compounds are thought to be intrinsic topological superconductors.

References

- 1 Wen, X.-G. J. I. J. o. M. P. B. Topological orders in rigid states. **4**, 239-271 (1990).
- 2 Thouless, D. J., Kohmoto, M., Nightingale, M. P. & den Nijs, M. J. P. r. l. Quantized Hall conductance in a two-dimensional periodic potential. **49**, 405 (1982).
- 3 Hatsugai, Y. J. P. r. l. Chern number and edge states in the integer quantum Hall effect. **71**, 3697 (1993).
- 4 Kane, C. L. & Mele, E. J. J. P. r. l. Quantum spin Hall effect in graphene. **95**, 226801 (2005).
- 5 Bernevig, B. A. & Zhang, S.-C. J. P. r. l. Quantum spin Hall effect. **96**, 106802 (2006).
- 6 Bernevig, B. A., Hughes, T. L. & Zhang, S.-C. J. s. Quantum spin Hall effect and topological phase transition in HgTe quantum wells. **314**, 1757-1761 (2006).
- 7 König, M. *et al.* Quantum Spin Hall Insulator State in HgTe Quantum Wells. **318**, 766-770, doi:10.1126/science.1148047 %J Science (2007).
- 8 Kane, C. L. & Mele, E. J. J. P. r. l. Z₂ topological order and the quantum spin Hall effect. **95**, 146802 (2005).
- 9 Wu, C., Bernevig, B. A. & Zhang, S.-C. J. P. r. l. Helical liquid and the edge of quantum spin Hall systems. **96**, 106401 (2006).
- 10 Xu, C. & Moore, J. E. J. P. R. B. Stability of the quantum spin Hall effect: Effects of interactions, disorder, and Z₂ topology. **73**, 045322 (2006).
- 11 Qi, X.-L., Hughes, T. L. & Zhang, S.-C. J. P. R. B. Topological invariants for the Fermi surface of a time-reversal-invariant superconductor. **81**, 134508 (2010).
- 12 Salomaa, M. & Volovik, G. J. P. R. B. Cosmiclike domain walls in superfluid B₃: Instantons and diabolical points in (k, r) space. **37**, 9298 (1988).
- 13 Volovik, G. E. J. J. l. Topological invariant for superfluid ³He-B and quantum phase transitions. **90**, 587-591 (2009).
- 14 Fu, L., Kane, C. L. & Mele, E. J. J. P. r. l. Topological insulators in three dimensions. **98**, 106803 (2007).
- 15 Moore, J. E. & Balents, L. J. P. R. B. Topological invariants of time-reversal-invariant band structures. **75**, 121306 (2007).
- 16 Roy, R. J. a. p. c.-m. Three dimensional topological invariants for time reversal invariant Hamiltonians and the three dimensional quantum spin Hall effect. (2006).
- 17 Qi, X.-L., Hughes, T. L., Raghu, S. & Zhang, S.-C. J. P. r. l. Time-reversal-invariant topological superconductors and superfluids in two and three dimensions. **102**, 187001 (2009).
- 18 Majorana, E. J. I. N. C. Teoria simmetrica dell'elettrone e del positrone. **14**, 171 (1937).
- 19 Alicea, J. J. R. o. p. i. p. New directions in the pursuit of Majorana fermions in solid state systems. **75**, 076501 (2012).
- 20 Beenakker, C. J. A. R. C. M. P. Search for Majorana fermions in superconductors. **4**, 113-136 (2013).
- 21 Kitaev, A. Y. J. A. o. P. Fault-tolerant quantum computation by anyons. **303**, 2-30 (2003).
- 22 Halperin, B. I. *et al.* Adiabatic manipulations of Majorana fermions in a three-dimensional network of quantum wires. **85**, 144501 (2012).
- 23 Read, N. & Green, D. J. P. R. B. Paired states of fermions in two dimensions with breaking of parity and time-reversal symmetries and the fractional quantum Hall effect. **61**, 10267 (2000).
- 24 Kitaev, A. J. A. o. P. Anyons in an exactly solved model and beyond. **321**, 2-111

- (2006).
- 25 Alicea, J., Oreg, Y., Refael, G., Von Oppen, F. & Fisher, M. P. J. N. P. Non-Abelian statistics and topological quantum information processing in 1D wire networks. **7**, 412 (2011).
- 26 Krygowski, T., Cyranski, M., Czarnocki, Z., Häfelinger, G. & Katritzky, A. R. Aromaticity: a theoretical concept of immense practical importance. *Tetrahedron* **13**, 1783-1796 (2000).
- 27 Kekulé, A. Sur la constitution des substances aromatiques. *Bulletin mensuel de la Société Chimique de Paris* **3**, 98 (1865).
- 28 Erlenmeyer, E. Studien über die sg aromatischen Säuren. *Annalen der Chemie und Pharmacie* **137**, 327-359 (1866).
- 29 Krygowski, T. M. & Cyranski, M. K. Structural aspects of aromaticity. *Chemical Reviews* **101**, 1385-1420 (2001).
- 30 Choi, K. H., Hwang, D. Y. & Suh, D. H. Dirac Metamaterial Assembled by Pyrene Derivative and its Topological Photonics. *arXiv preprint arXiv:2101.04359* (2021).
- 31 Choi, K. H. & Suh, D. H. Experimental realization of Majorana hinge and corner modes in intrinsic organic topological superconductor without magnetic field at room temperature. *arXiv preprint arXiv:2101.05978* (2021).
- 32 Schleyer, P. v. R. Introduction: Aromaticity. *Chemical Reviews* **101**, 1115-1118, doi:10.1021/cr0103221 (2001).
- 33 Yao, S. & Wang, Z. Edge states and topological invariants of non-Hermitian systems. *Physical review letters* **121**, 086803 (2018).
- 34 van Lenthe, J. H., Havenith, R. W. A., Dijkstra, F. & Jenneskens, L. W. 1,3,5-Cyclohexatriene captured in computro; the importance of resonance. *Chemical Physics Letters* **361**, 203-208, doi:[https://doi.org/10.1016/S0009-2614\(02\)00873-4](https://doi.org/10.1016/S0009-2614(02)00873-4) (2002).
- 35 Heeger, A. J., Kivelson, S., Schrieffer, J. R. & Su, W. P. Solitons in conducting polymers. *Reviews of Modern Physics* **60**, 781-850, doi:10.1103/RevModPhys.60.781 (1988).
- 36 Burrezo, P. M., Zafra, J. L., López Navarrete, J. T. & Casado, J. Quinoidal/Aromatic Transformations in π -Conjugated Oligomers: Vibrational Raman studies on the Limits of Rupture for π -Bonds. **56**, 2250-2259, doi:10.1002/anie.201605893 (2017).
- 37 Schnyder, A. P., Ryu, S., Furusaki, A. & Ludwig, A. W. W. Classification of topological insulators and superconductors in three spatial dimensions. *Physical Review B* **78**, 195125, doi:10.1103/PhysRevB.78.195125 (2008).
- 38 Little, W. J. P. R. Possibility of synthesizing an organic superconductor. **134**, A1416 (1964).
- 39 London, F. Théorie quantique des courants interatomiques dans les combinaisons aromatiques. *J. phys. radium* **8**, 397-409 (1937).
- 40 Hirsch, J. Spin-split states in aromatic molecules. *Modern Physics Letters B* **4**, 739-749 (1990).
- 41 Hirsch, J. E. Spin-split states in aromatic molecules and superconductors. *Physics Letters A* **374**, 3777-3783, doi:<https://doi.org/10.1016/j.physleta.2010.07.023> (2010).
- 42 Schnyder, A. P., Ryu, S., Furusaki, A. & Ludwig, A. W. J. P. R. B. Classification of topological insulators and superconductors in three spatial dimensions. **78**, 195125 (2008).
- 43 Platt, J. R. J. T. J. o. C. P. The box model and electron densities in conjugated systems. **22**, 1448-1455 (1954).
- 44 Clar, E. & Schoental, R. *Polycyclic hydrocarbons*. Vol. 2 (Springer, 1964).
- 45 Randic, M. J. J. o. t. A. C. S. Aromaticity and conjugation. **99**, 444-450 (1977).
- 46 Yin, C., Jiang, H., Li, L., Lü, R. & Chen, S. Geometrical meaning of winding number

and its characterization of topological phases in one-dimensional chiral non-Hermitian systems. *Physical Review A* **97**, 052115, doi:10.1103/PhysRevA.97.052115 (2018).

Figures.

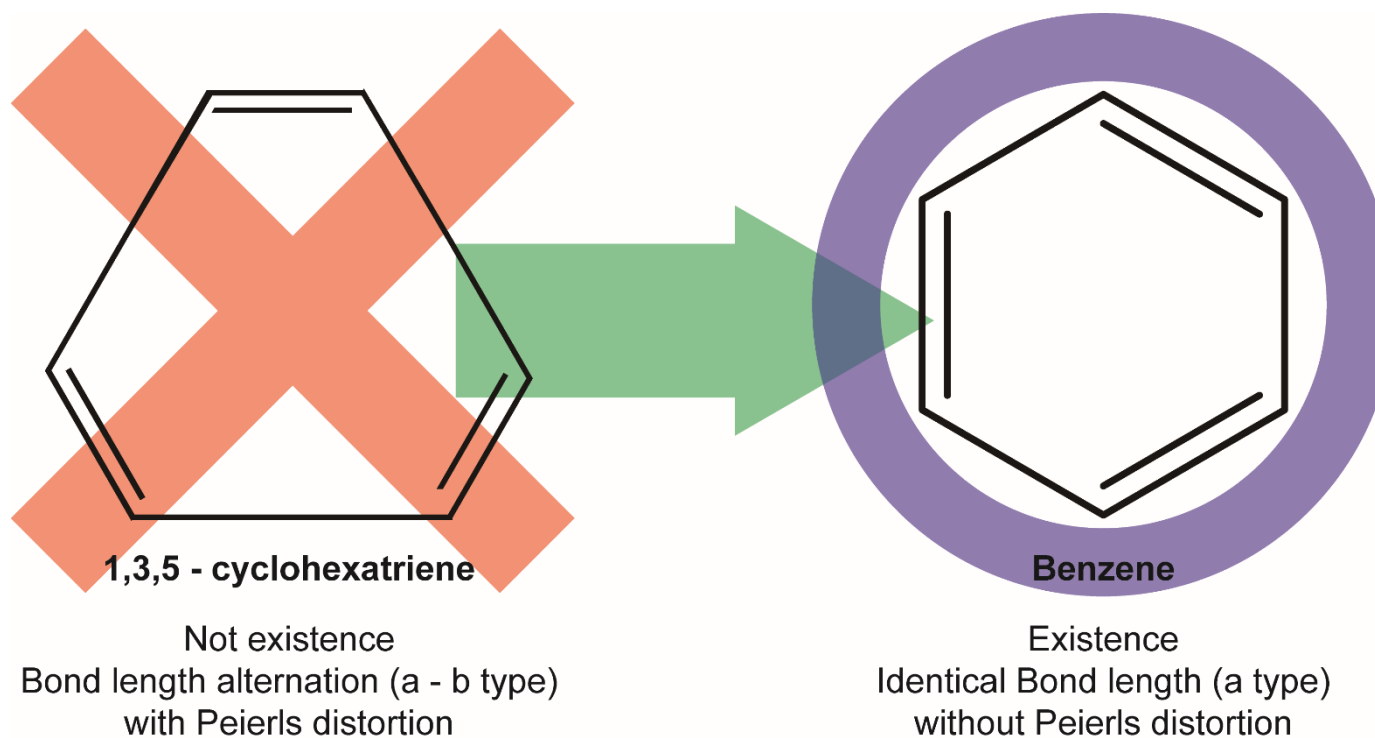


Fig. 1. Differences between 1,3,5-cyclohexatriene and benzene. Although Peierls distortion is a very important theory explaining the stability of molecules, benzene does not follow it. Recent topological studies show that odd number of Kramers doublet guarantees robustness of Peierls distortion.

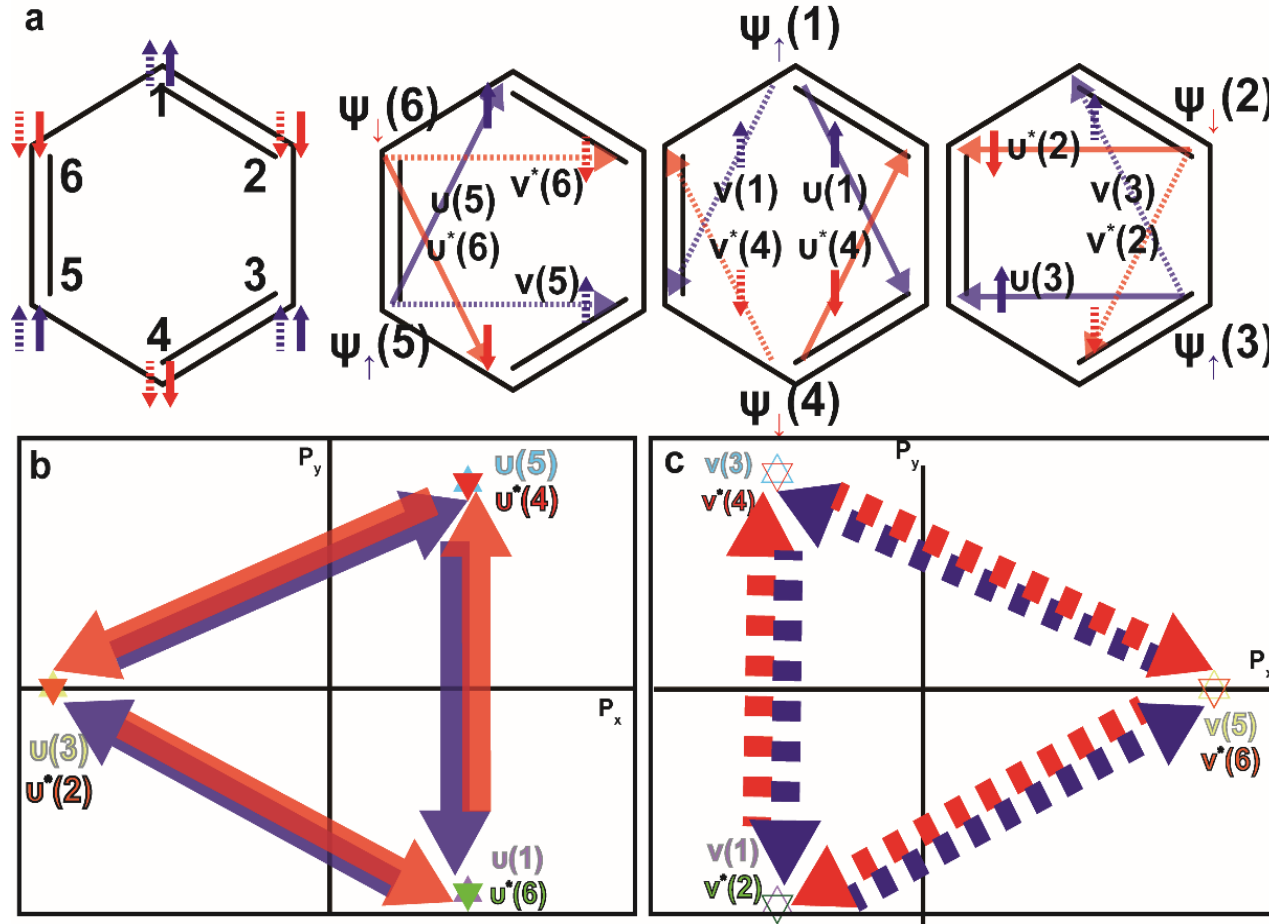


Fig. 2. Next Nearest Neighbor(NNN) Hopping scheme and momentum space of benzene. **a.** Benzene has three different momentum vectors for each particle and hole. ($\psi_{\uparrow}(n) = u(n)c_{\uparrow}(n) + u^*(n)c_{\uparrow}^{\dagger}(n)$, $\psi_{\downarrow} = v(m)c_{\downarrow}(m) + v^*(m)c_{\downarrow}^{\dagger}(m)$). ($\psi_{k1,\uparrow}$, $\psi_{-k1,\downarrow}$) consists of Kramers' doublets and a totally odd number of Kramers doublets exists in benzene. Therefore, benzene is robust against Peierls distortion. **b and c.** Momentum space for electron and hole. Up-spin and down-spin particles have chirality and up-spin particles and antiparticles also have chirality like the quantum spin Hall model. It shows NNN hopping of benzene has a non-trivial phase.

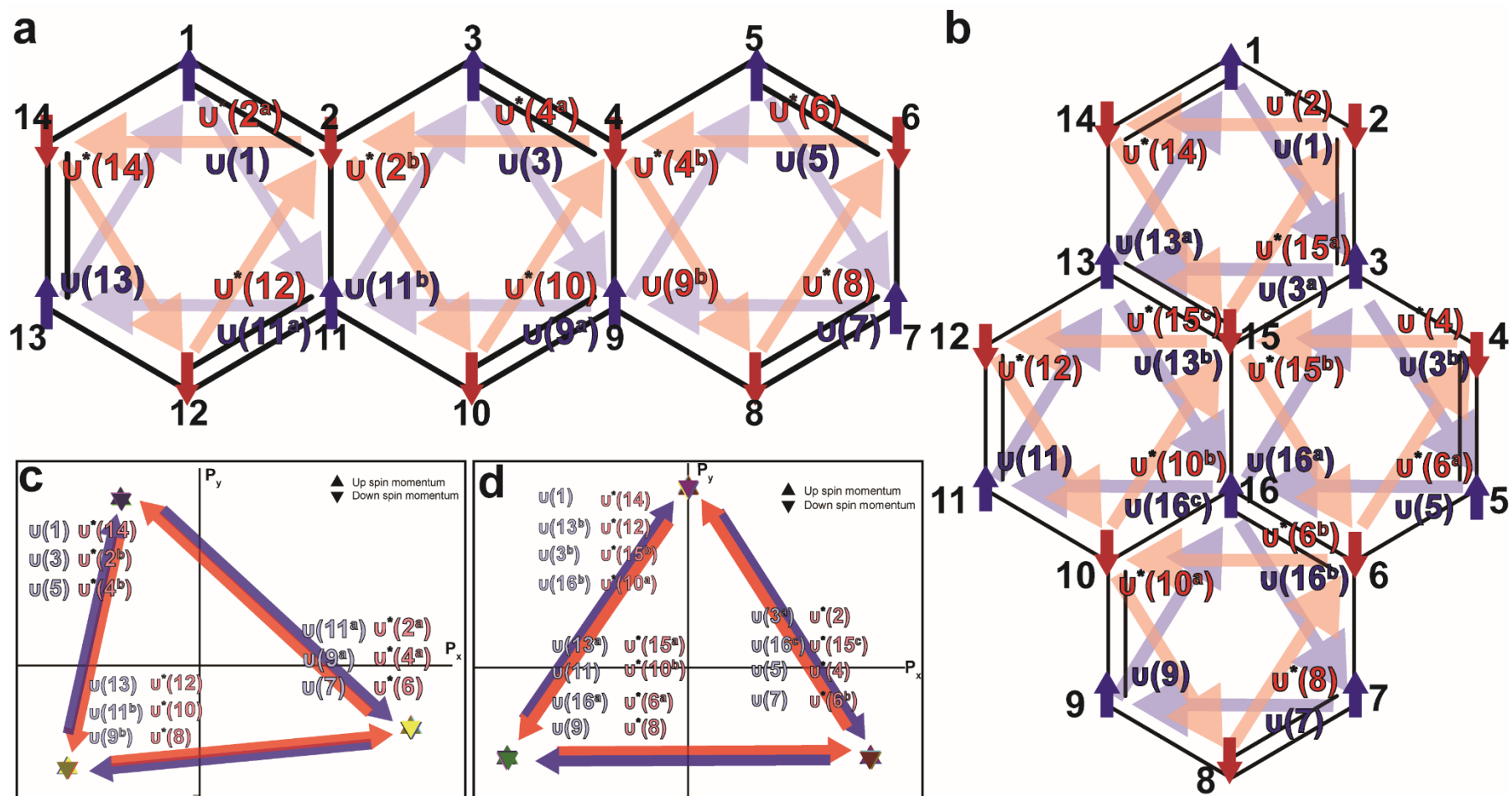


Fig. 3. Non-trivial state for anthracene and pyrene. a and b. NNN hopping scheme for anthracene(a) and pyrene(b). **c. and d.** Momentum space of anthracene(c) and pyrene(d).

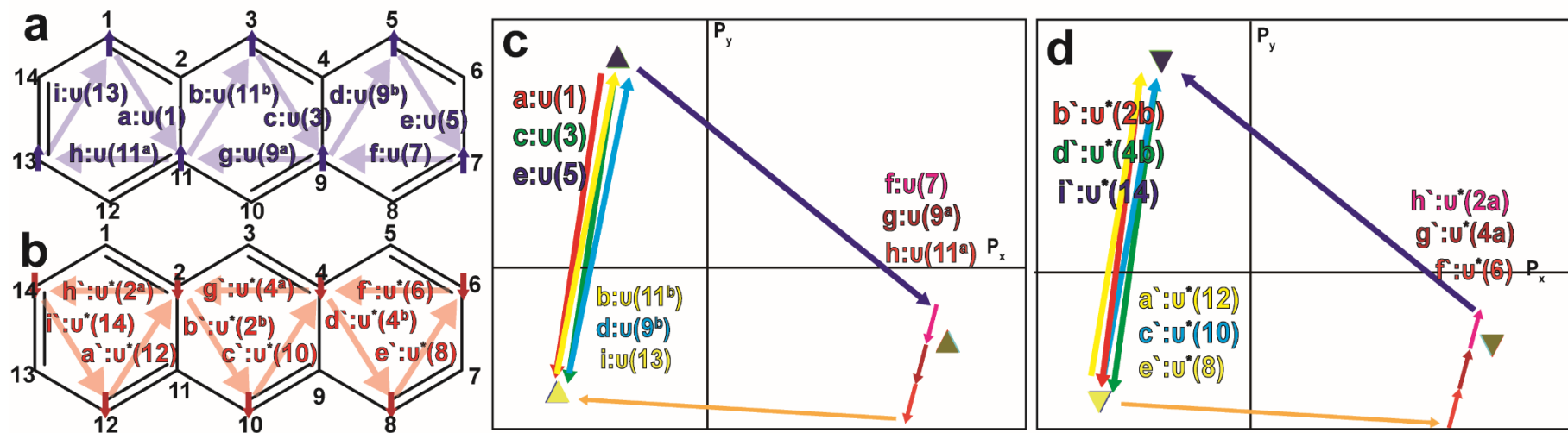


Fig. 4. Scheme and momentum space of Global NNN hopping for anthracene. a and b. Scheme of NNN hopping model of up-spin(a) and down-spin(b) for anthracene. **c. and d.** Momentum vectors of up-spin(c) and down-spin(d) of anthracene for global NNN hopping

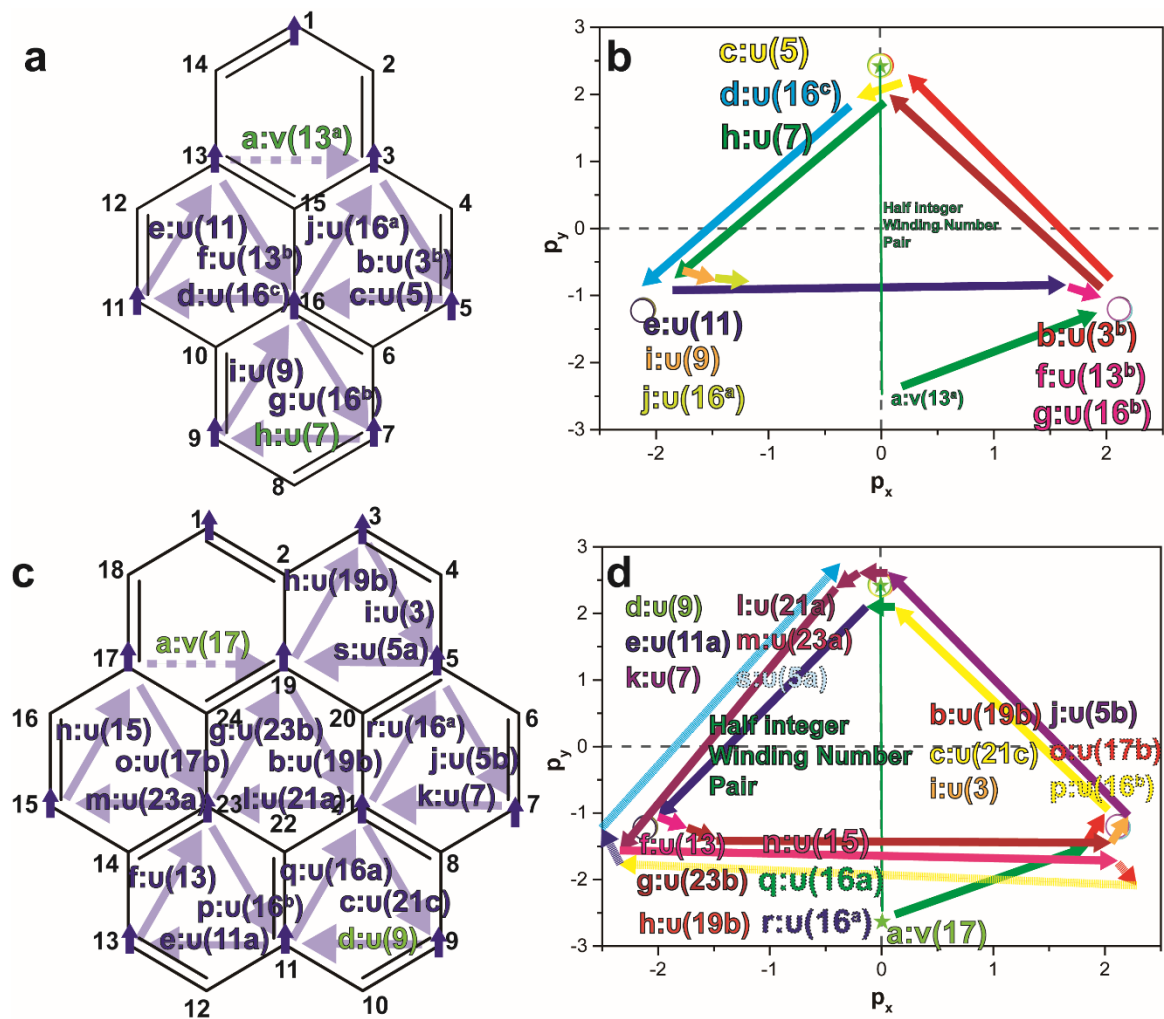


Fig. 5. Scheme and momentum space of Global NNN hopping for pyrene and coronene. a Scheme of NNN hopping model of up-spin for pyrene. **b.** Momentum vectors of up-spin of pyrene for global NNN hopping **c.** Scheme of NNN hopping model of up-spin for coronene **d.** Momentum vectors of up-spin of coronene for global NNN hopping

Methods

All molecules can be either drawn in Chemdraw. The Chemdraw drawing needs to be checked for stereochemical accuracy and the file is saved as a CDX file. The file is either opened in Chem3D or the structure is simply copied and pasted in Chem3D side window. The most stable structure of all molecules can be obtained by using a MM2 force field method which is optimized structure with little steric interactions. The carbon coordinates were then used as the position vector. A detail method for calculation of bond characteristics and modified bond dissociation energy in PAHs are discussed in supplementary information.

Supplementary information is available in the online version of the paper

Acknowledgements

This research was supported by Basic Science Research Program through the National Research Foundation of Korea(NRF) funded by the Ministry of Education (2018R1D1A1A02047853).

Author contribution

Dong Hack Suh designed, initiated and directed this research. Kyoung Hwan Choi performed the experiment. Dong Hack Suh and Kyoung Hwan Choi discussed the experiment, the data, the results and co-wrote the manuscript.

Competing interest. The authors declare no competing interests.

Supplementary information is available for this paper

Reprints and permissions information is available

Supplementary information for

**The origin of aromaticity: Aromatic compound as
the Intrinsic Topological Superconductor with a
Majorana Fermion.**

Supplementary Note 1: According to the definition of momentum ($P=mv$), the difference between the two position vectors has the same physical meaning as the momentum vector when the mass is constant. Therefore, momentum vectors of each PAHs are calculated from their position vector. For instance, benzene has six carbons, and each has their position (Supplementary table 2) and momentum vector for NNN hopping can be calculated (Supplementary table 3).

Carbon number	X position	Y position
1	0.0000	1.3990
2	1.2116	0.6995
3	1.2116	-0.6995
4	0.0000	-1.3990
5	-1.2116	-0.6995
6	-1.2116	0.6995

Table S1. Position vector of carbons in benzene

Particle/antiparticle	Up / down spin	Momentum vector	x	y	z
Electron	Up spin	u(1)	1.2116	-2.0985	0
		u(3)	-2.4231	0.0000	0
		u(5)	1.2116	2.0985	0
	Down spin	u*(2)	-2.4231	0.0000	0
		u*(4)	1.2116	2.0985	0
		u*(6)	1.2116	-2.0985	0
Hole	Up spin	v(1)	-1.2116	-2.0985	0
		v(3)	-1.2116	2.0985	0
		v(5)	2.4231	0.0000	0
	Down spin	v*(2)	-1.2116	-2.0985	0
		v*(4)	-1.2116	2.0985	0
		v*(6)	2.4231	0.0000	0

Table S2. Momentum vectors of fermions in benzene

Carbon number	X position	Y position	Z position
1	2.513	0.304	-1.24
2	1.258	0.159	-0.626
3	0.194	1.03	-0.918
4	-1.061	0.884	-0.304
5	-2.125	1.754	-0.596
6	-3.366	1.597	0.023
7	-3.56	0.568	0.939
8	-2.513	-0.304	1.24
9	-1.258	-0.159	0.626
10	-0.194	-1.03	0.918
11	1.61	-0.884	0.304
12	2.124	-1.754	0.596
13	3.366	-1.597	-0.023
14	3.56	-0.569	-0.94

Table S3. Position vector of carbons in anthracene

Particle/antiparticle	Up / down spin	Momentum vector	x	y	z
Electron	Up spin	u(1)	-1.452	-1.188	1.544
		u(11a)	2.305	-0.713	-0.327
		u(13)	-0.853	1.901	-1.217
		u(3)	-1.452	-1.189	1.544
		u(9a)	2.319	-0.725	-0.322
		u(11b)	-0.867	1.914	-1.222
		u(5)	-1.435	-1.186	1.535
		u(7)	2.302	-0.727	-0.313
	Down spin	u(9b)	-0.867	1.913	-1.222
		u*(2a)	2.302	-0.728	-0.314
		u*(14)	-1.436	-1.185	1.536
		u*(12)	-0.866	1.913	-1.222
		u*(4a)	2.319	-0.725	-0.322
		u*(2b)	-1.452	-1.189	1.544
		u*(10)	-0.867	1.914	-1.222
		u*(6)	2.305	-0.713	-0.327
Hole	Up spin	u*(4b)	-1.452	-1.188	1.544
		u*(8)	-0.853	1.901	-1.217
		v(1)	0.853	-1.901	1.217
		v(13)	-2.305	0.713	0.327
		v(11a)	1.452	1.188	-1.544
		v(3)	0.867	-1.914	1.222
		v(11b)	-2.319	0.725	0.322
		v(9a)	1.452	1.189	-1.544
	Down spin	v(5)	0.867	-1.913	1.222
		v(9b)	-2.302	0.727	0.313
		v(7)	1.435	1.186	-1.535
		v*(14)	-2.302	0.728	0.314
		v*(2a)	0.866	-1.913	1.222
		v*(12)	1.436	1.185	-1.536
		v*(2b)	-2.319	0.725	0.322
		v*(4a)	0.867	-1.914	1.222
v*(10)	1.452	1.189	-1.544		
v*(4b)	-2.305	0.713	0.327		
v*(6)	0.853	-1.901	1.217		
v*(8)	1.452	1.188	-1.544		

Table S4. Momentum vectors of fermions in anthracene

Carbon number	X position	Y position	Z position
1	-3.513	-0.007	-0.106
2	-2.814	-1.214	-0.1
3	-1.412	-1.228	-0.058
4	-0.693	-2.43	-0.051
5	0.704	-2.427	-0.009
6	1.418	-1.222	0.028
7	2.82	-1.202	0.07
8	3.513	0.007	0.106
9	2.814	1.214	0.1
10	1.412	1.228	0.058
11	0.693	2.43	0.051
12	-0.704	2.428	0.009
13	-1.418	1.222	-0.028
14	-2.82	1.203	-0.07
15	-0.708	-0.001	-0.021
16	0.708	0.001	0.021

Table S5. Position vector of carbons in pyrene

Particle/antiparticle	Up / down spin	Momentum vector	x	y	z	
Electron	Up spin	u(1)	2.101	-1.221	0.048	
		u(3a)	-0.006	2.45	0.03	
		u(13a)	-2.095	-1.229	-0.078	
		u(13b)	2.126	-1.221	0.049	
		u(16c)	-0.015	2.429	0.03	
		u(11)	-2.111	-1.208	-0.079	
		u(3b)	2.116	-1.199	0.049	
		u(5)	0.004	2.428	0.03	
		u(16a)	-2.12	-1.229	-0.079	
		u(16b)	2.112	-1.203	0.049	
		u(7)	-0.006	2.416	0.03	
		u(9)	-2.106	-1.213	-0.079	
		u*(2)	-0.006	2.417	0.03	
	u*(14)	2.112	-1.204	0.049		
	u*(15a)	-2.106	-1.213	-0.079		
	u*(15c)	0.004	2.429	0.03		
	u*(12)	2.116	-1.2	0.049		
	u*(10b)	-2.12	-1.229	-0.079		
	u*(4)	-0.015	2.429	0.03		
	u*(15b)	2.126	-1.221	0.049		
	u*(6a)	-2.111	-1.208	-0.079		
	u*(6b)	-0.006	2.45	0.03		
	u*(10a)	2.101	-1.221	0.048		
	u*(8)	-2.095	-1.229	-0.078		
		Down spin				

Table S6. Momentum vectors of particles in pyrene

Particle/antiparticle	Up / down spin	Momentum vector	x	y	z	
		v(1)	2.095	1.229	0.078	
		v(13a)	0.006	-2.45	-0.03	
		v(3a)	-2.101	1.221	-0.048	
		v(13b)	2.111	1.208	0.079	
		v(11)	0.015	-2.429	-0.03	
	Up spin	v(16a)	-2.126	1.221	-0.049	
		v(3b)	2.12	1.229	0.079	
		v(16b)	-0.004	-2.428	-0.03	
		v(5)	-2.116	1.199	-0.049	
		v(16c)	2.106	1.213	0.079	
		v(9)	0.006	-2.416	-0.03	
Hole		v(7)	-2.112	1.203	-0.049	
		v*(2)	0.006	-2.417	-0.03	
		v*(15a)	2.106	1.213	0.079	
		v*(14)	-2.112	1.204	-0.049	
		v*(12)	-0.004	-2.429	-0.03	
		v*(15b)	2.12	1.229	0.079	
		Down spin	v*(10a)	-2.116	1.2	-0.049
			v*(15c)	0.015	-2.429	-0.03
			v*(4)	2.111	1.208	0.079
			v*(6a)	-2.126	1.221	-0.049
			v*(10b)	0.006	-2.45	-0.03
			v*(6b)	2.095	1.229	0.078
		v*(8)	-2.101	1.221	-0.048	

Table S7. Momentum vectors of antiparticles in pyrene

Carbon number	X position	Y position	Z position
1	3.575	-0.022	0.005
2	2.75	1.099	0.001
3	1.351	0.971	0
4	0.556	2.12	-0.004
5	-0.833	2.027	-0.006
6	-1.468	0.782	-0.004
7	-2.872	0.723	-0.006
8	-3.541	-0.498	-0.004
9	-2.81	-1.677	0
10	-1.413	-1.631	0.002
11	-0.695	-0.408	0
12	0.743	-0.311	0.002
13	1.618	-1.428	0.006
14	3.009	-1.287	0.008

Table S8. Position vector of carbons in phenanthrene

Particle/antiparticle	Up / down spin	Momentum vector	x	y	z
Electron	Up spin	u(1)	-2.224	0.993	-0.005
		u(3a)	0.267	-2.399	0.006
		u(13)	1.957	1.406	-0.001
		u(3b)	-2.184	1.056	-0.006
		u(5)	0.138	-2.435	0.006
		u(11a)	2.046	1.379	0
		u(11b)	-2.177	1.131	-0.006
	Down spin	u(7)	0.062	-2.4	0.006
		u(9)	2.115	1.269	0
		u*(2)	0.259	-2.386	0.007
		u*(14)	-2.266	0.976	-0.006
		u*(12a)	2.007	1.41	-0.001
		u*(4)	0.187	-2.431	0.006
		u*(12b)	-2.211	1.093	-0.006
Hole	Up spin	u*(6a)	2.024	1.338	0
		u*(6b)	0.055	-2.413	0.006
		u*(10)	-2.128	1.133	-0.006
		u*(8)	2.073	1.28	0
		v(1)	-1.957	-1.406	0.001
		v(13)	-0.267	2.399	-0.006
		v(3a)	2.224	-0.993	0.005
	Down spin	v(3b)	-2.046	-1.379	0
		v(11a)	-0.138	2.435	-0.006
		v(5)	2.184	-1.056	0.006
		v(11b)	-2.115	-1.269	0
		v(9)	-0.062	2.4	-0.006
		v(7)	2.177	-1.131	0.006
		v*(14)	-0.259	2.386	-0.007
Down spin	v*(2)	-2.007	-1.41	0.001	
	v*(12a)	2.266	-0.976	0.006	
	v*(12b)	-0.187	2.431	-0.006	
	v*(4)	-2.024	-1.338	0	
	v*(6)	2.211	-1.093	0.006	
	v*(10)	-0.055	2.413	-0.006	
	v*(6)	-2.073	-1.28	0	
	v*(8)	2.128	-1.133	0.006	

Table S9. Momentum vectors of fermions in phenanthrene

Carbon number	X position	Y position	Z position
1	3.921	0.58	0.032
2	2.515	0.566	0.04
3	1.822	1.765	0.168
4	0.429	1.787	0.18
5	-0.35	0.617	0.065
6	-1.797	0.647	0.078
7	-2.581	1.826	0.204
8	-3.98	1.803	0.211
9	-4.651	0.597	0.093
10	-3.921	-0.58	-0.032
11	-2.515	-0.566	-0.041
12	-1.823	-1.766	-0.168
13	-0.429	-1.787	-0.18
14	0.35	-0.617	-0.065
15	1.797	-0.647	-0.078
16	2.581	-1.826	-0.204
17	3.98	-1.803	-0.211
18	4.651	-0.597	-0.093

Table S1. Position vector of carbons in chrysene

Particle/antiparticle	Up / down spin	Momentum vector	x	y	z
Electron	Up spin	u(1)	-2.124	-1.227	-0.11
		u(15a)	2.183	-1.156	-0.133
		u(17)	-0.059	2.383	0.243
		u(3)	-2.172	-1.148	-0.103
		u(5a)	2.147	-1.264	-0.143
		u(15b)	0.025	2.412	0.246
		u(5b)	-2.165	-1.183	-0.106
		u(11a)	2.086	-1.221	-0.139
		u(13)	0.079	2.404	0.245
		u(7)	-2.07	-1.229	-0.111
		u(9)	2.136	-1.163	-0.134
		u(11b)	-0.066	2.392	0.245
	Down spin	u*(2a)	2.136	-1.163	-0.133
		u*(18)	-2.07	-1.229	-0.111
		u*(16)	-0.066	2.392	0.244
		u*(4)	2.086	-1.221	-0.14
		u*(2b)	-2.165	-1.183	-0.105
		u*(14a)	0.079	2.404	0.245
		u*(6a)	2.147	-1.264	-0.143
		u*(14b)	-2.173	-1.149	-0.103
		u*(12)	0.026	2.413	0.246
		u*(8)	2.183	-1.156	-0.133
		u*(6b)	-2.124	-1.227	-0.11
		u*(10)	-0.059	2.383	0.243

Table S2. Momentum vectors of particles in chrysene

Particle/antiparticle	Up / down spin	Momentum vector	x	y	z
Hole	Up spin	v(1)	0.059	-2.383	-0.243
		v(17)	-2.183	1.156	0.133
		v(15a)	2.124	1.227	0.11
		v(3)	-0.025	-2.412	-0.246
		v(15b)	-2.147	1.264	0.143
		v(5a)	2.172	1.148	0.103
		v(5b)	-0.079	-2.404	-0.245
		v(13)	-2.086	1.221	0.139
		v(11a)	2.165	1.183	0.106
		v(7)	0.066	-2.392	-0.245
		v(11b)	-2.136	1.163	0.134
		v(9)	2.07	1.229	0.111
		v*(18)	-2.136	1.163	0.133
		v*(2a)	0.066	-2.392	-0.244
	Down spin	v*(16)	2.07	1.229	0.111
		v*(2b)	-2.086	1.221	0.14
		v*(4)	-0.079	-2.404	-0.245
		v*(14a)	2.165	1.183	0.105
		v*(14b)	-2.147	1.264	0.143
		v*(6a)	-0.026	-2.413	-0.246
		v*(12)	2.173	1.149	0.103
		v*(6b)	-2.183	1.156	0.133
		v*(8)	0.059	-2.383	-0.243
		v*(10)	2.124	1.227	0.11

Table S3. Momentum vectors of antiparticles in chrysene

Carbon number	X position	Y position	Z position
1	0.686	-3.685	0.015
2	1.416	-2.453	0.008
3	2.848	-2.437	0.007
4	3.534	-1.249	0.002
5	2.833	0	-0.004
6	3.534	1.247	-0.006
7	2.849	2.436	-0.012
8	1.417	2.453	-0.018
9	0.686	3.684	-0.021
10	-0.686	3.685	-0.024
11	-1.417	2.453	-0.021
12	-2.849	2.436	-0.018
13	-3.534	1.248	-0.008
14	-2.833	-0.001	-0.003
15	-3.534	-1.249	0.008
16	-2.848	-2.437	0.017
17	-1.416	-2.454	0.013
18	-0.685	-3.685	0.019
19	0.716	-1.24	-0.001
20	1.432	0	-0.008
21	0.716	1.24	-0.016
22	-0.716	1.24	-0.017
23	-1.432	0	-0.008
24	-0.716	-1.24	0.001

Table S4. Position vector of carbons in coronene

Particle/antiparticle	Up / down spin	Momentum vector	x	y	z
Electron	Up spin	u(1)	0.03	2.445	-0.016
		u(19a)	-2.132	-1.214	0.014
		u(17a)	2.102	-1.231	0.002
		u(3)	-0.015	2.437	-0.011
		u(5a)	-2.117	-1.24	0.003
		u(19b)	2.132	-1.197	0.008
		u(7b)	-0.016	2.454	-0.021
		u(23a)	-2.102	-1.249	0.016
		u(15)	2.118	-1.205	0.005
		u(19c)	0	2.48	-0.015
		u(21a)	-2.148	-1.24	0.008
		u(23b)	2.148	-1.24	0.007
		u(5b)	0.016	2.436	-0.008
		u(7)	-2.133	-1.196	-0.004
		u(21b)	2.117	-1.24	0.012
		u(23c)	0.015	2.453	-0.013
		u(11a)	-2.117	-1.205	0.013
		u(13)	2.102	-1.248	0
		u(21c)	-0.03	2.444	-0.005
		u(9)	-2.103	-1.231	0
		u(11b)	2.133	-1.213	0.005
	u*(2a)	-2.101	-1.232	0.011	
	u*(18)	-0.031	2.445	-0.018	
	u*(24a)	2.132	-1.213	0.007	
	u*(4)	-2.118	-1.204	0.006	
	u*(2b)	0.016	2.453	-0.016	
	u*(20a)	2.102	-1.249	0.01	
	u*(24b)	-2.132	-1.197	0.016	
	u*(16)	0.015	2.436	-0.02	
	u*(14a)	2.117	-1.239	0.004	
	u*(20b)	-2.148	-1.24	0.009	
	u*(24c)	0	2.48	-0.018	
	u*(22a)	2.148	-1.24	0.009	
	u*(6)	-2.102	-1.247	-0.002	
	u*(20c)	-0.015	2.453	-0.01	
	u*(8a)	2.117	-1.206	0.012	
	u*(22b)	-2.117	-1.241	0.014	
	u*(14b)	-0.016	2.437	-0.015	
	u*(12)	2.133	-1.196	0.001	
	u*(8b)	-2.133	-1.213	0.001	
	u*(22c)	0.03	2.445	-0.007	
	u*(10)	2.103	-1.232	0.006	
	Down spin				

Table S5. Momentum vectors of particles in coronene

Particle/antiparticle	Up / down spin	Momentum vector	x	y	z
		v(1)	-2.102	1.231	-0.002
		v(17)	2.132	1.214	-0.014
		v(19a)	-0.03	-2.445	0.016
		v(3)	-2.132	1.197	-0.008
		v(19b)	2.117	1.24	-0.003
		v(5a)	0.015	-2.437	0.011
		v(17b)	-2.118	1.205	-0.005
		v(15)	2.102	1.249	-0.016
		v(23a)	0.016	-2.454	0.021
		v(19c)	-2.148	1.24	-0.007
	Up spin	v(23b)	2.148	1.24	-0.008
		v(21a)	0	-2.48	0.015
		v(5b)	-2.117	1.24	-0.012
		v(21b)	2.133	1.196	0.004
		v(7)	-0.016	-2.436	0.008
		v(23c)	-2.102	1.248	0
		v(13)	2.117	1.205	-0.013
		v(11a)	-0.015	-2.453	0.013
		v(121c)	-2.133	1.213	-0.005
		v(11b)	2.103	1.231	0
Hole		v(9)	0.03	-2.444	0.005
		v*(18)	2.101	1.232	-0.011
		v*(2a)	-2.132	1.213	-0.007
		v*(24a)	0.031	-2.445	0.018
		v*(2b)	2.118	1.204	-0.006
		v*(4)	-2.102	1.249	-0.01
		v*(20a)	-0.016	-2.453	0.016
		v*(16)	2.132	1.197	-0.016
		v*(24b)	-2.117	1.239	-0.004
		v*(14a)	-0.015	-2.436	0.02
		v*(24c)	2.148	1.24	-0.009
	Down spin	v*(20b)	-2.148	1.24	-0.009
		v*(22a)	0	-2.48	0.018
		v*(20c)	2.102	1.247	0.002
		v*(6)	-2.117	1.206	-0.012
		v*(8a)	0.015	-2.453	0.01
		v*(14b)	2.117	1.241	-0.014
		v*(22b)	-2.133	1.196	-0.001
		v*(12)	0.016	-2.437	0.015
		v*(22c)	2.133	1.213	-0.001
		v*(8)	-2.103	1.232	-0.006
		v*(10)	-0.03	-2.445	0.007

Table S6. Momentum vectors of antiparticles in coronene

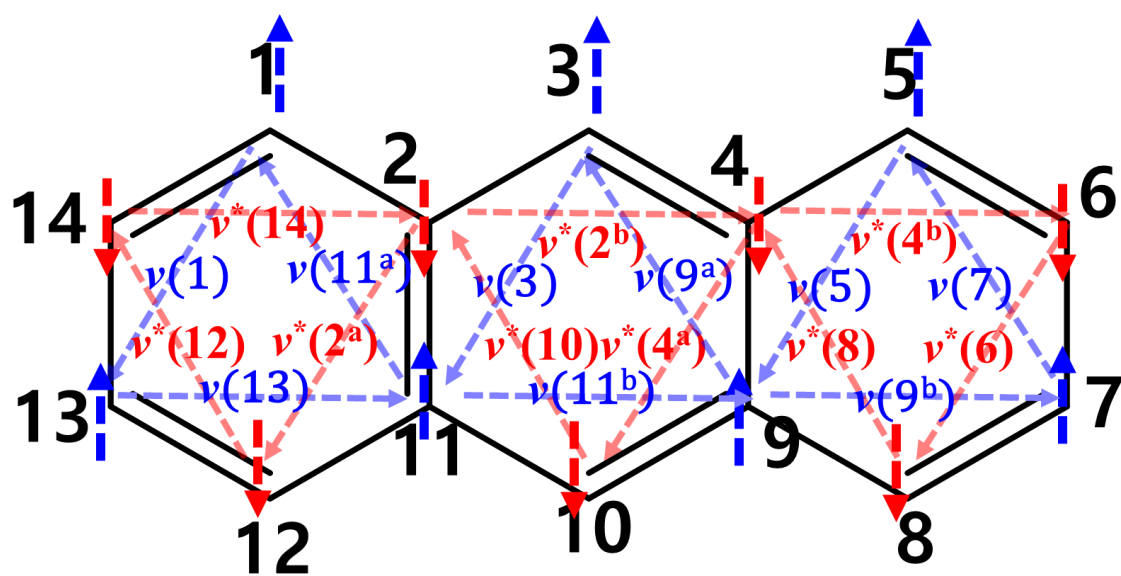


Figure S1. Momentum vectors of antiparticle fermions in anthracene

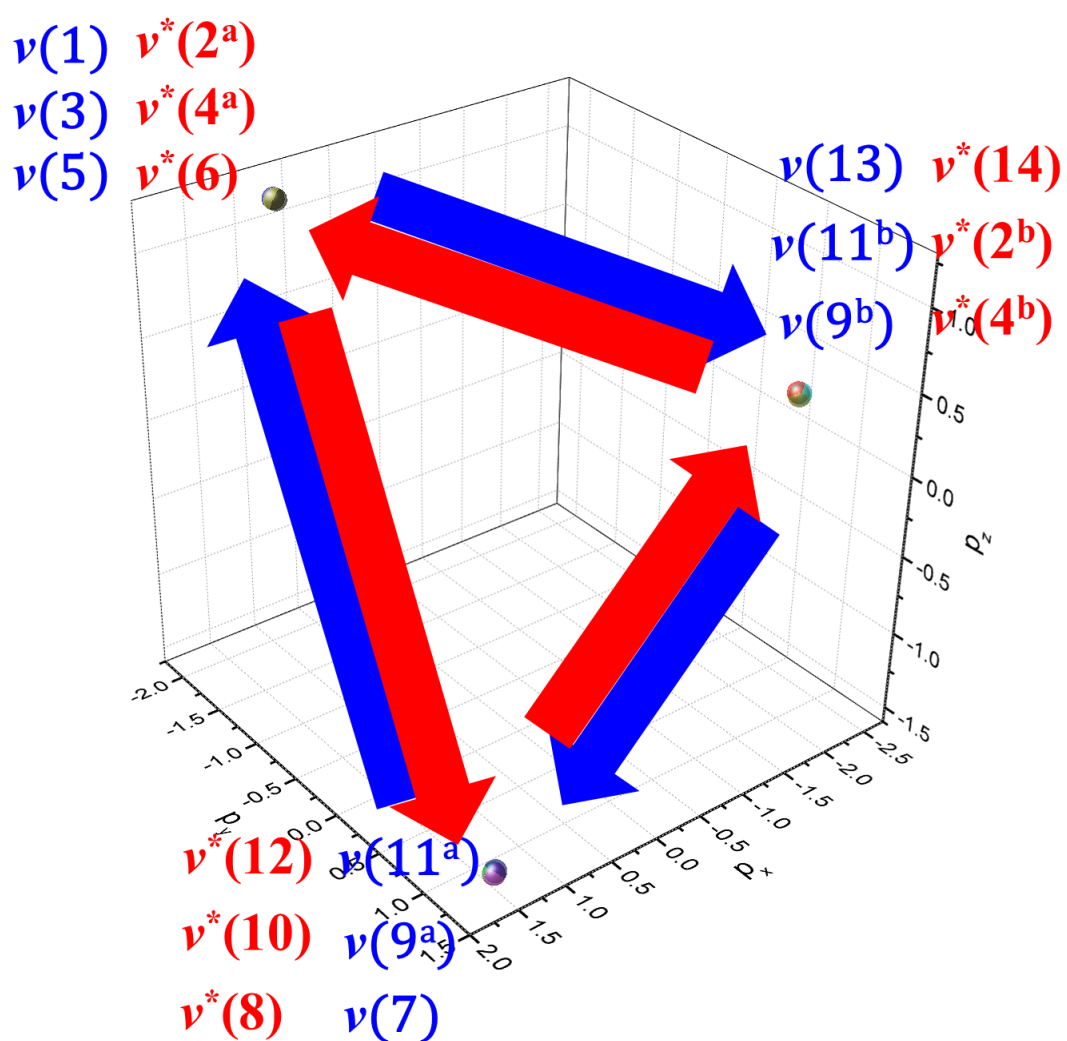


Figure S2. Momentum space of antiparticle fermions in anthracene

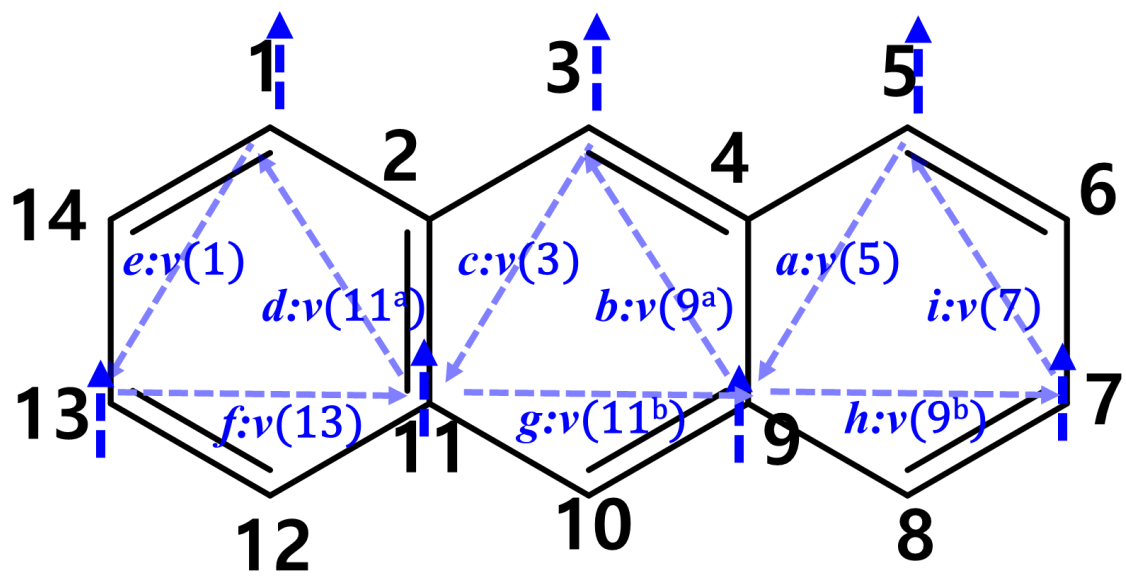


Figure S3. Momentum vector for global NNN hopping of up spin antiparticle of anthracene

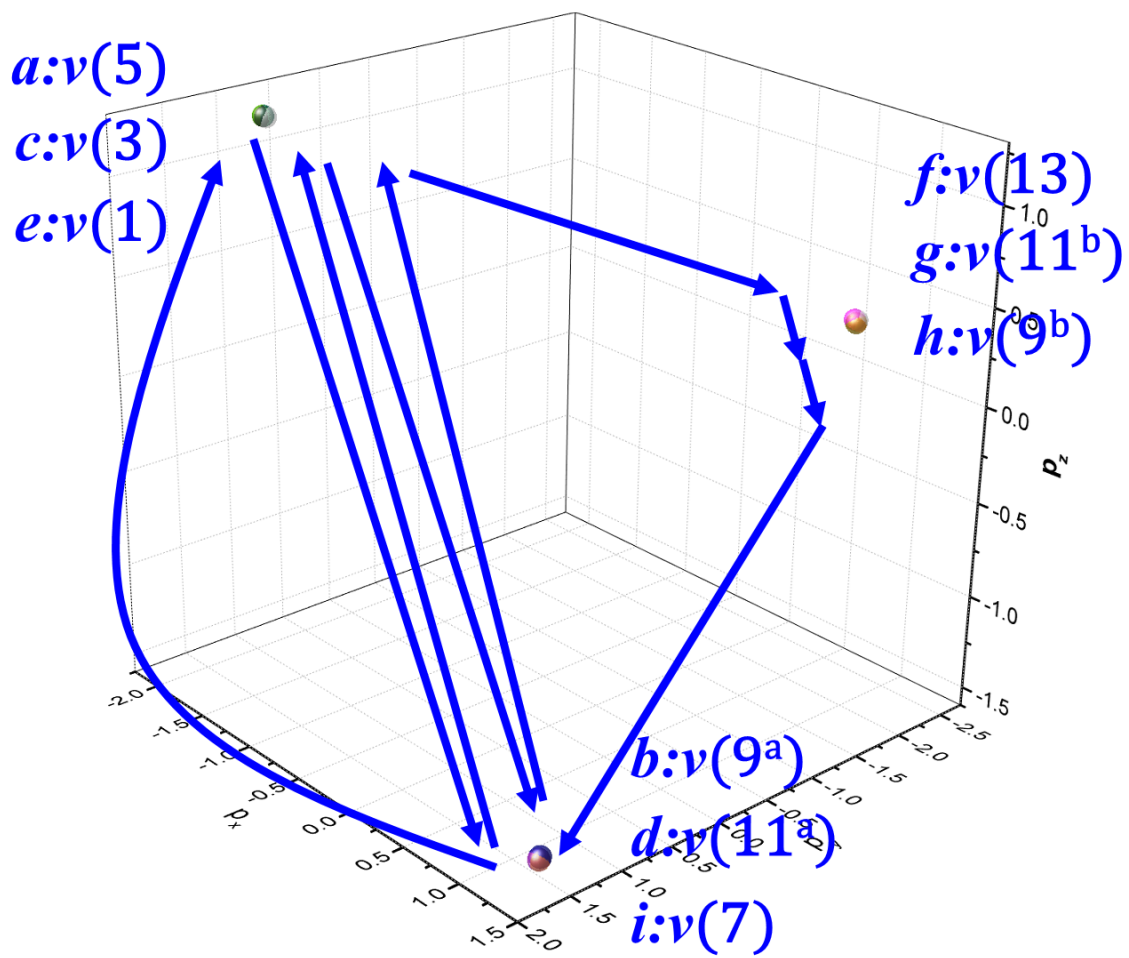


Figure S4. Momentum space for global NNN hopping of up spin antiparticle of anthracene

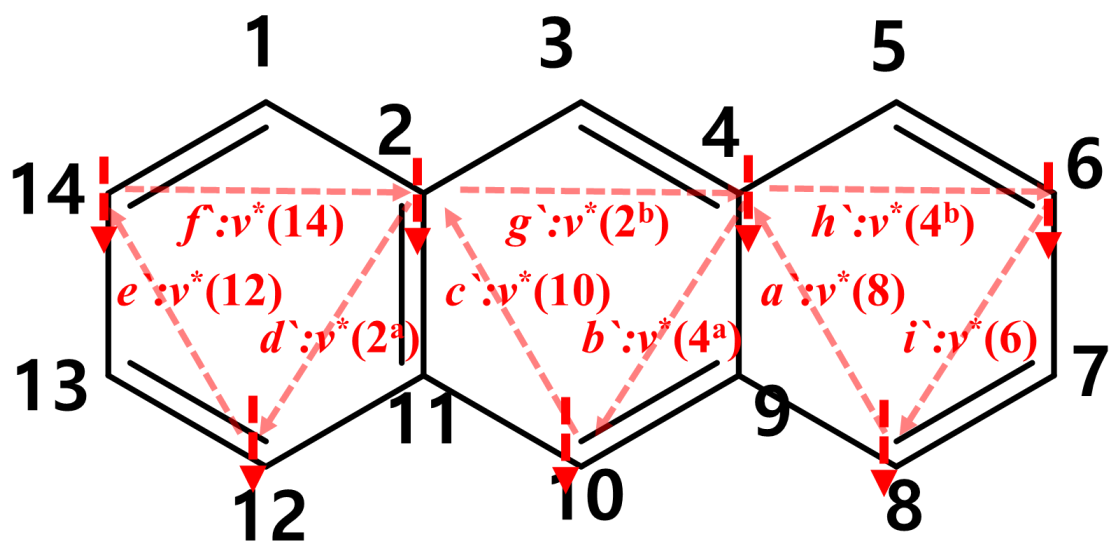


Figure S5. Momentum vector for global NNN hopping of down spin antiparticle of anthracene

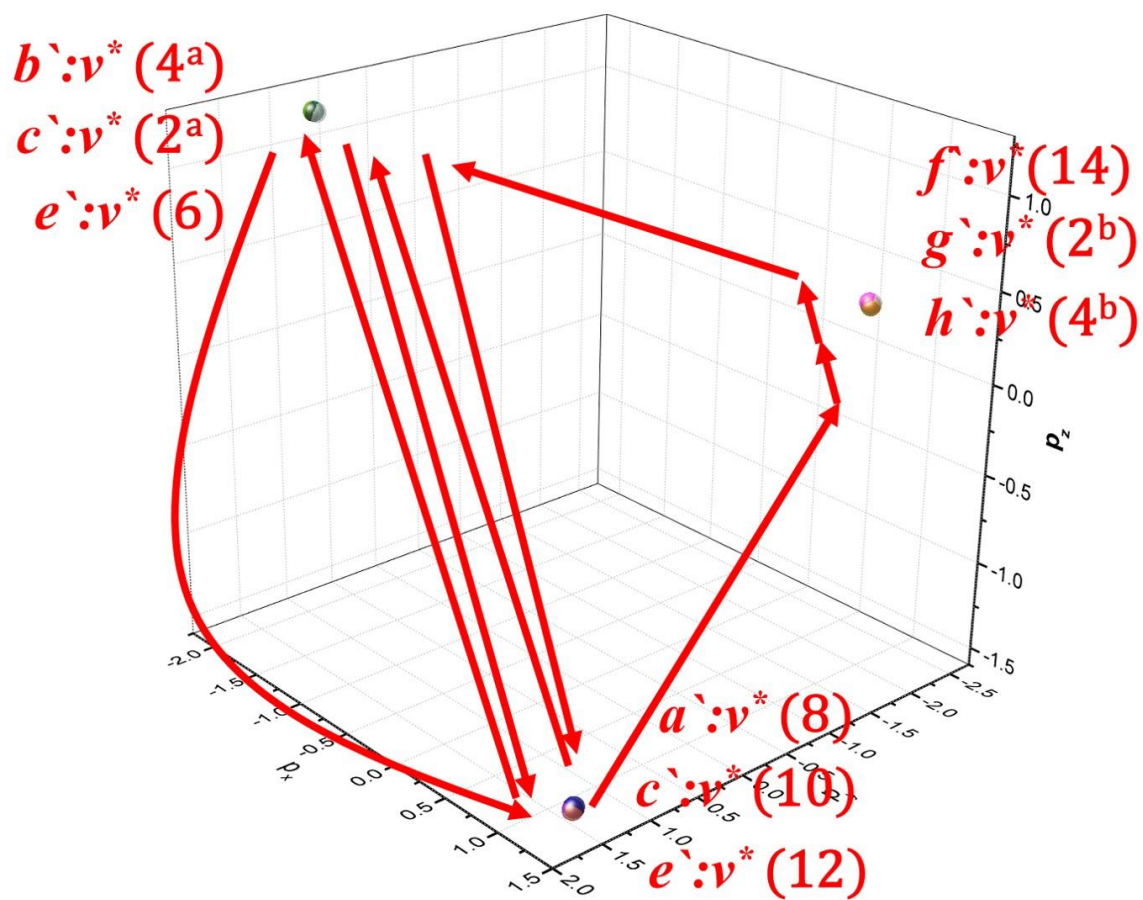


Figure S6. Momentum space for global NNN hopping of down spin antiparticle of anthracene

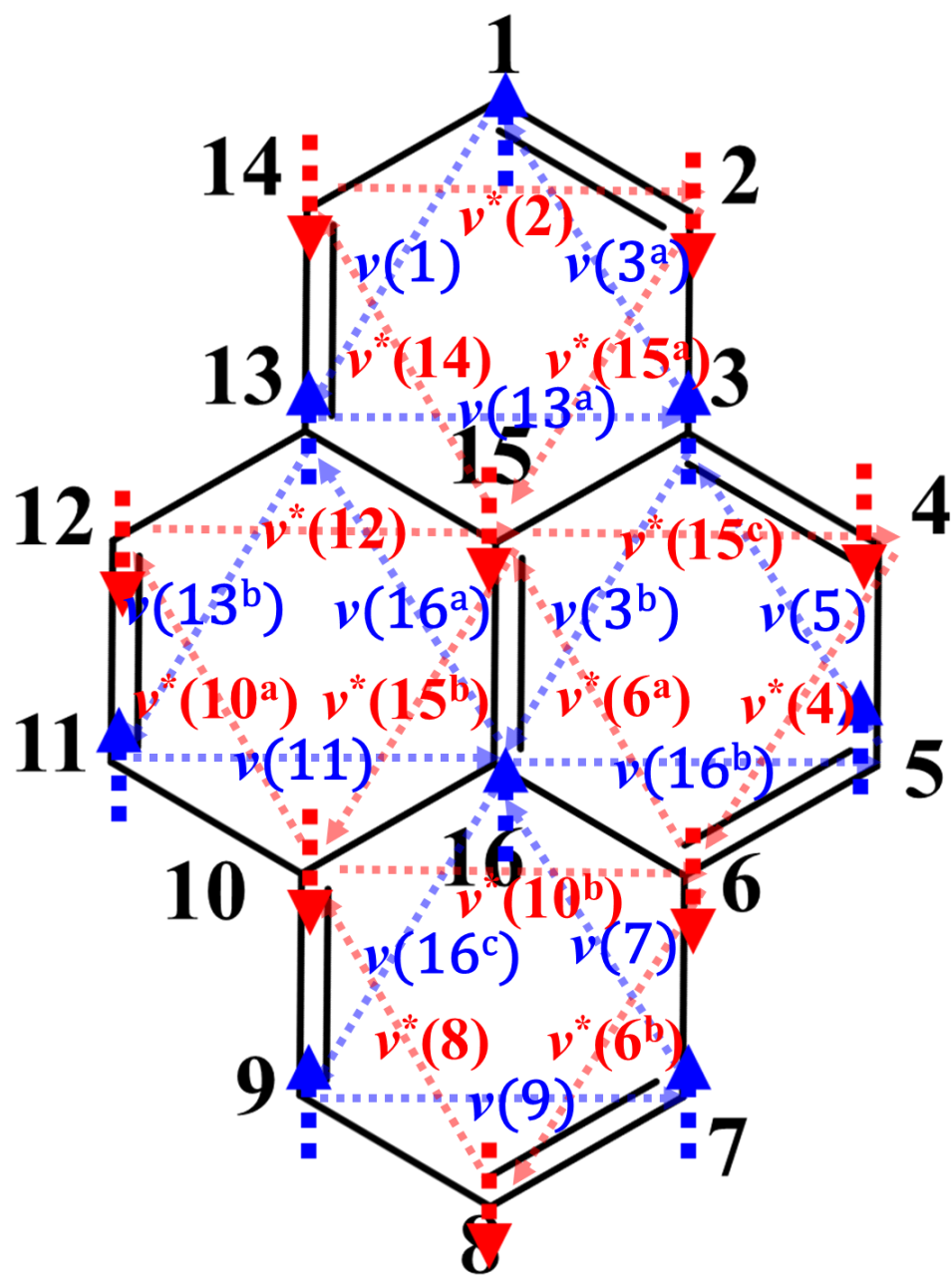


Figure S7. Momentum vectors of antiparticle fermions in pyrene.

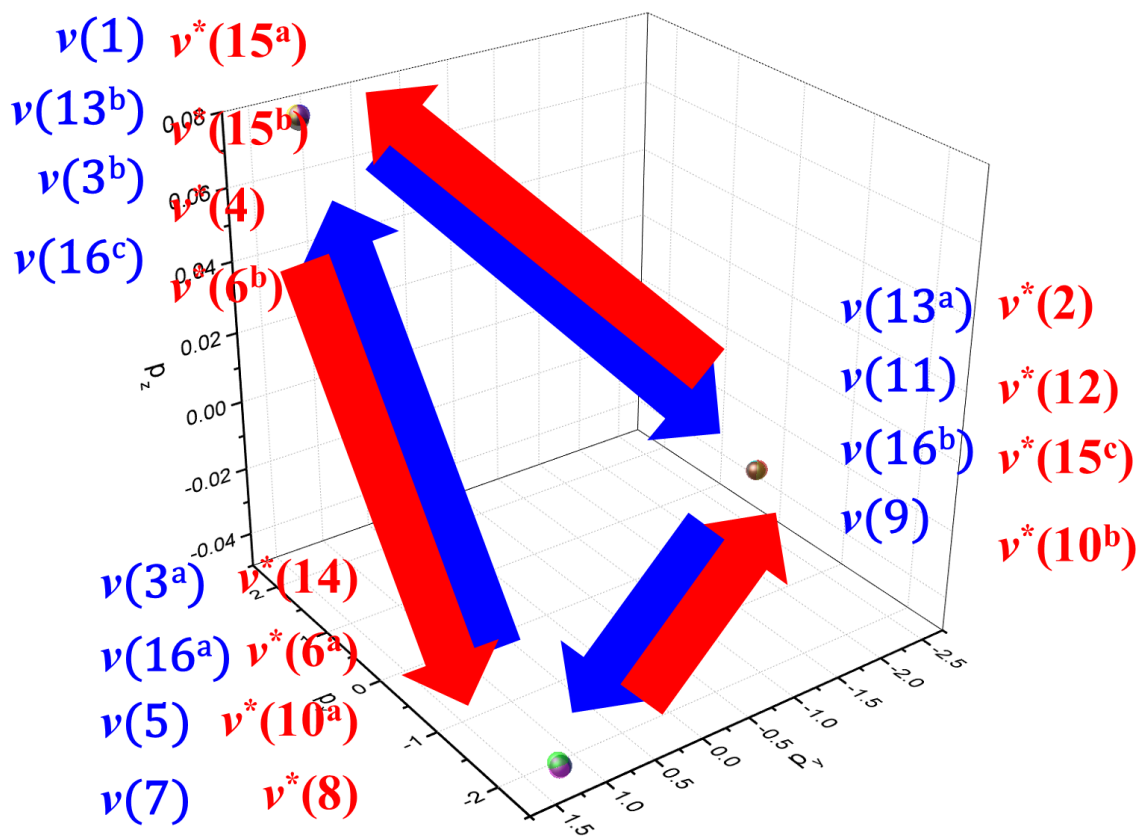


Figure S8. Momentum space of antiparticle fermions in pyrene

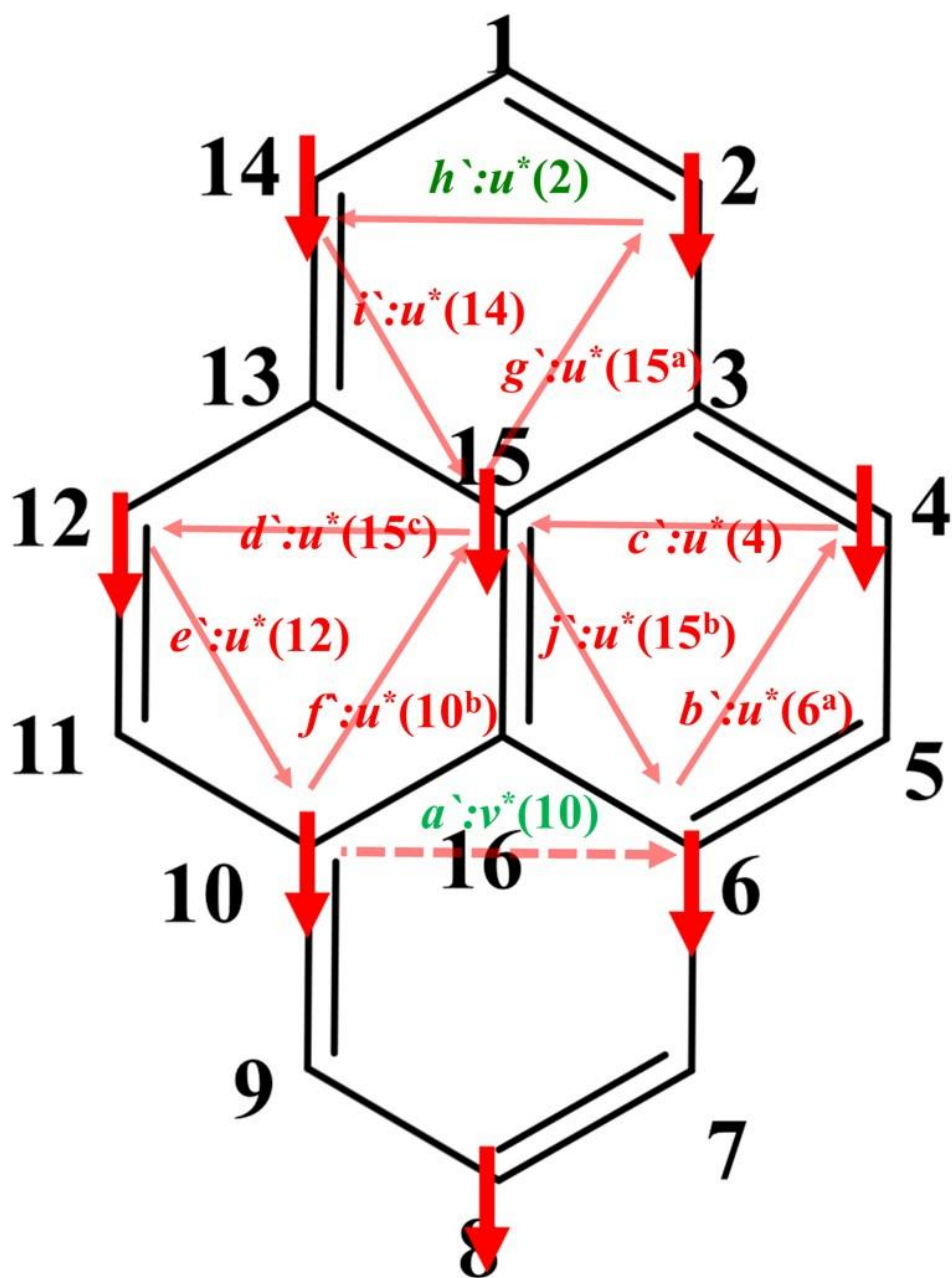


Figure S9. Momentum vector for global NNN hopping of down spin particle of pyrene

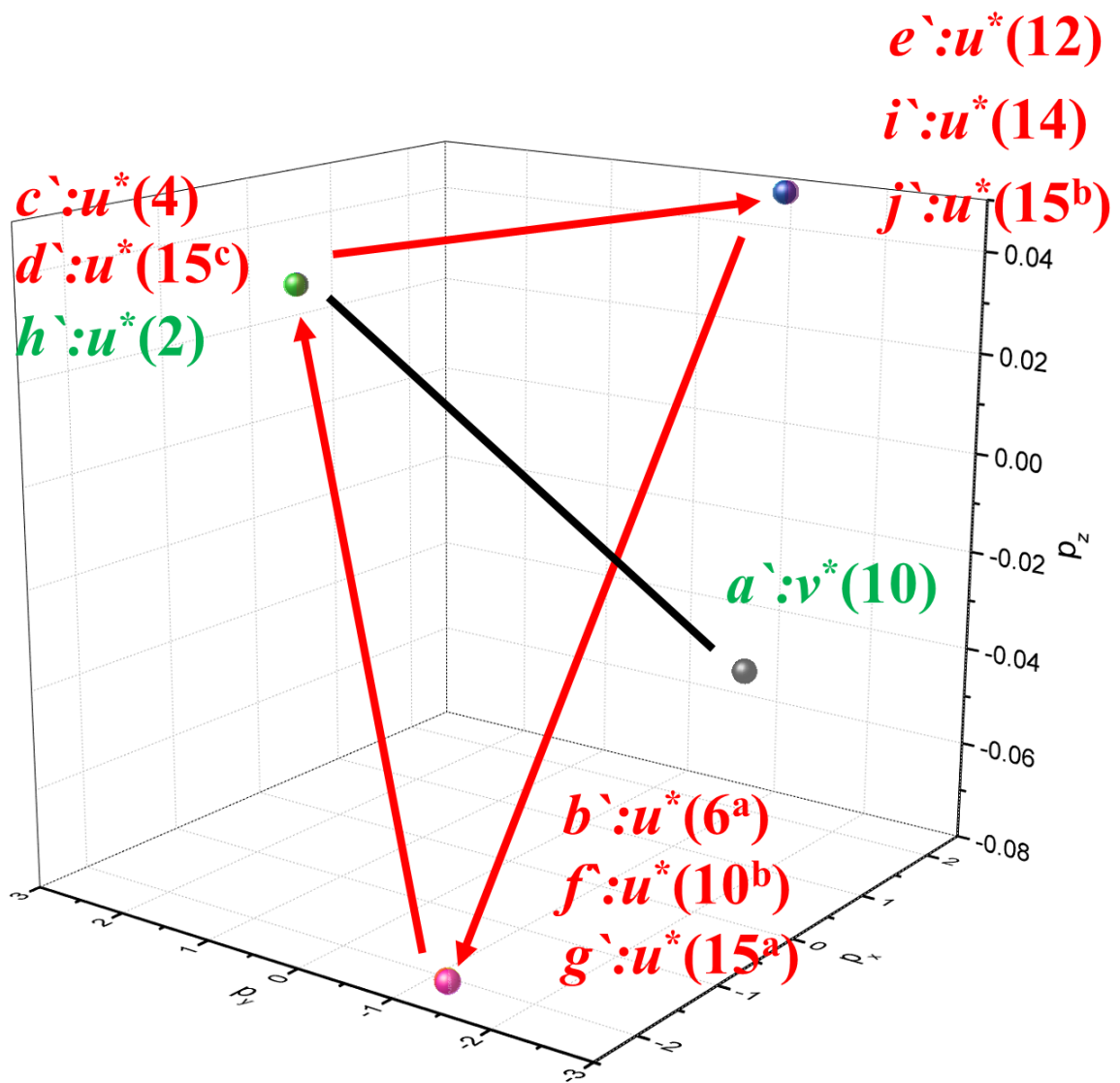


Figure S10. Momentum space for global NNN hopping of down spin particle of pyrene.

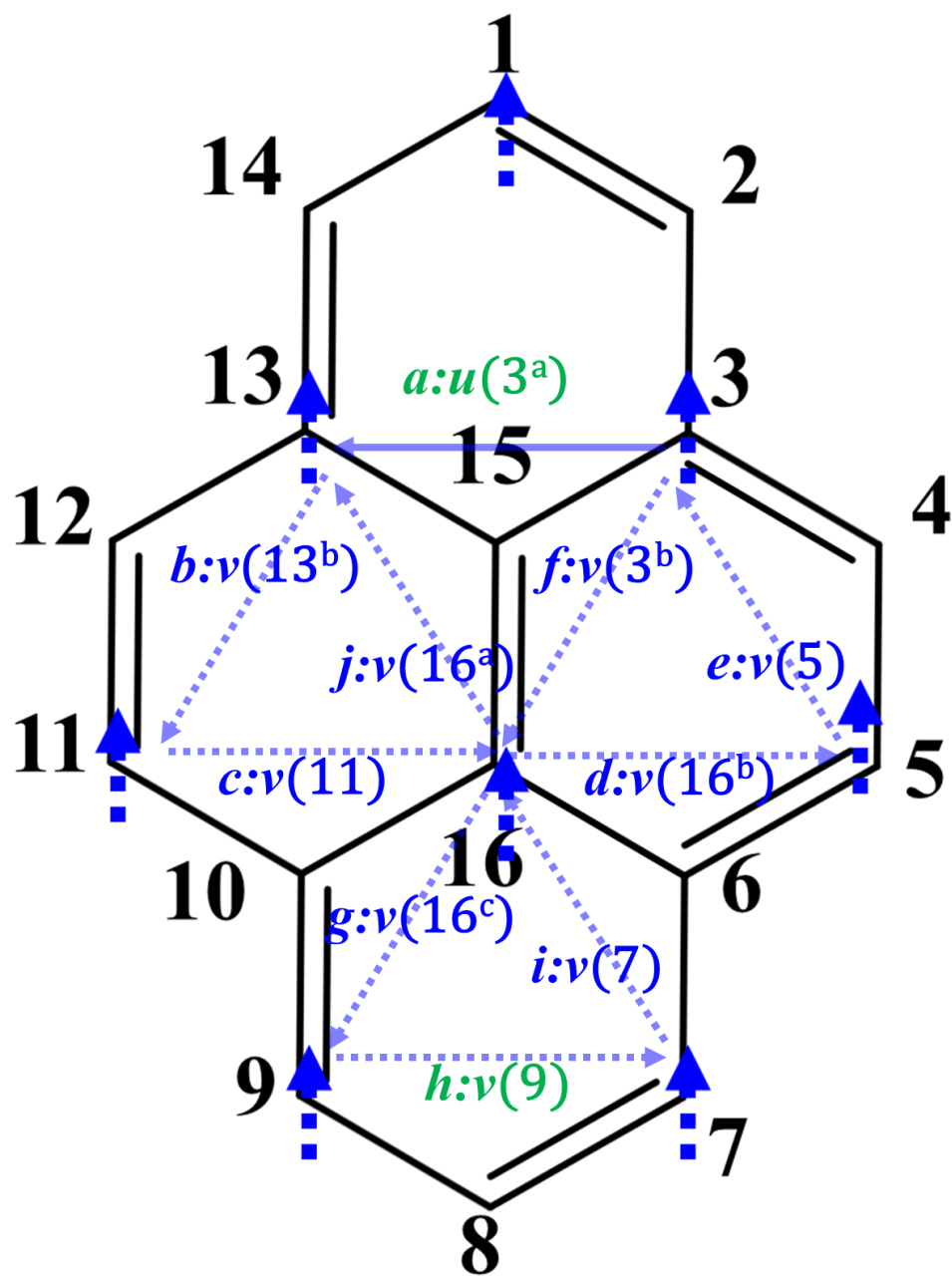


Figure S11. Momentum vector for global NNN hopping of up spin antiparticle of pyrene

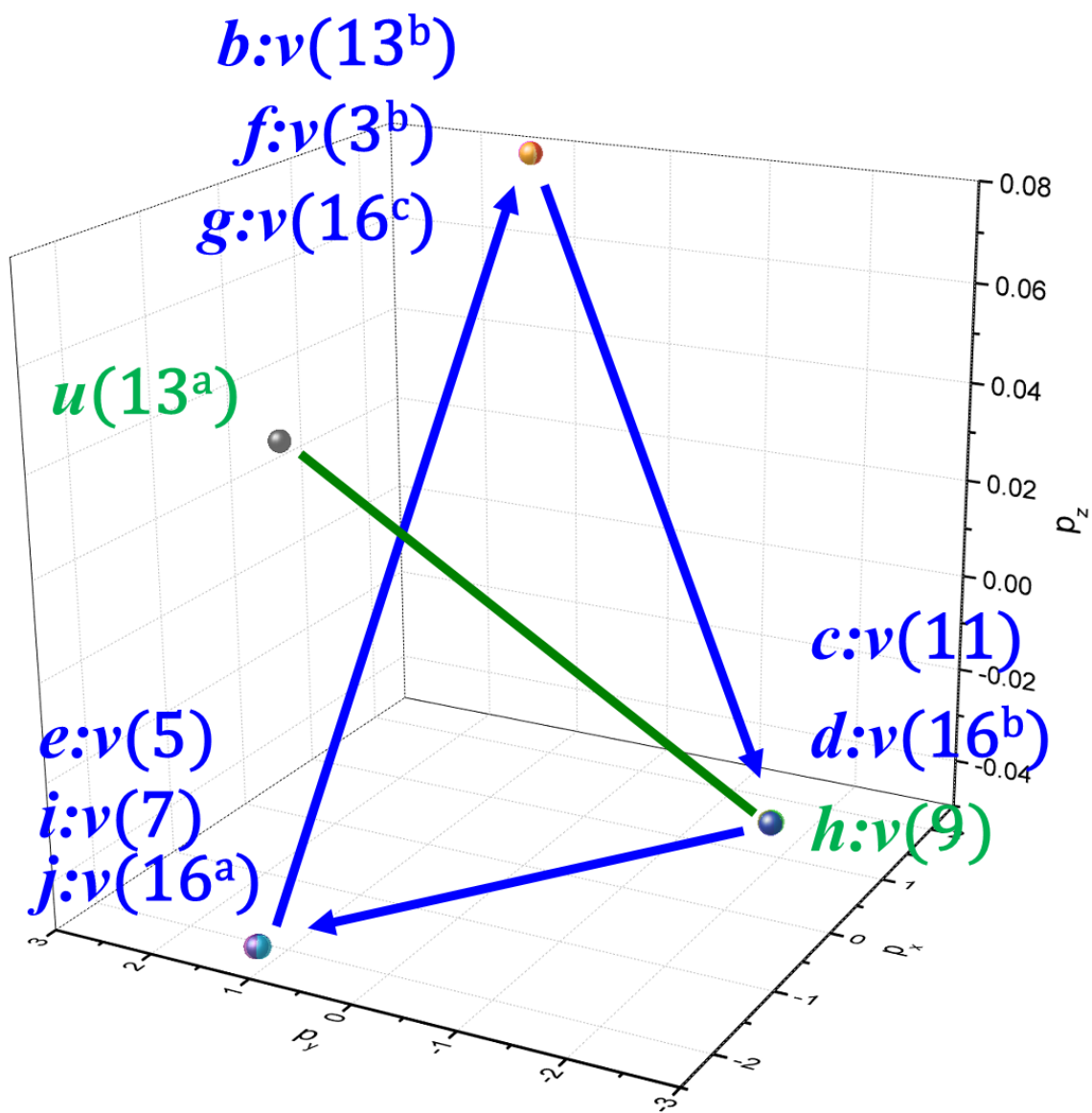


Figure S1. Momentum space for global NNN hopping of up spin antiparticle of pyrene

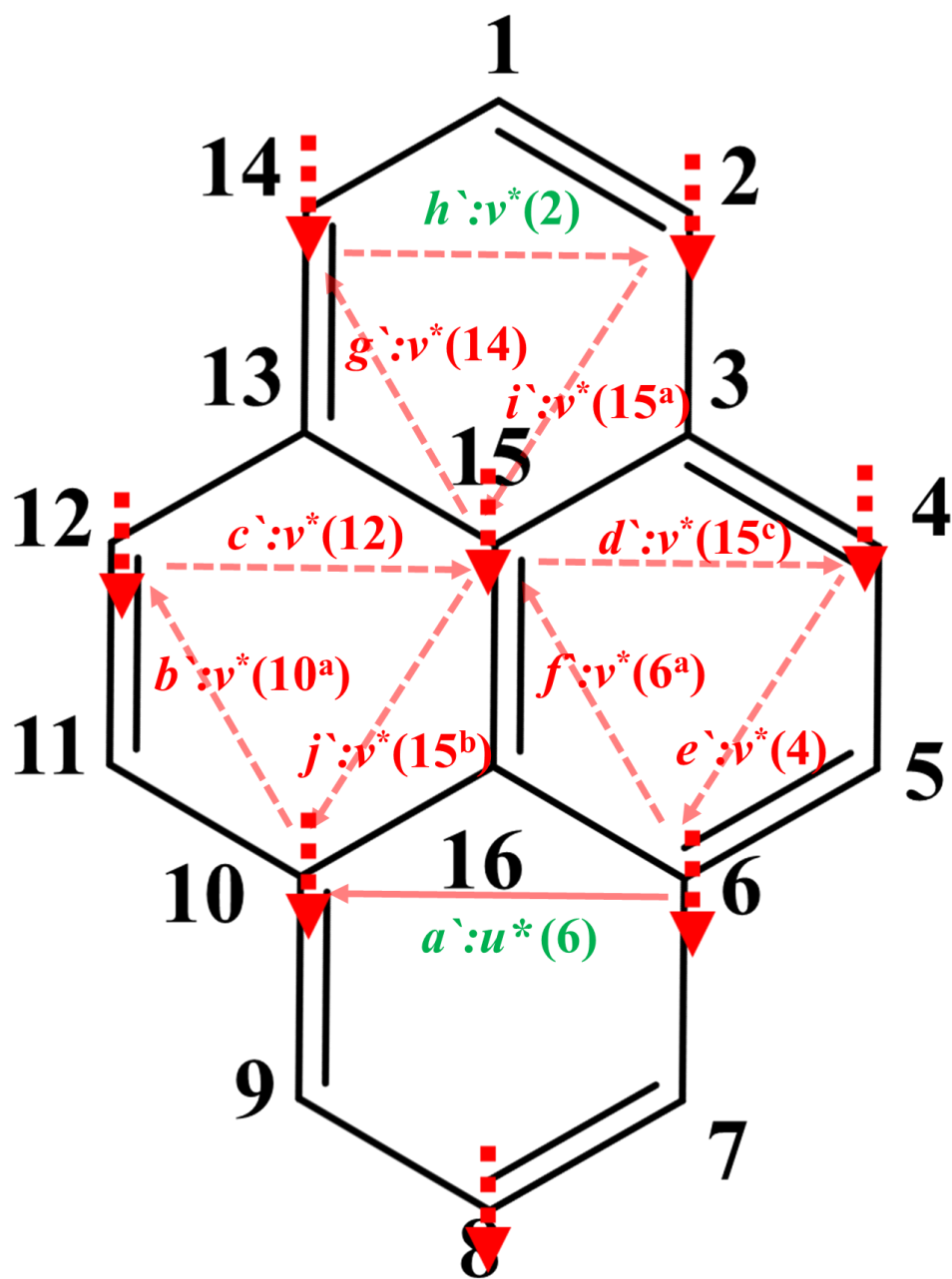


Figure S13. Momentum vector for global NNN hopping of down spin antiparticle of pyrene

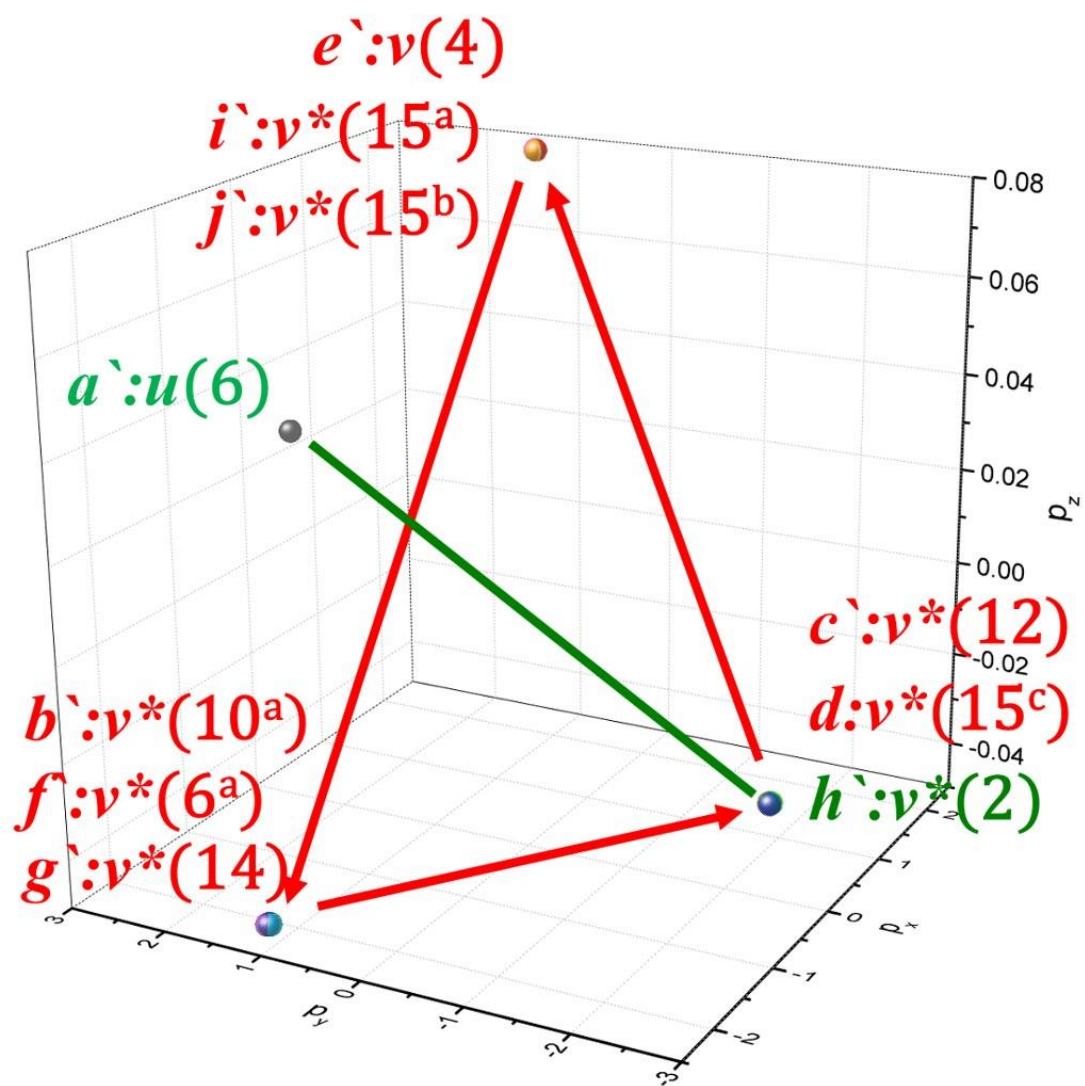


Figure S14. Momentum space for global NNN hopping of down spin antiparticle of pyrene

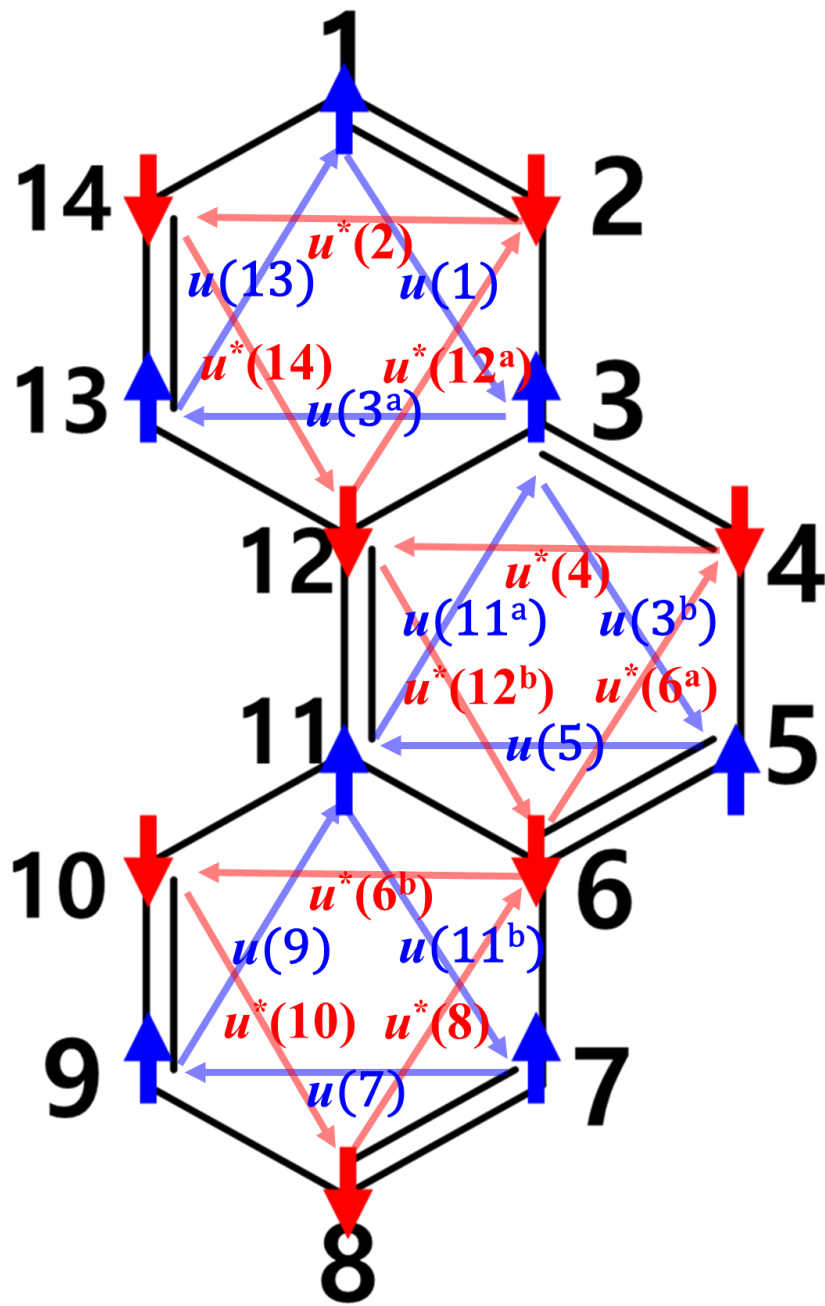


Figure S15. Momentum vectors of particle fermions in phenanthrene

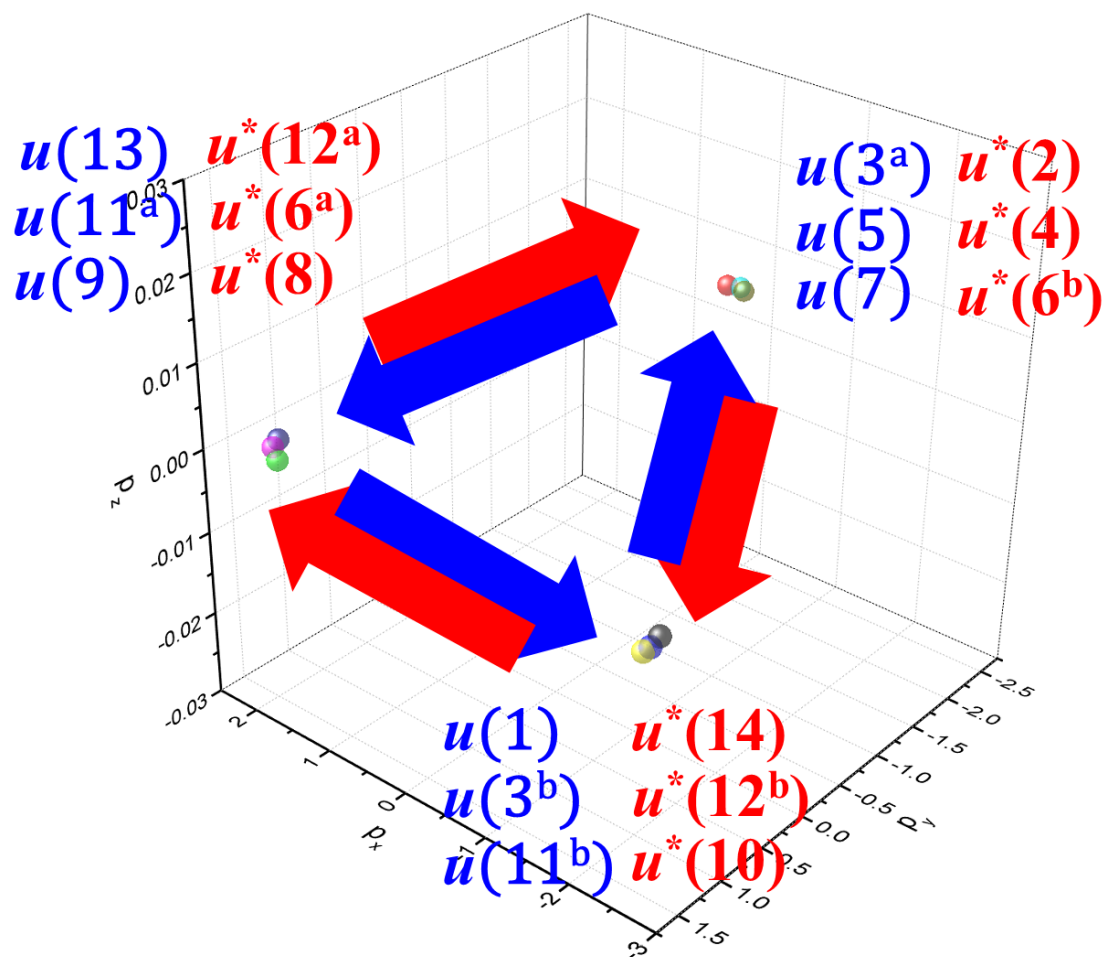


Figure S16. Momentum space of particle fermions in phenanthrene

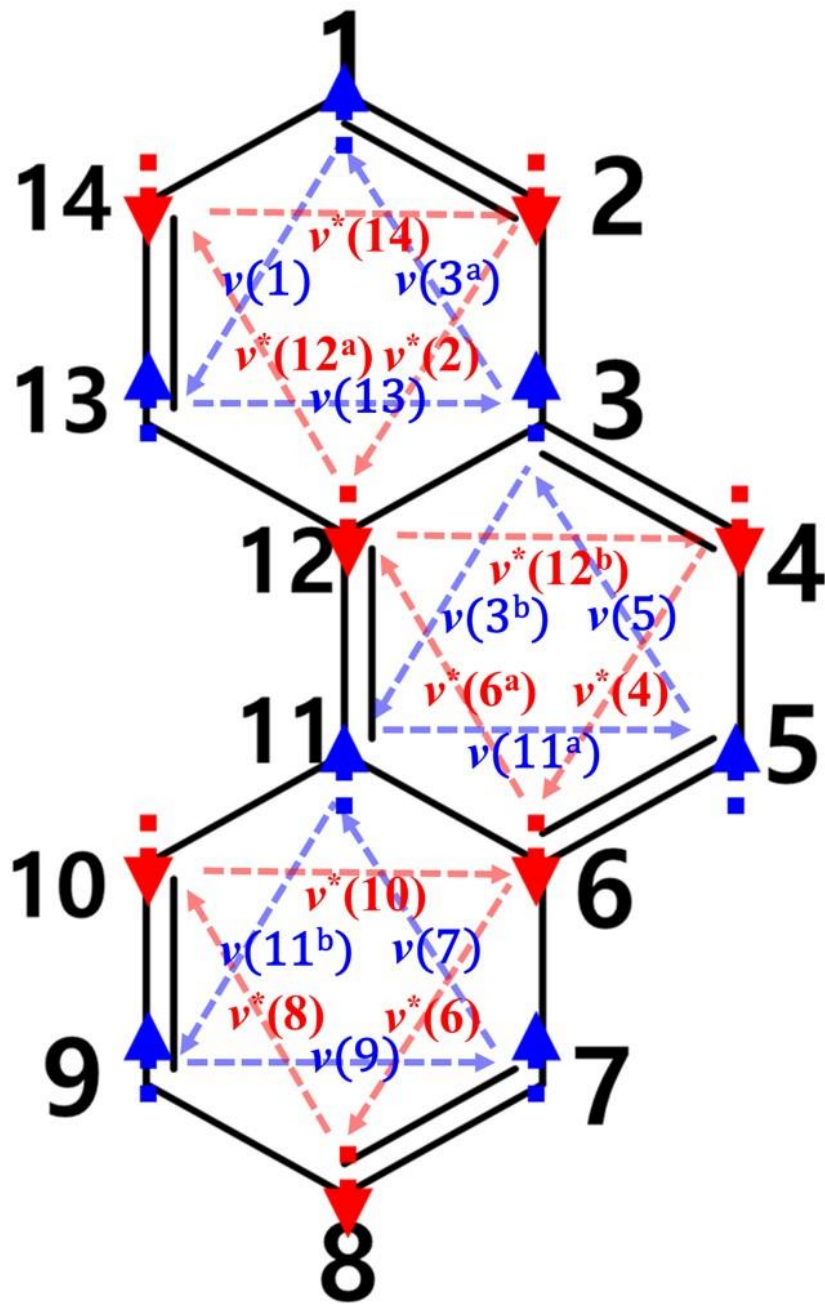


Figure S17. Momentum vectors of antiparticle fermions in phenanthrene

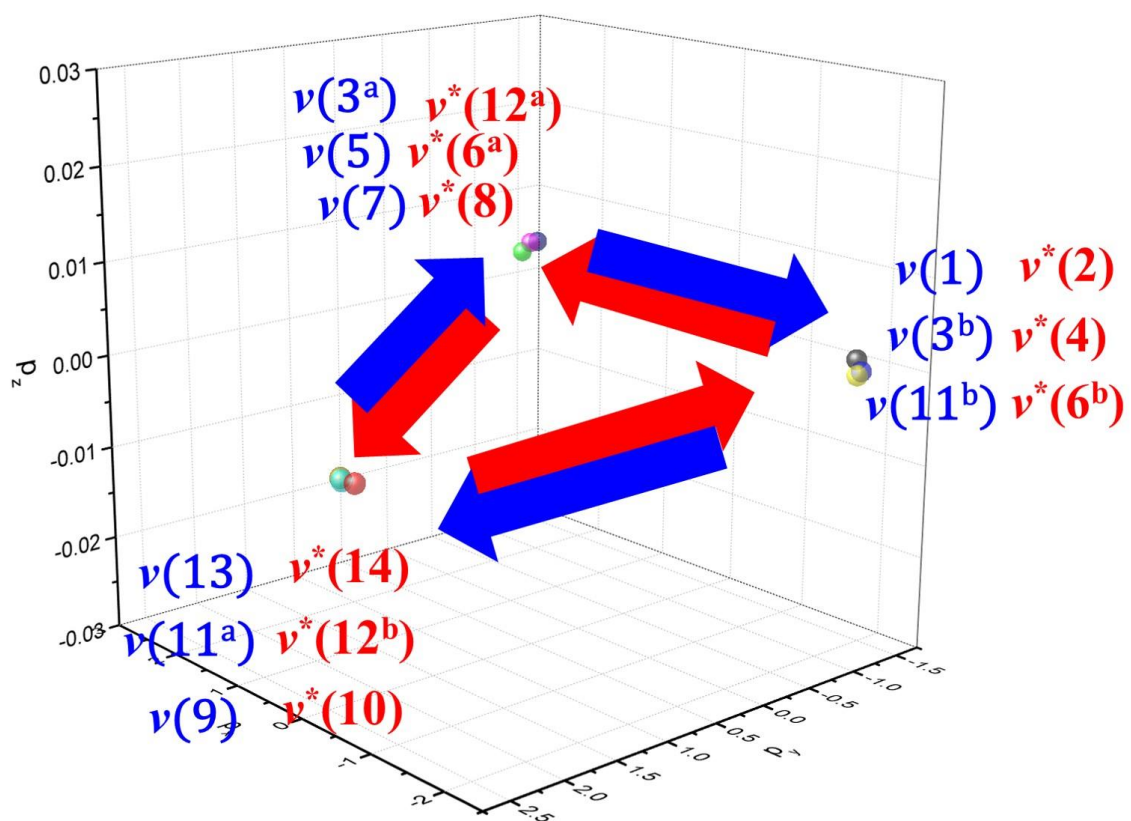


Figure S18. Momentum space of antiparticle fermions in phenanthrene

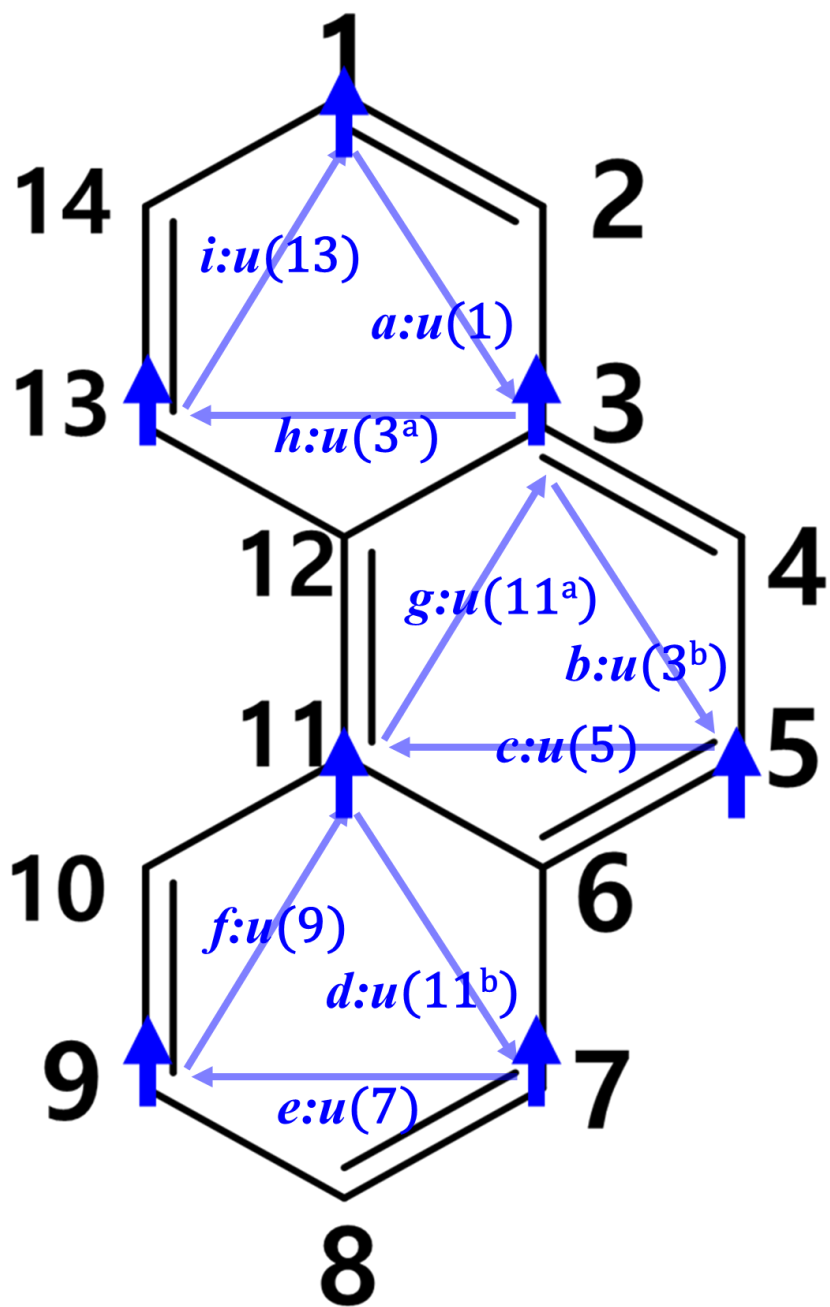


Figure S19. Momentum vector for global NNN hopping of up spin particle of phenanthrene

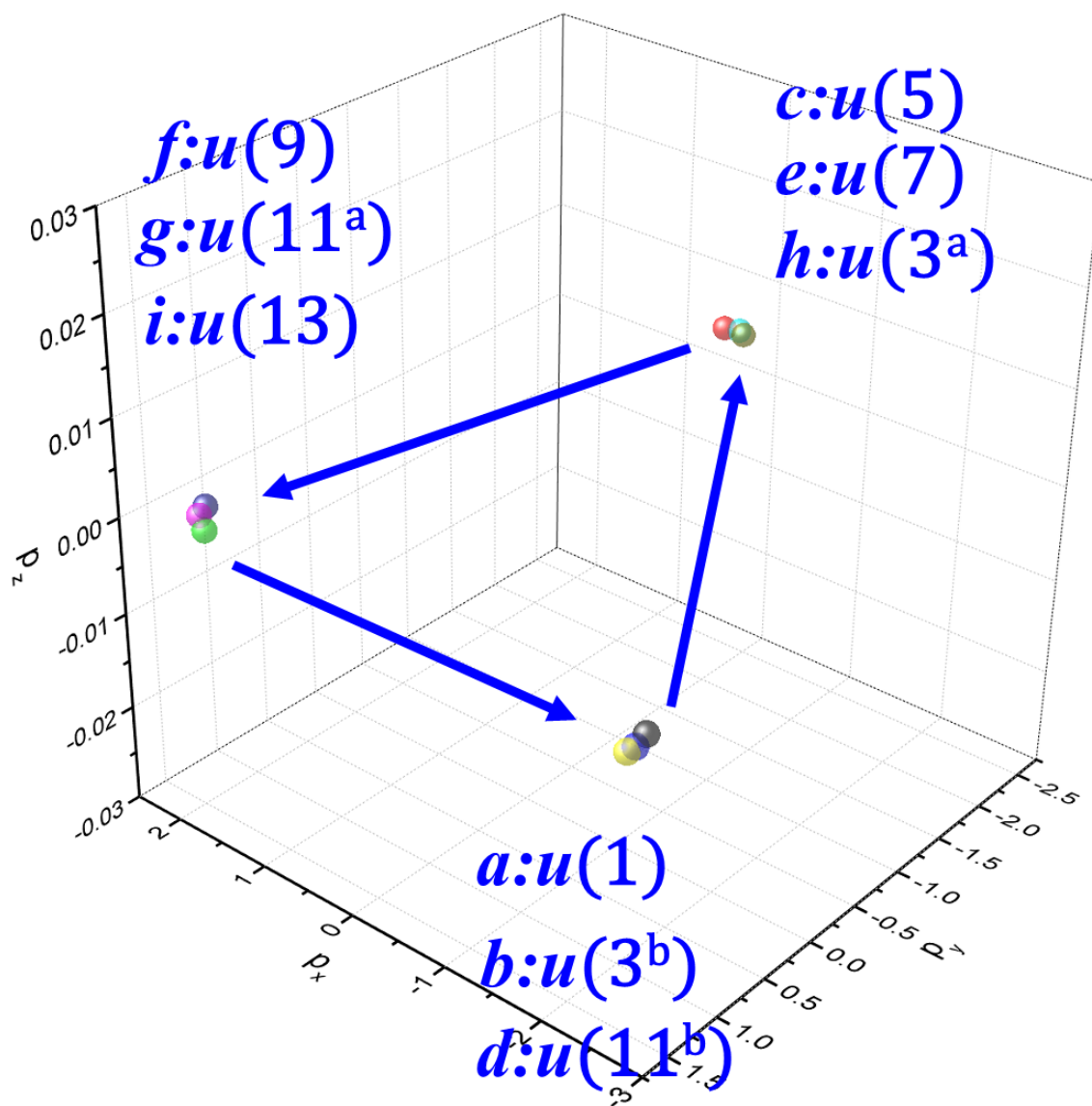


Figure S20. Momentum space for global NNN hopping of up spin particle of phenanthrene

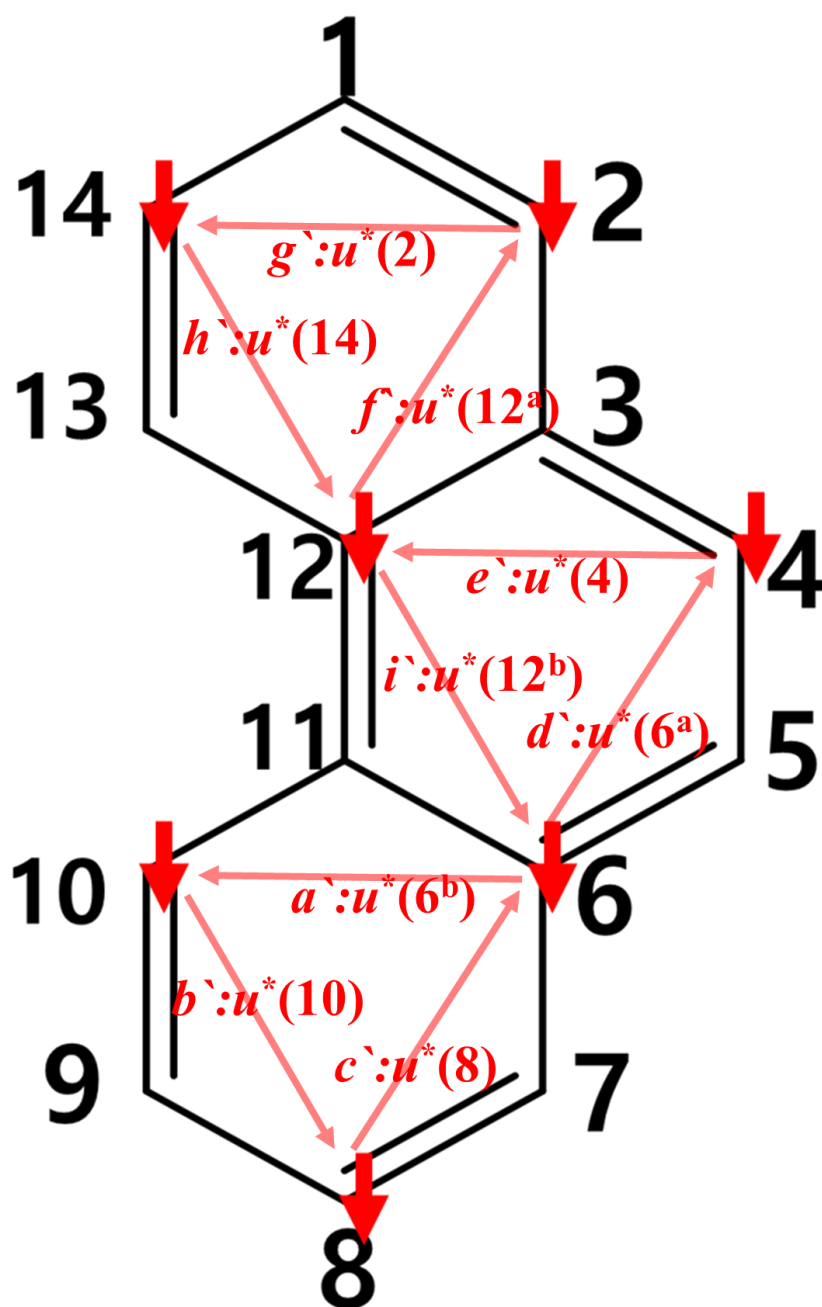


Figure S21. Momentum vector for global NNN hopping of down spin particle of phenanthrene

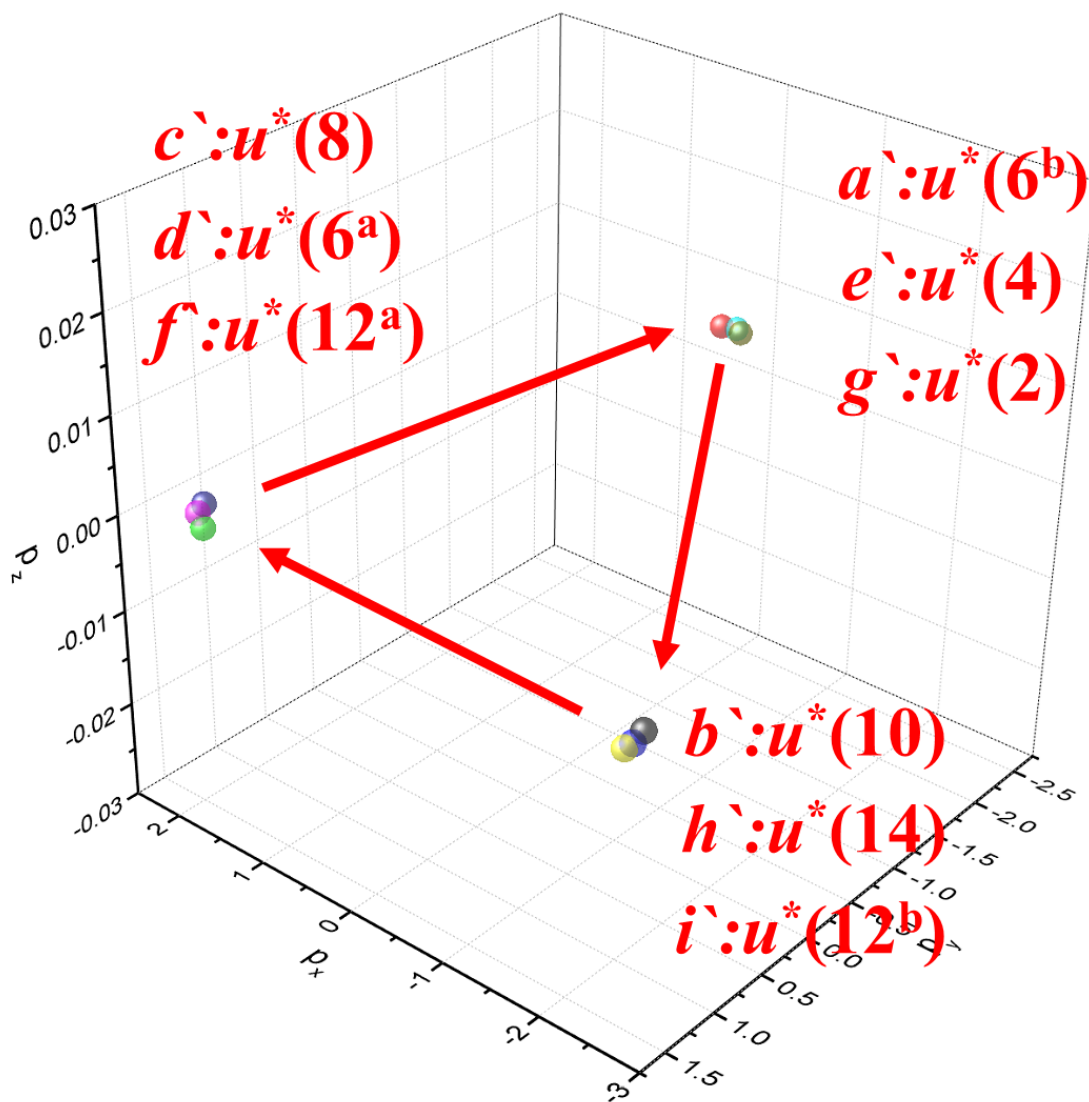


Figure S22. Momentum space for global NNN hopping of down spin particle of phenanthrene

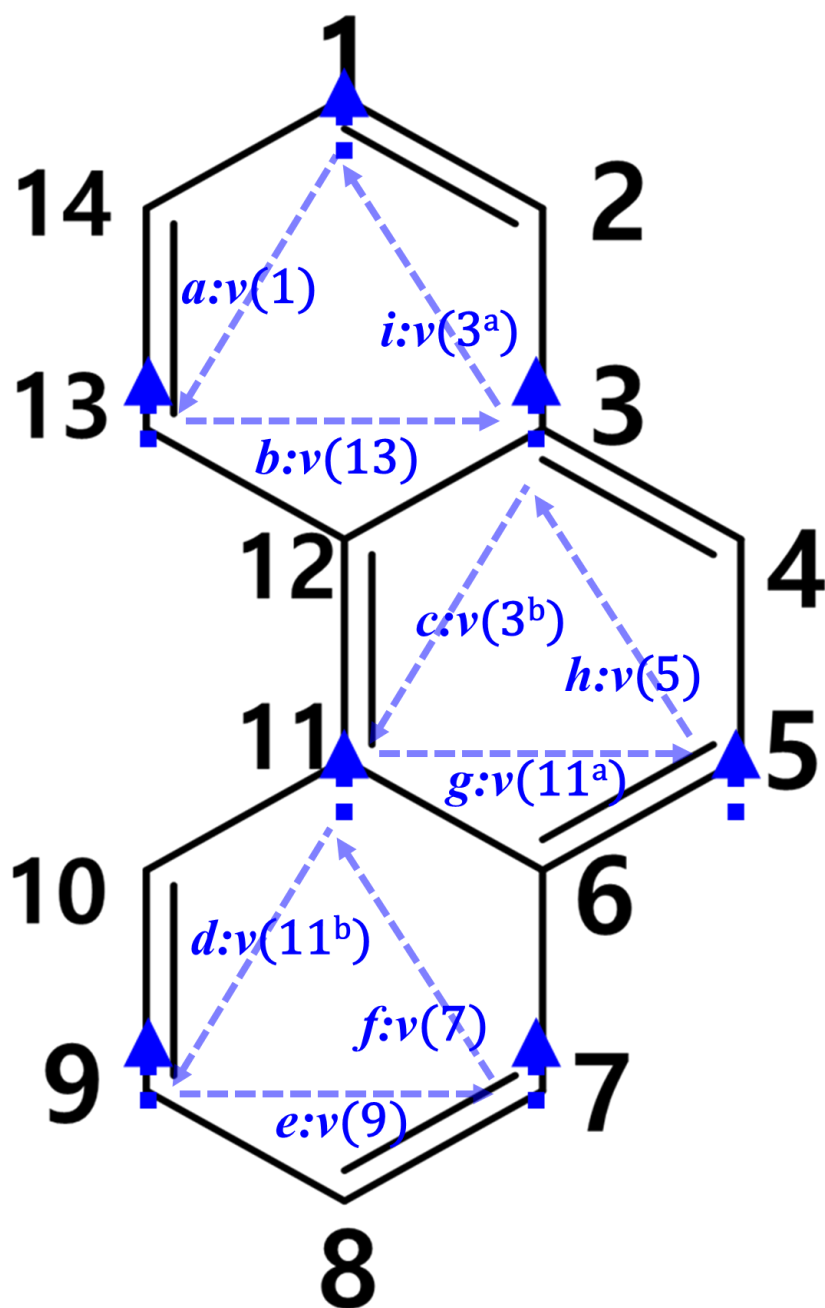


Figure S23. Momentum vector for global NNN hopping of up spin antiparticle of phenanthrene.

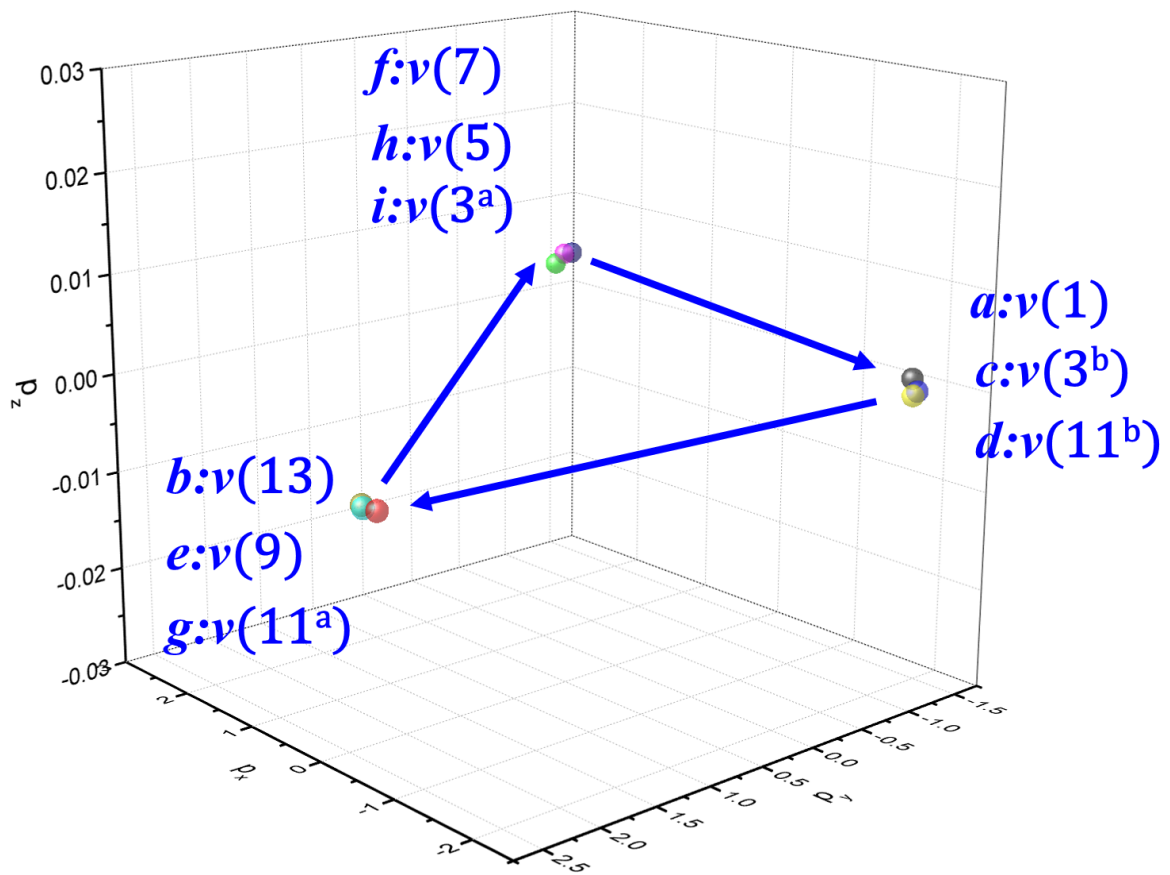


Figure S24. Momentum space for global NNN hopping of up spin antiparticle of anthracene

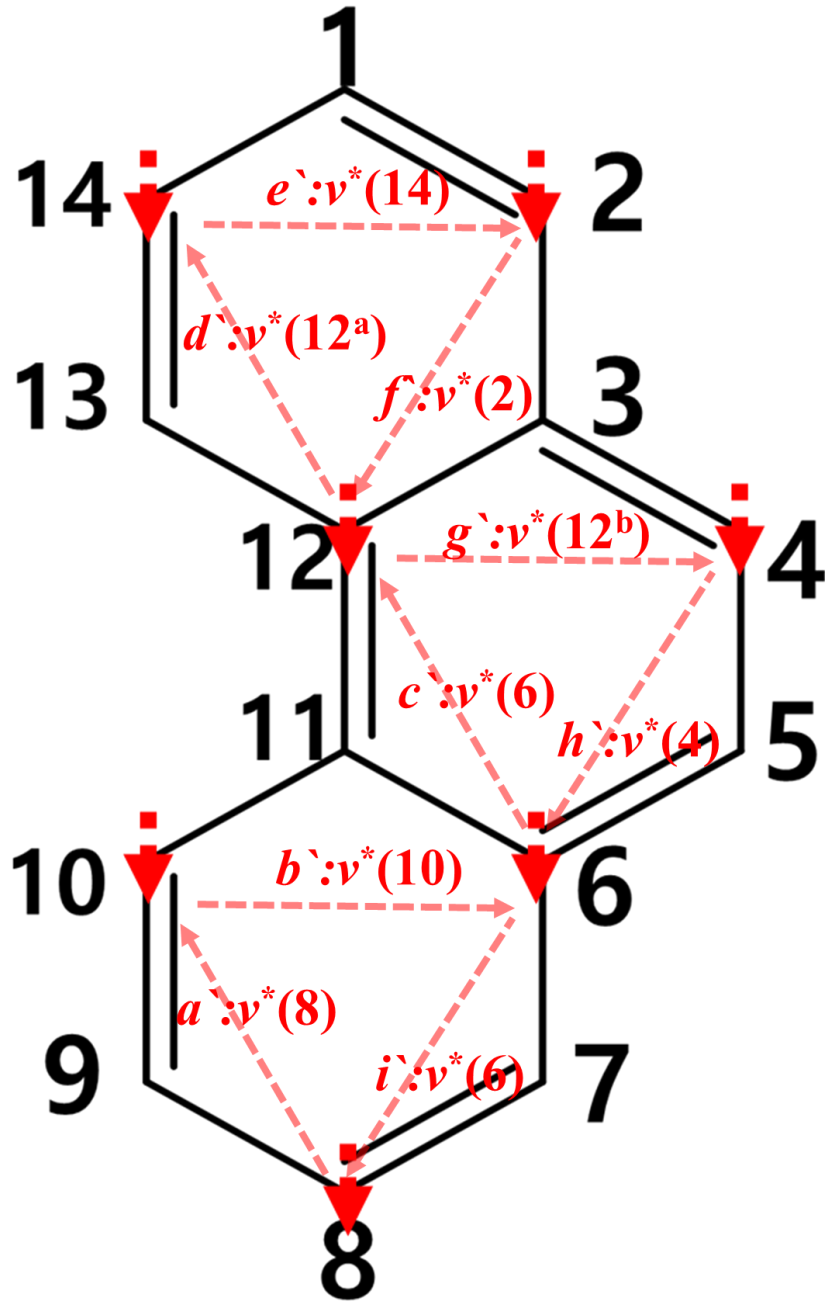


Figure S25. Momentum vector for global NNN hopping of down spin antiparticle of phenanthrene.

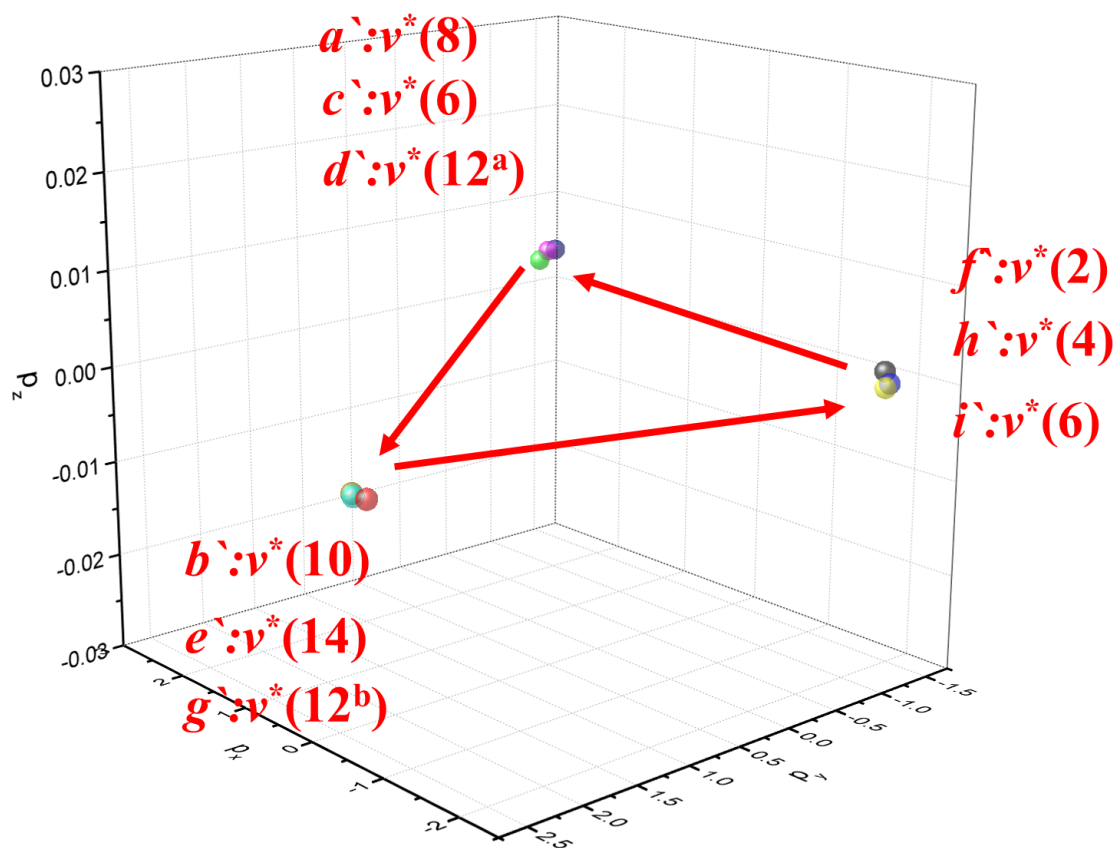


Figure S26. Momentum space for global NNN hopping of down spin antiparticle of phenanthrene.

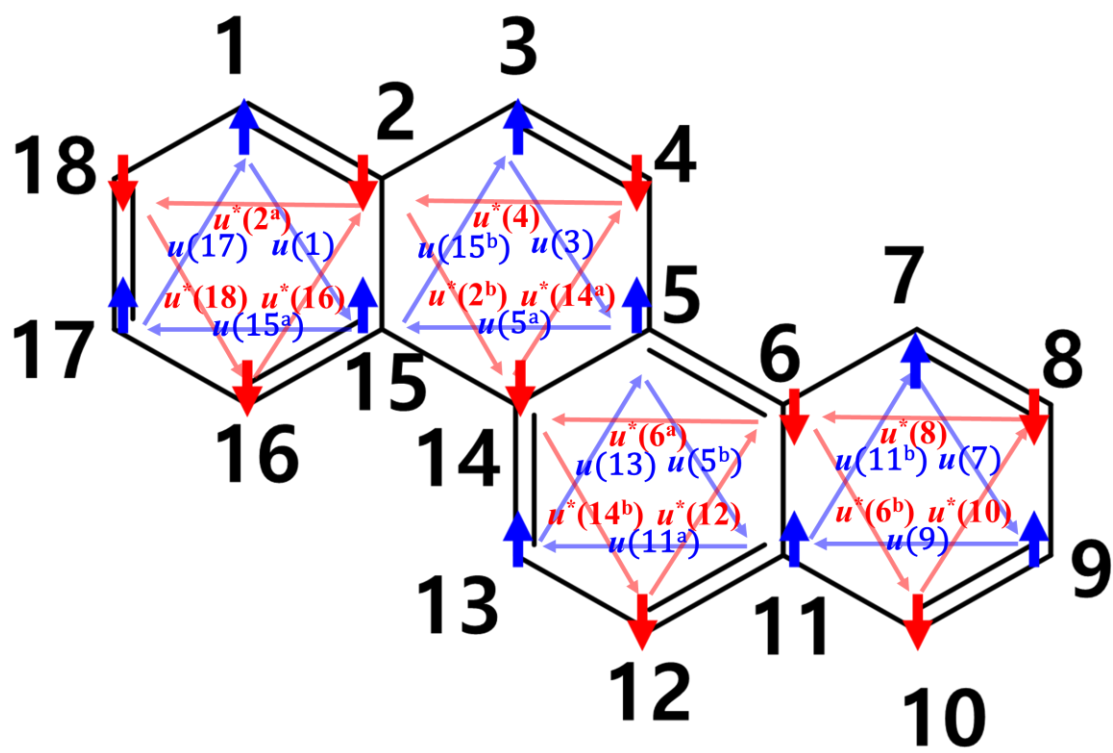


Figure S27. Momentum vectors of particle fermions in chrysene.

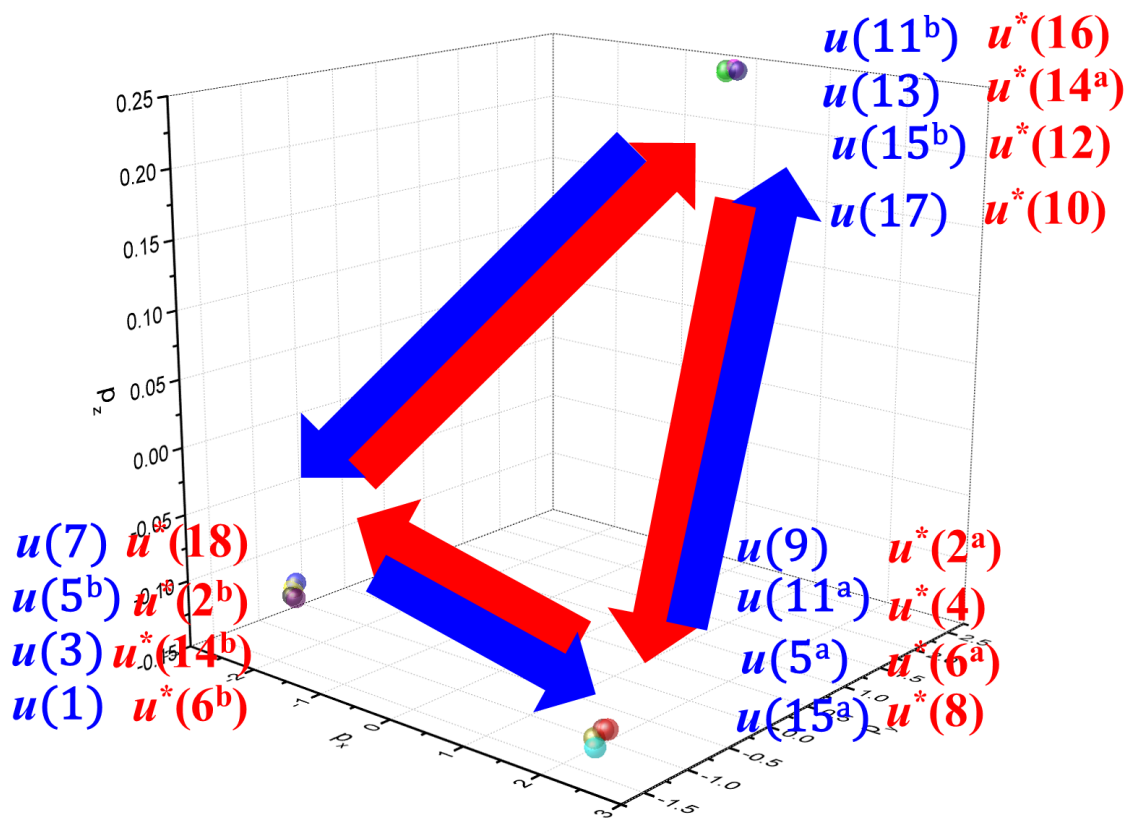


Figure S28. Momentum space of particle fermions in phenanthrene.

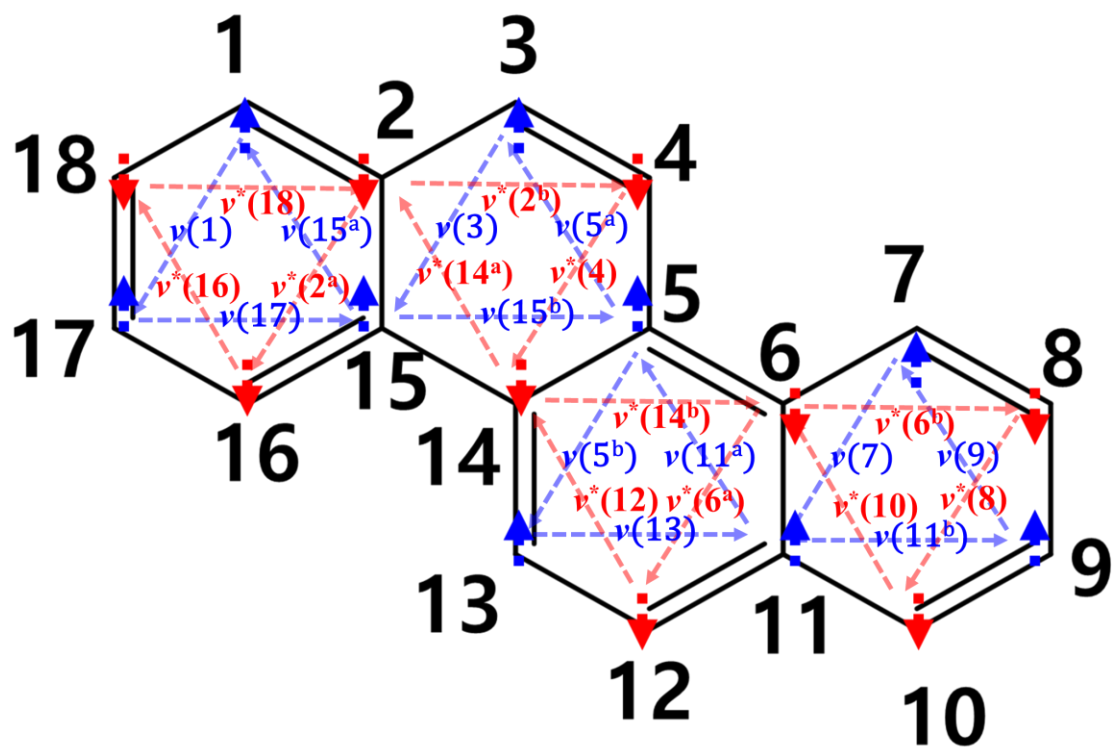


Figure S29. Momentum vectors of antiparticle fermions in phenanthrene.

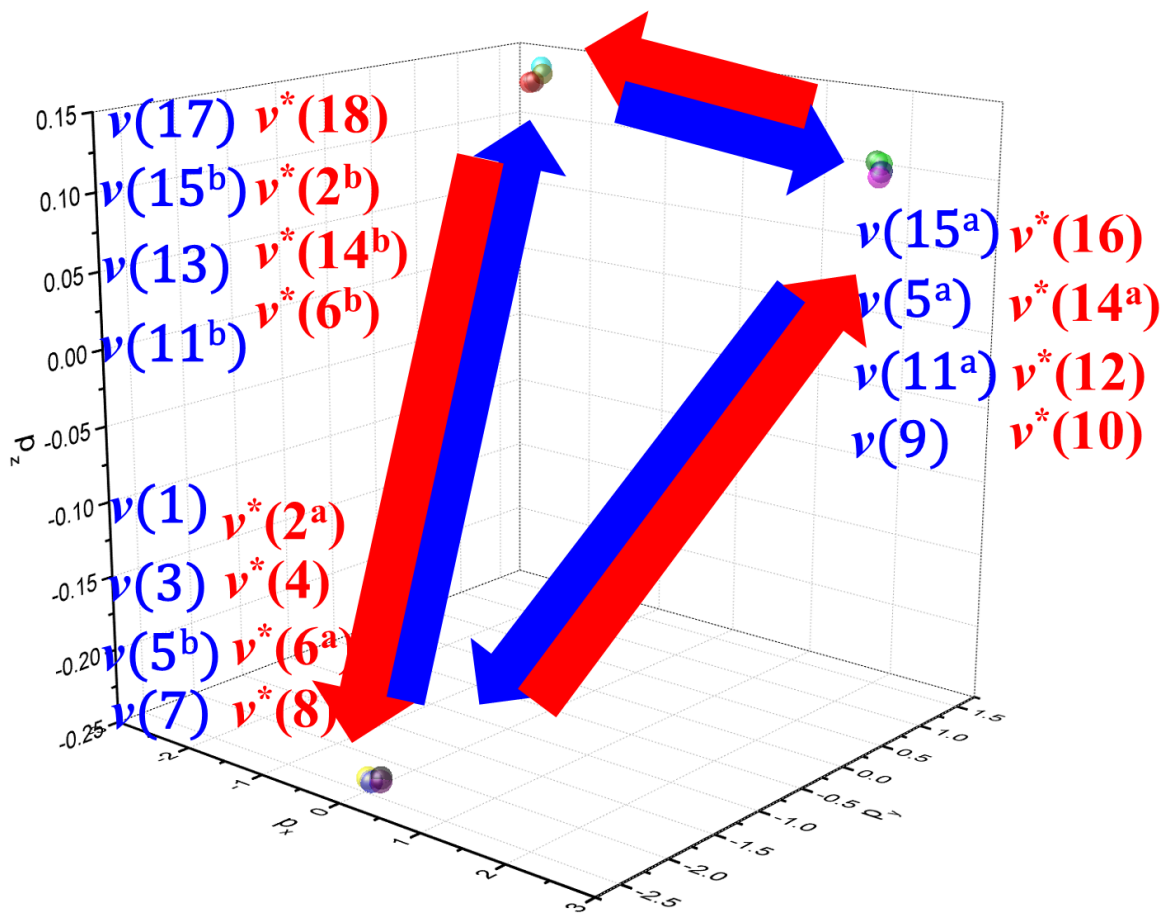


Figure S30. Momentum space of antiparticle fermions in chrysene

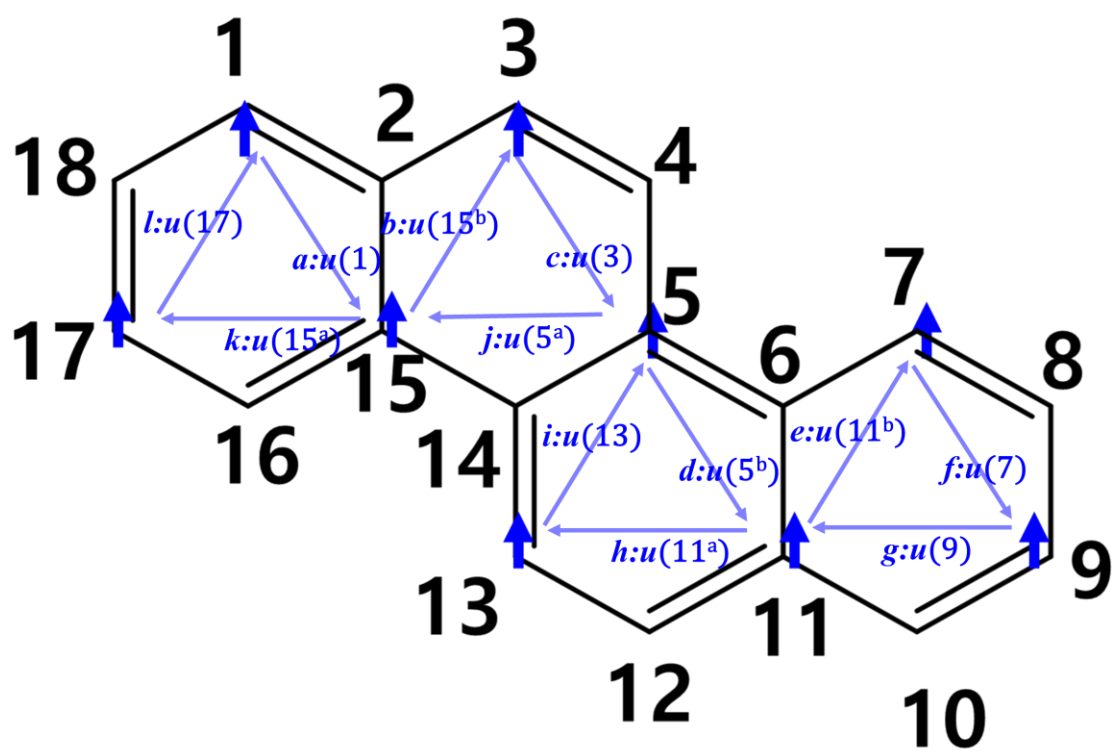


Figure S31. Momentum vector for global NNN hopping of up spin particle of chrysene.

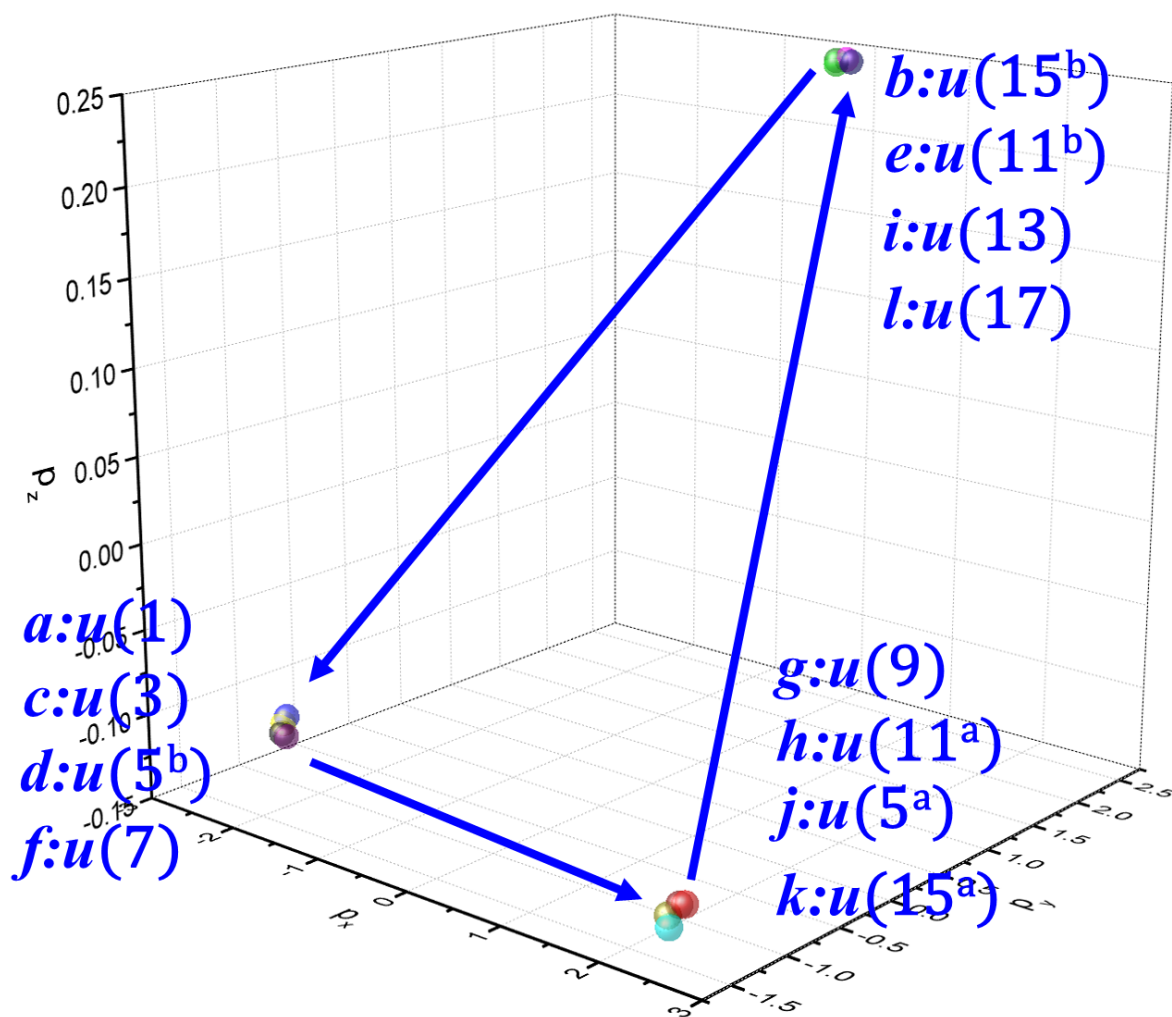


Figure S32. Momentum space for global NNN hopping of up spin particle of phenanthrene.

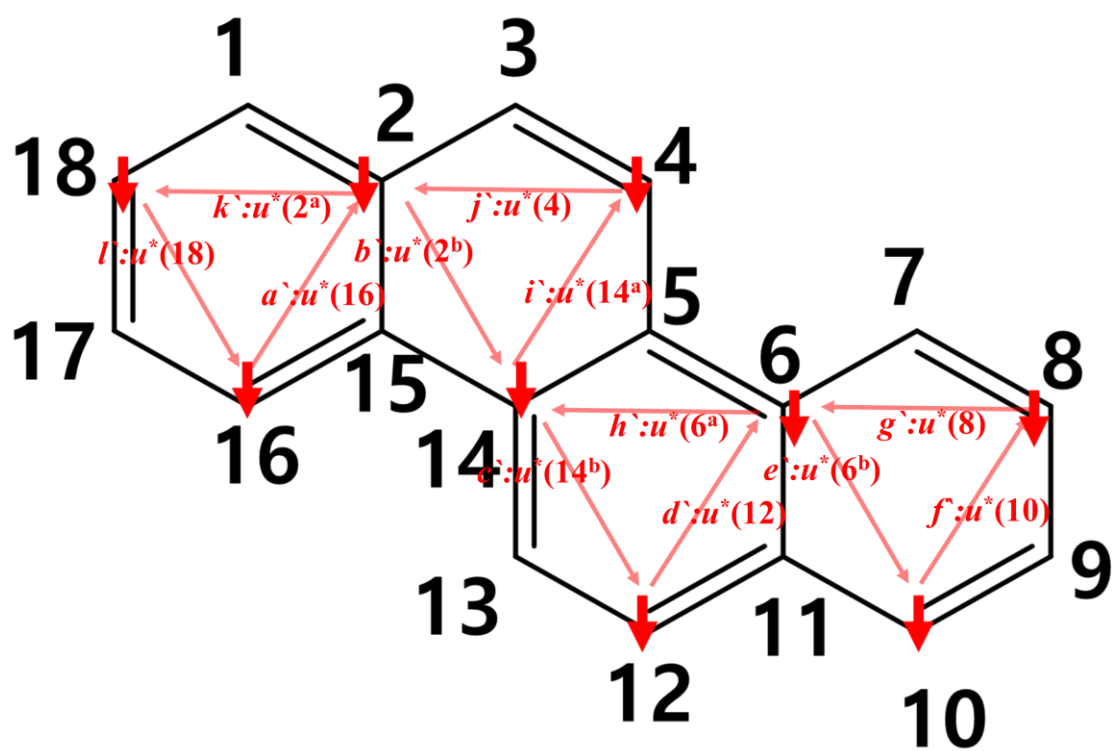


Figure S33. Momentum vector for global NNN hopping of down spin particle of chrysene.

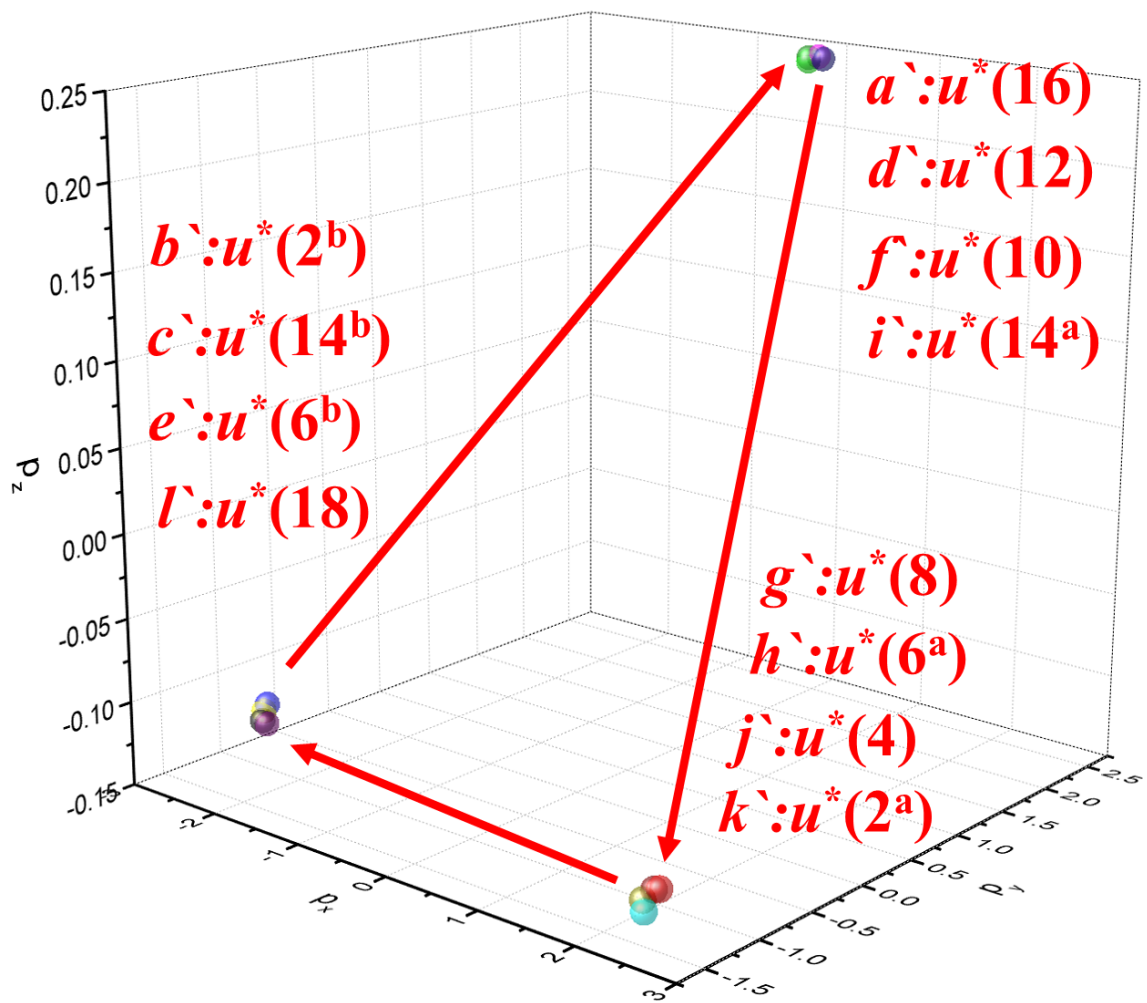


Figure S34. Momentum space for global NNN hopping of down spin particle of chrysene

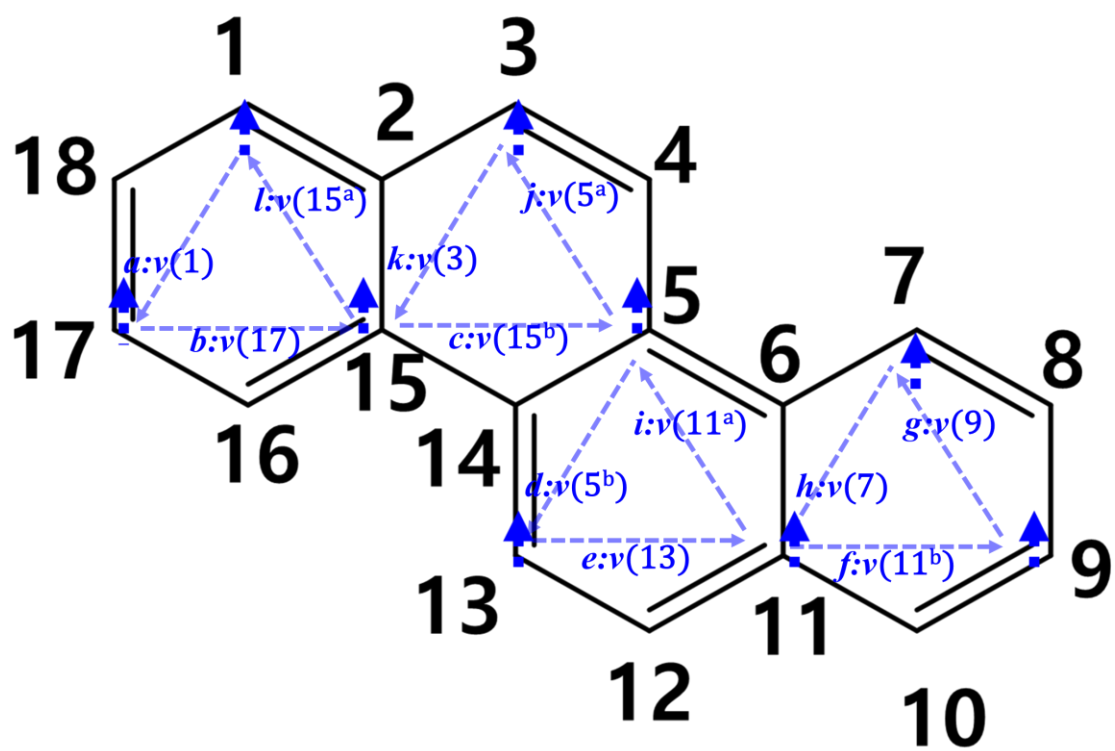


Figure S35. Momentum vector for global NNN hopping of up spin antiparticle of chrysene.

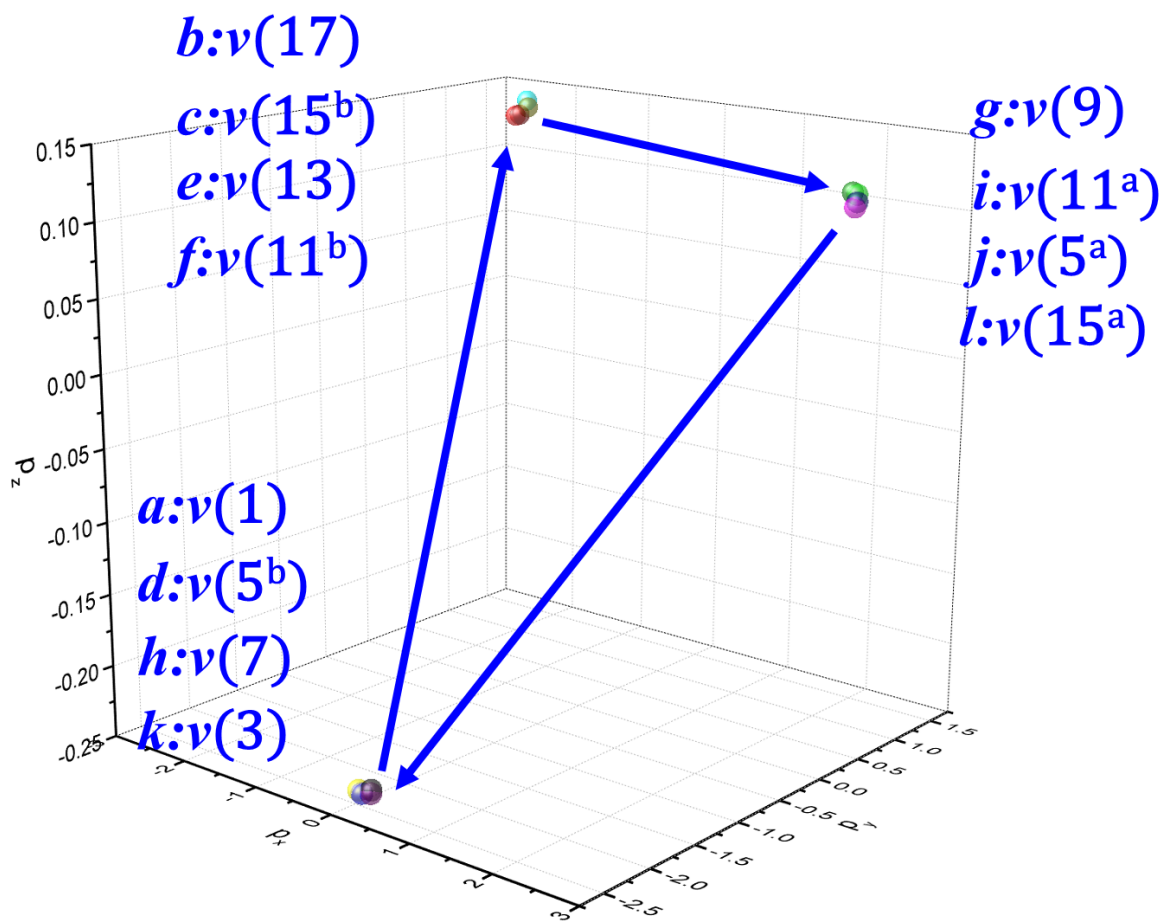


Figure S36. Momentum space for global NNN hopping of up spin antiparticle of chrysenes

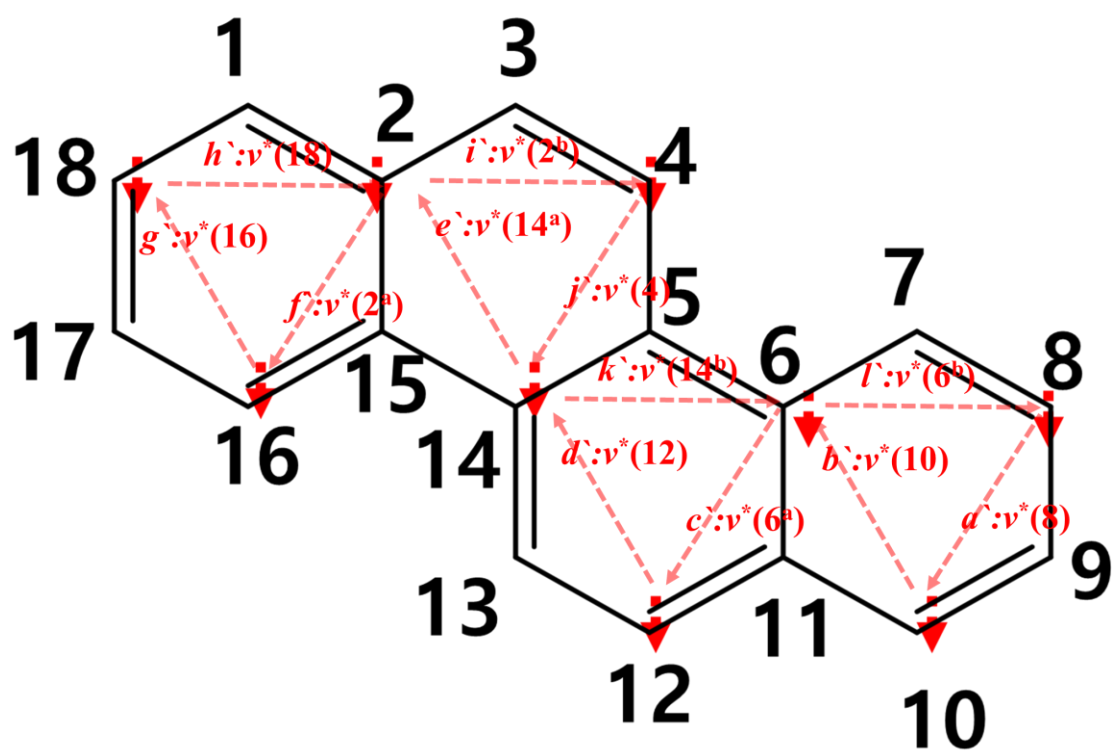


Figure S37. Momentum vector for global NNN hopping of down spin antiparticle of phenanthrene

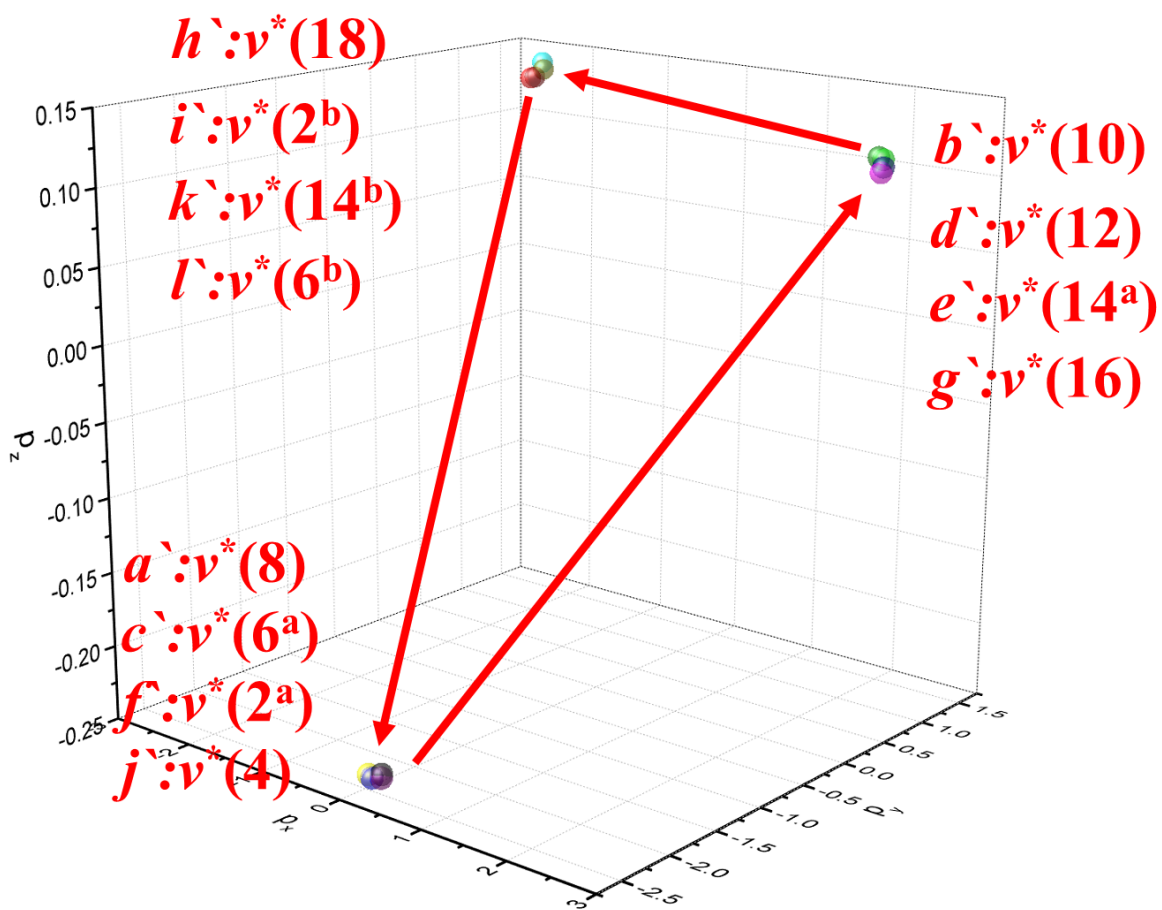


Figure S38. Momentum space for global NNN hopping of down spin antiparticle of phenanthrene.

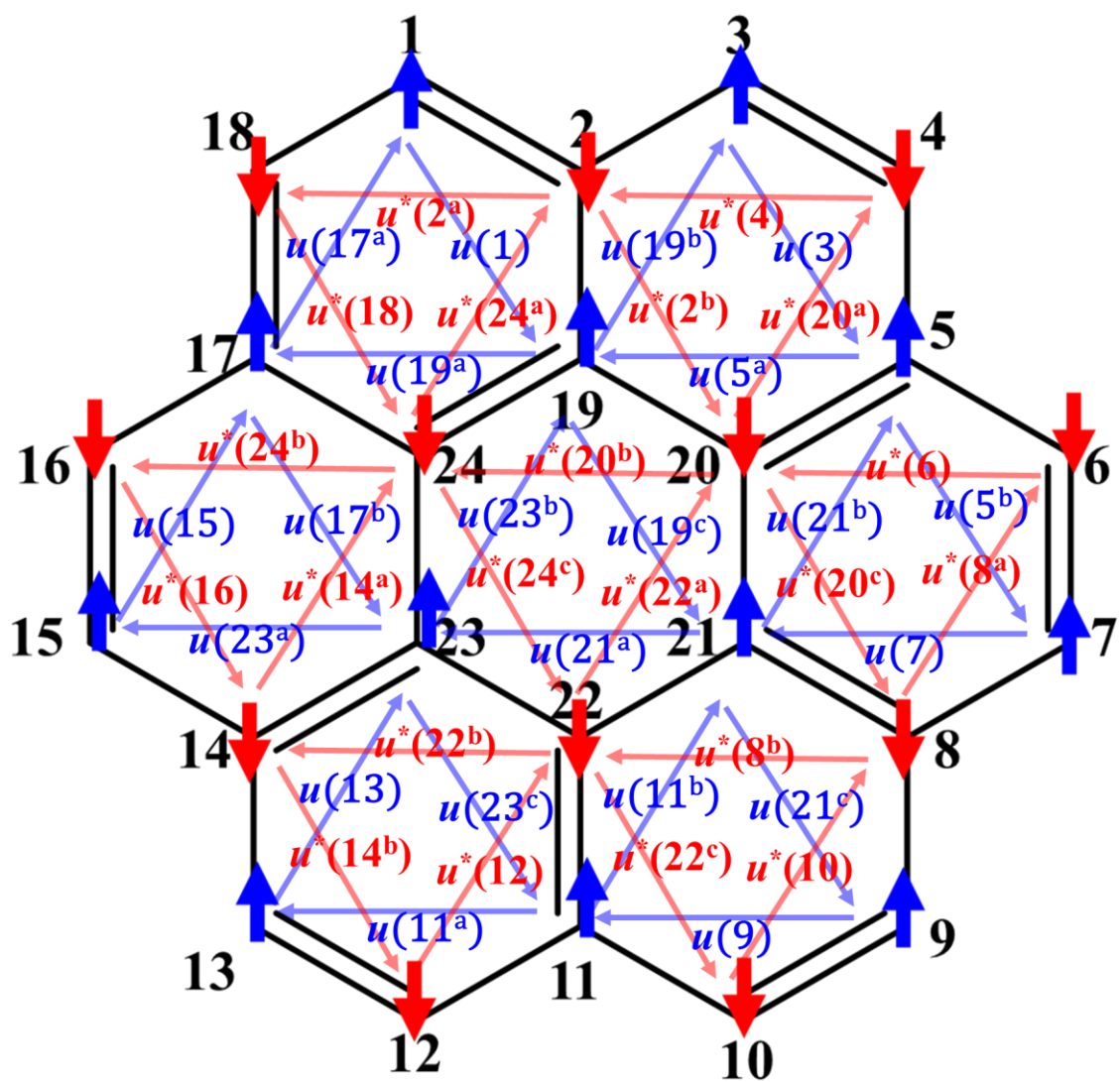


Figure S39. Momentum vectors of particle fermions in coronene.

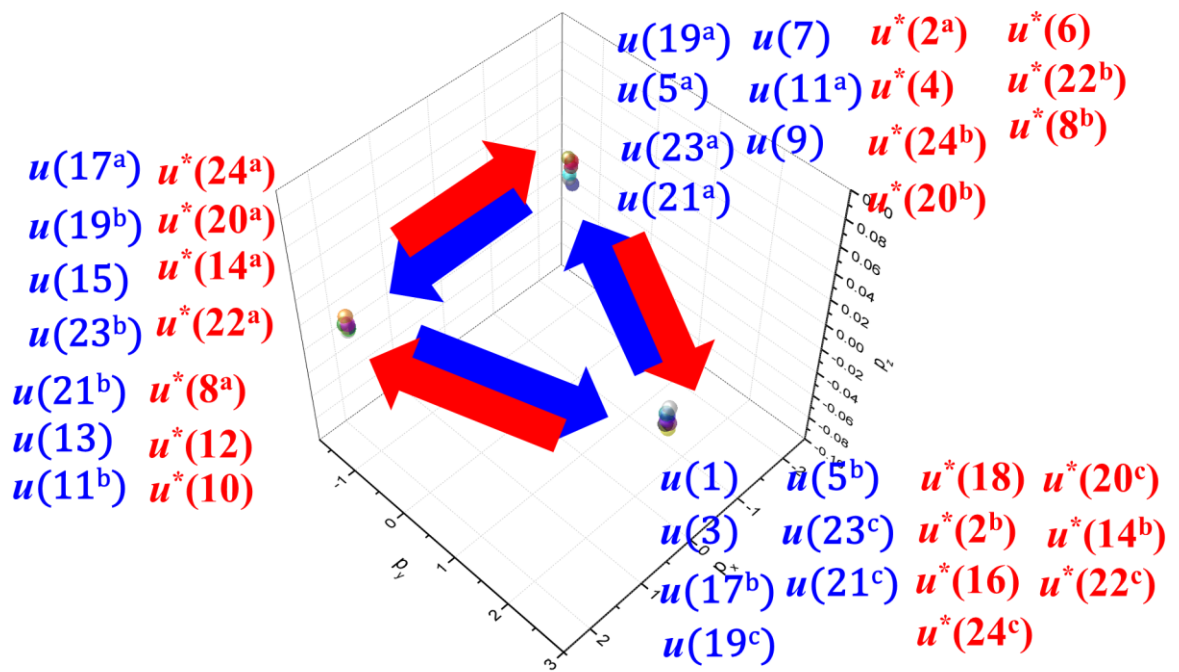


Figure S40. Momentum space of particle fermions in coronene.

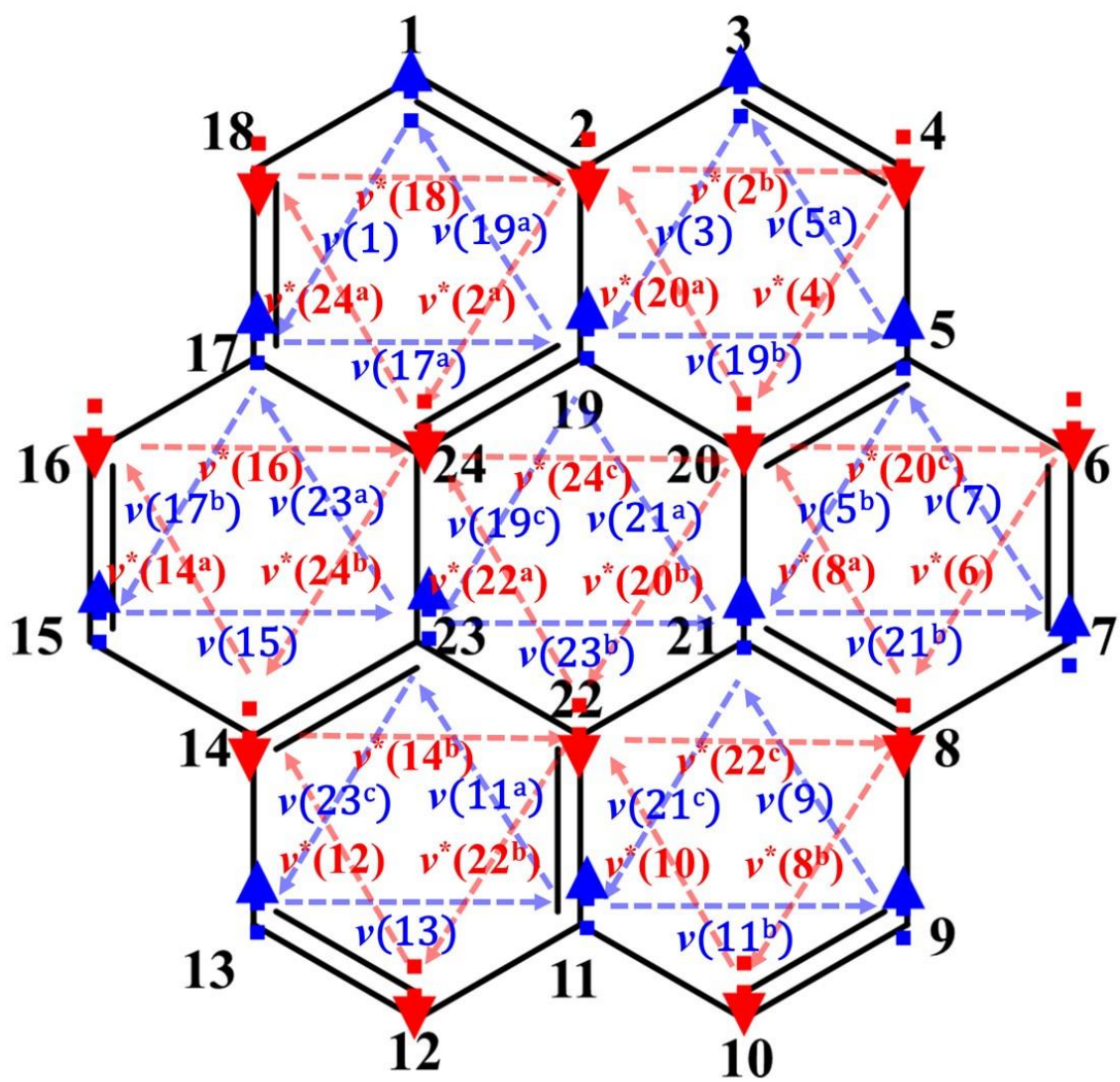


Figure S41. Momentum vectors of antiparticle fermions in coronene

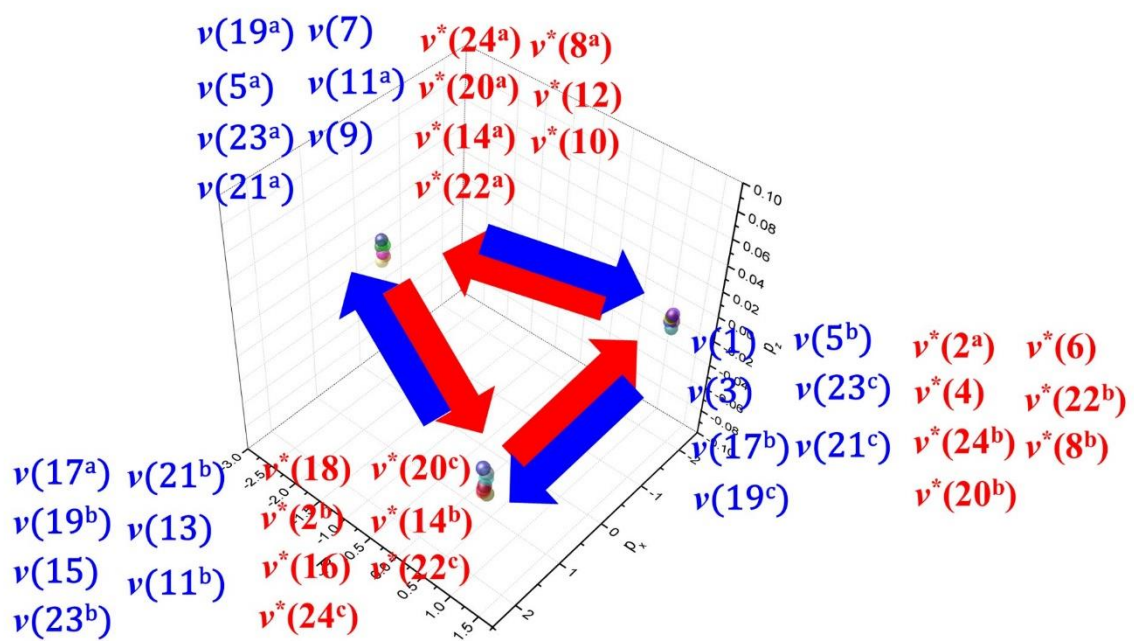


Figure S42. Momentum space of antiparticle fermions in coronene

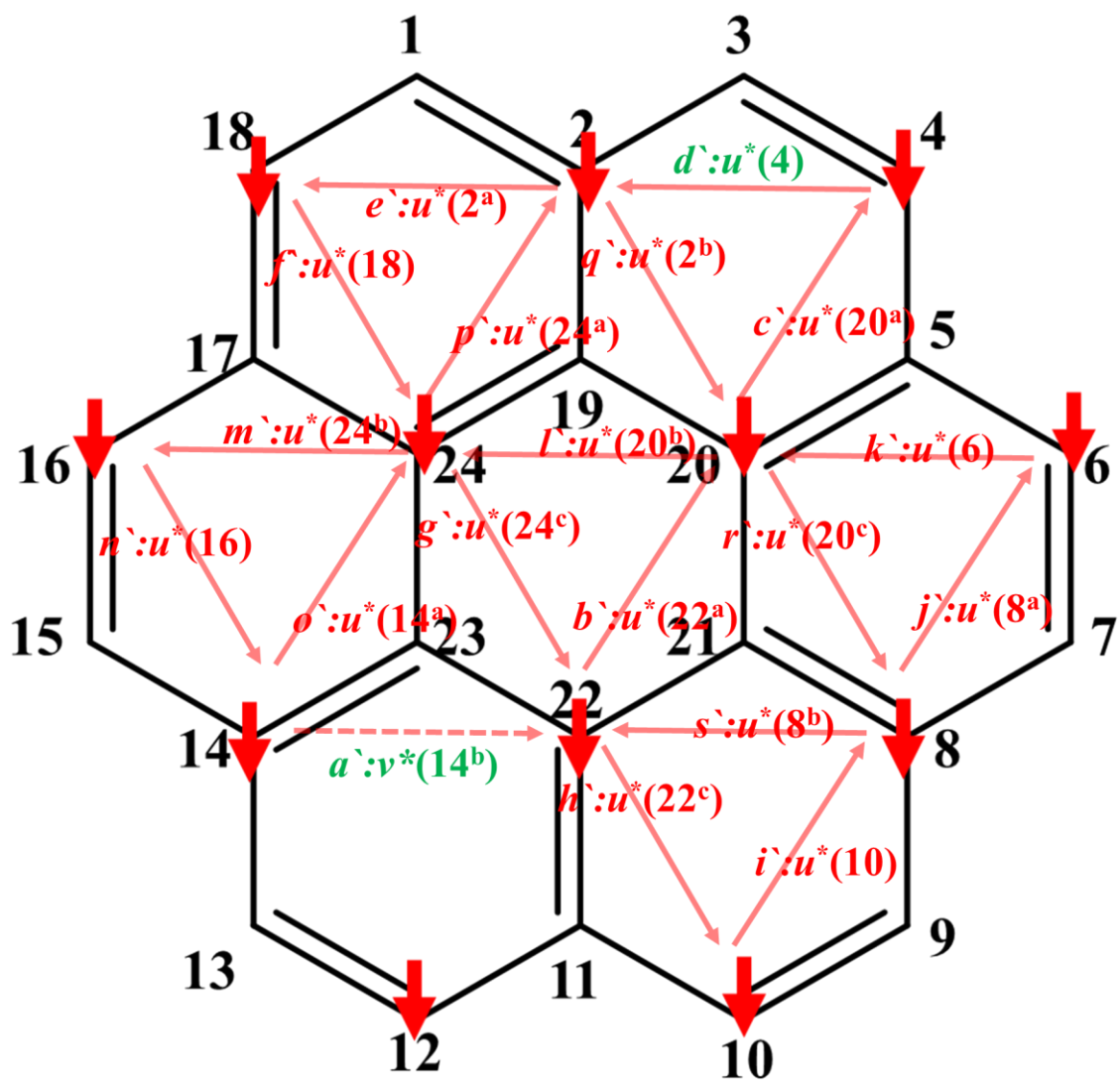


Figure S43. Momentum vector for global NNN hopping of down spin particle of coronene.

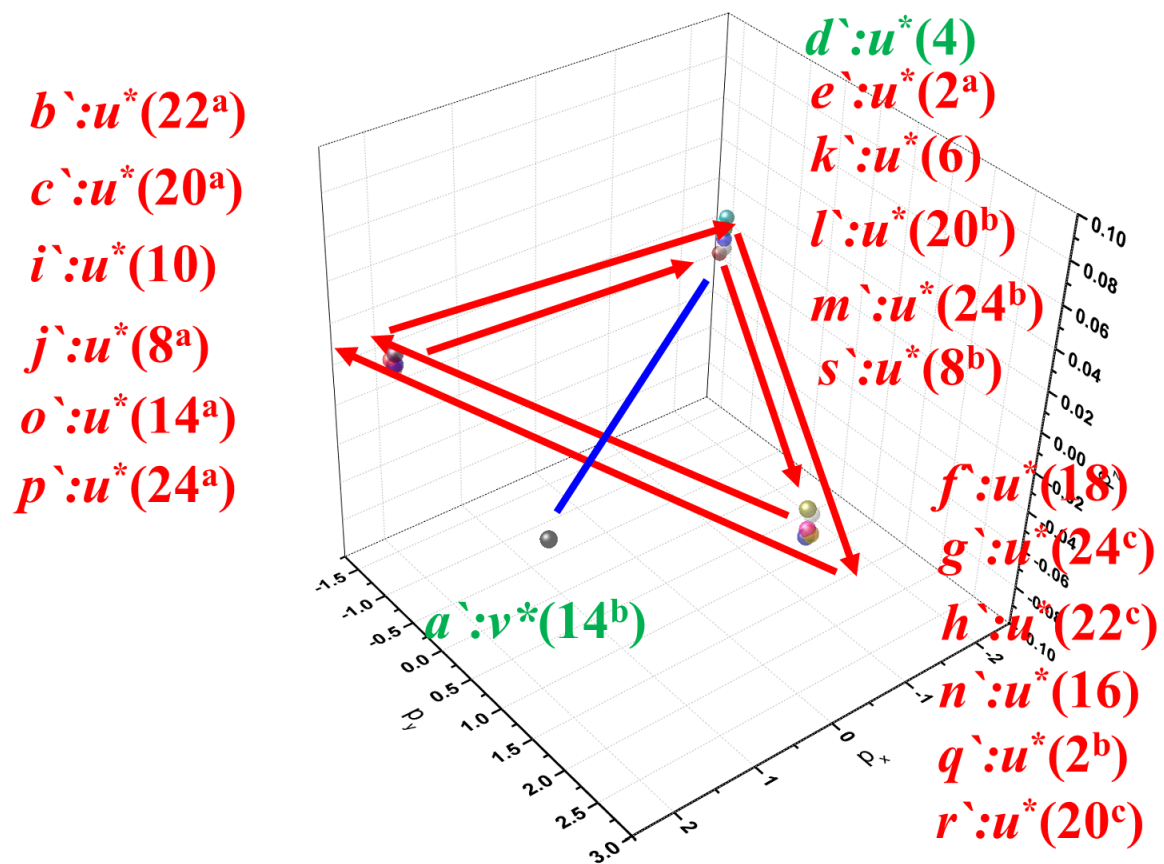


Figure S44. Momentum space for global NNN hopping of down spin particle of coronene.

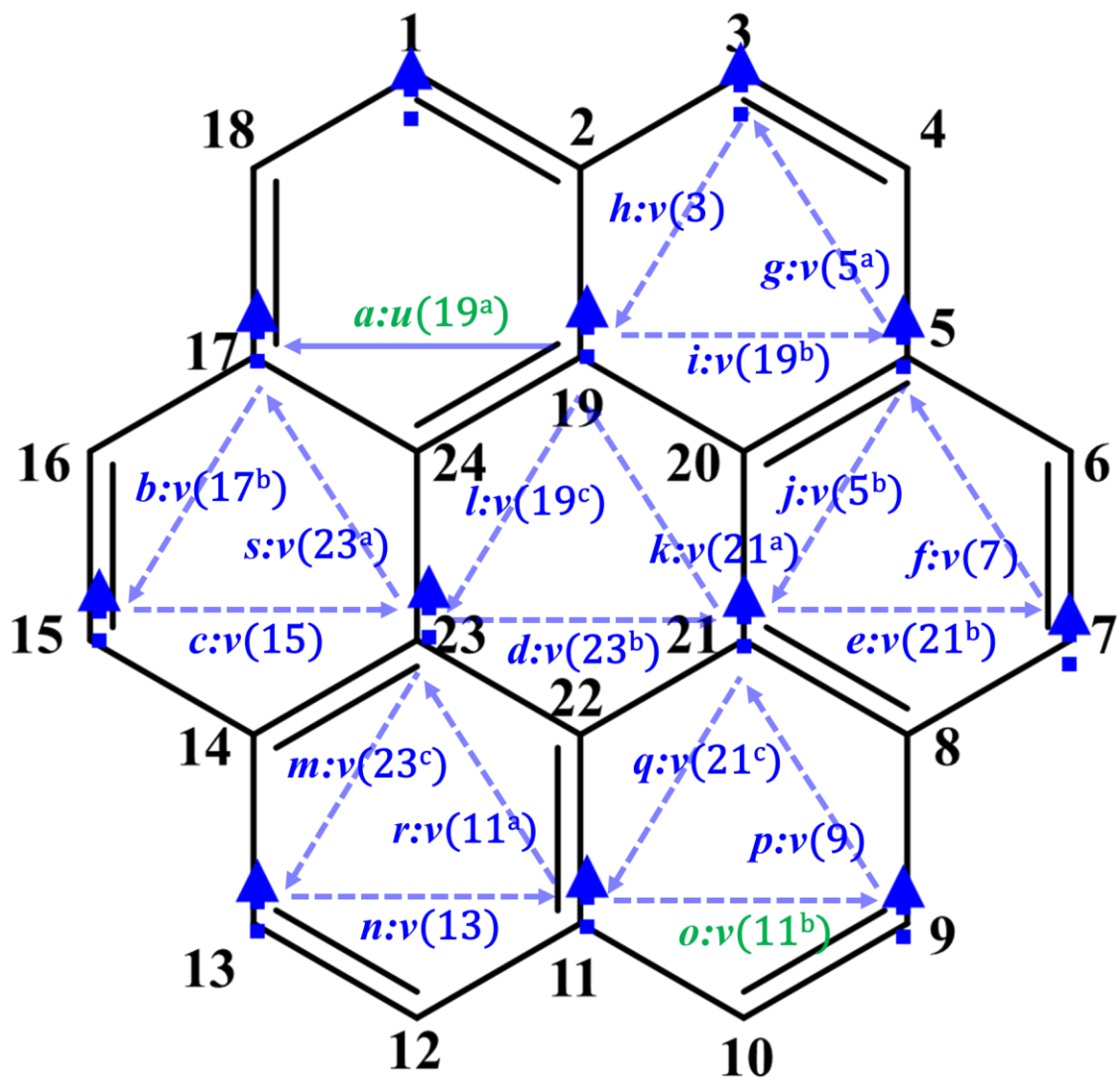


Figure S45. Momentum vector for global NNN hopping of up spin antiparticle of coronene.

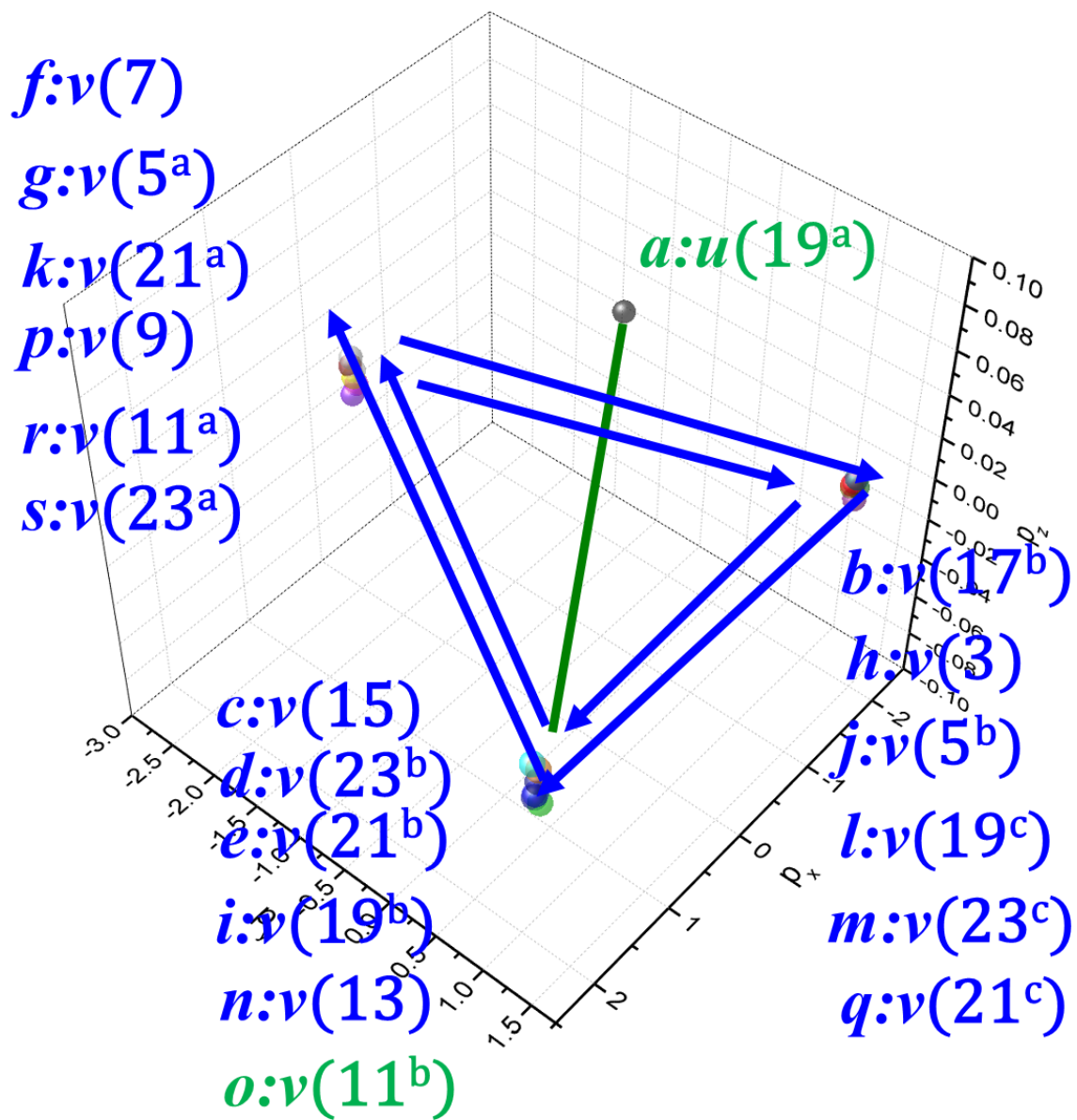


Figure S46. Momentum space for global NNN hopping of up spin antiparticle of coronene

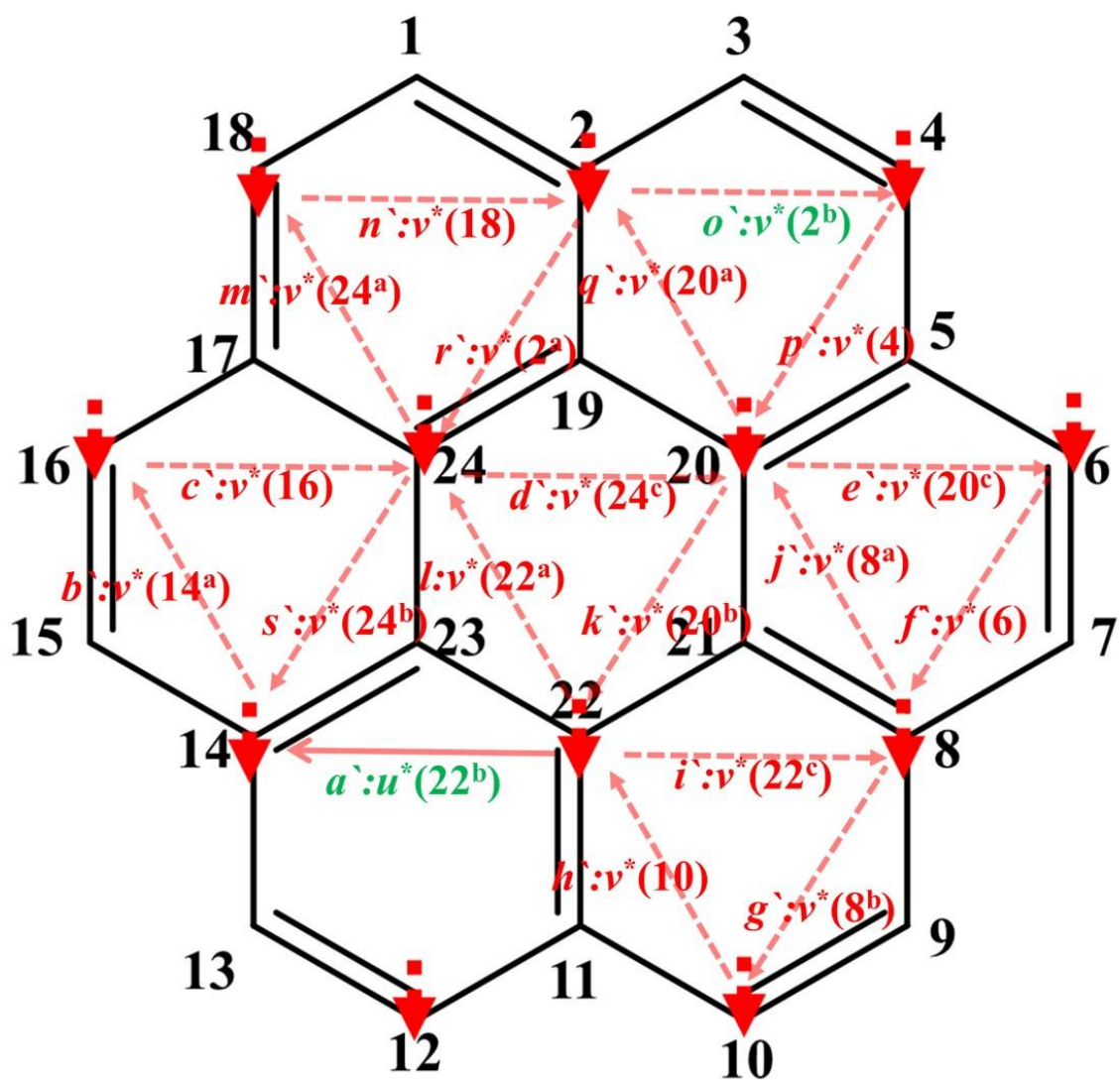


Figure S47. Momentum vector for global NNN hopping of down spin antiparticle of coronene

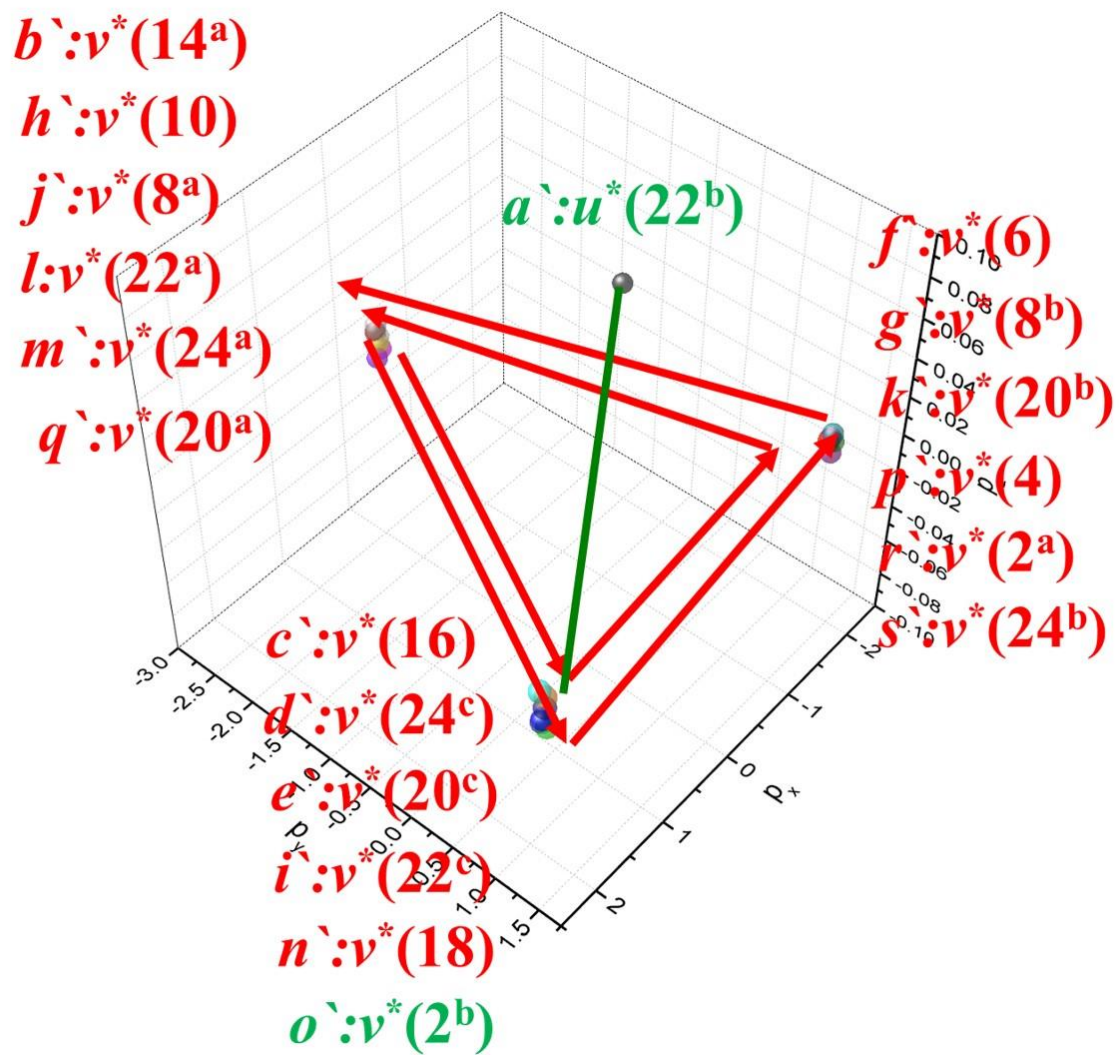


Figure S48. Momentum space for global NNN hopping of down spin antiparticle of coronene.

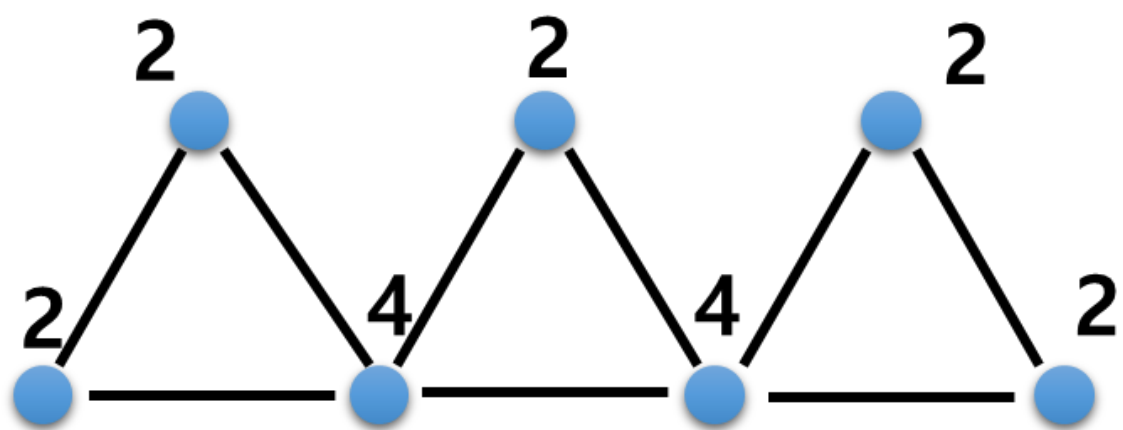


Figure S49. Eulerian graph of anthracene for up spin. Because all vertices in the graph have an even degree, it can make Eulerian circuit.

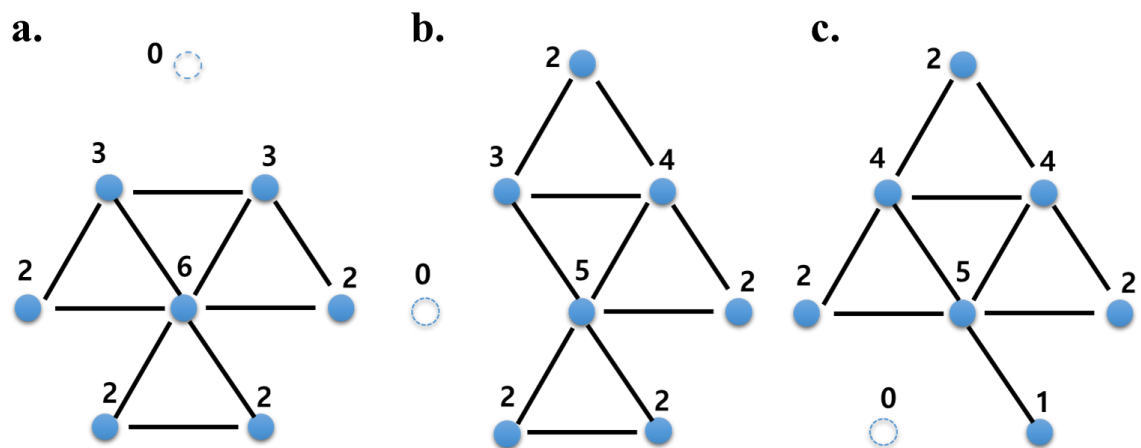


Figure S50. Eulerian graph of pyrene that can make odd number of Kramers doublet and Eulerian trail.